# Unstructured Adiabatic Quantum Optimization

Thesis submitted in partial fulfillment
of the requirements for the degree of

*Master of Science in Computer Science and Engineering by Research*

by

Alapan Chaudhuri
2019111023
alapan.chaudhuri@research.iiit.ac.in

Centre for Quantum Science and Technology (CQST)
International Institute of Information Technology (IIIT)
Hyderabad - 500032, India
February 2026

International Institute of Information Technology
Hyderabad, India

# CERTIFICATE

It is certified that the work contained in this thesis, titled "Unstructured Adiabatic Quantum Optimization" by Alapan Chaudhuri, has been carried out under my supervision and is not submitted elsewhere for a degree.

Date | Adviser: Prof. Indranil Chakrabarty

Date | Co-Adviser: Prof. Shantanav Chakraborty

To a world that feels like it's splitting apart.
May we keep repairing what we can.

“Computers are more forgiving than bare-bone nature or mathematics
— both of which are infinitely more forgiving than academia."

# Abstract

[TODO]

# Acknowledgement

# Contents


**1 Introduction** **1**

**2 Physics and Computation** **2**

**3 Quantum Computation** **3**

**4 Adiabatic Quantum Computation** **4**

**5 Adiabatic Quantum Optimization** **5**
5.1 The Problem . . . 6
5.2 Spectral Parameters . . . 7
5.3 Symmetry Reduction . . . 8
5.4 The Avoided Crossing . . . 10
5.5 Gap Structure . . . 12
5.6 The Central Questions . . . 13

**6 Spectral Analysis** **14**
6.1 Gap to the Left of the Crossing . . . 14
6.2 Gap to the Right of the Crossing . . . 16
6.3 The Complete Gap Profile . . . 20

**7 Optimal Schedule** **22**
7.1 Prior Adiabatic Theorems . . . 22
7.2 The Adiabatic Error Bound . . . 23
7.3 The Adaptive Schedule . . . 26
7.4 Runtime of Adiabatic Quantum Optimization . . . 28

**8 Hardness of Optimality** **32**
8.1 NP-Hardness of Estimating $A_1$ . . . 32
8.2 #P-Hardness of Computing $A_1$ Exactly . . . 35
8.3 The Intermediate Regime . . . 37

**9 Information Gap** **42**
9.1 The Cost of Ignorance . . . 42
9.2 Partial Knowledge and Hedging . . . 44
9.3 Quantum Bypass . . . 45
9.4 Gap Geometry and Schedule Optimality . . . 48
9.5 Anatomy of the Barrier . . . 51
9.6 Computational Nature of $A_1$ . . . 53
9.7 The Complexity Landscape . . . 55

**10 Formalization** **58**

**11 Conclusion** **59**

# List of Theorems


5.2.1 Definition (Spectral parameters) . . . 7
5.2.2 Definition (Spectral condition) . . . 7
5.3.1 Lemma (Eigenvalue equation) . . . 9
5.4.1 Lemma (Validity of approximation) . . . 10
5.4.2 Lemma (Gap within the crossing window) . . . 11
5.5.1 Lemma (Gap to the left of the crossing) . . . 12
5.5.2 Lemma (Gap to the right of the crossing) . . . 12

6.1.1 Lemma (Gap to the left of the crossing) . . . 14
6.2.1 Lemma (Gap to the right of the crossing) . . . 17
6.3.1 Theorem (Complete gap profile) . . . 20

7.2.1 Lemma (Adiabatic error bound [14, 23]) . . . 24
7.2.2 Lemma (Projector derivative bounds [14]) . . . 24
7.2.3 Theorem (Constant-rate runtime) . . . 25
7.3.1 Theorem (Adaptive rate [14]) . . . 26
7.3.2 Corollary . . . 27
7.3.3 Lemma (Grover gap integral) . . . 28
7.4.1 Theorem (Runtime of AQO — Main Result 1 [14]) . . . 30

8.1.1 Lemma (Disambiguation [14]) . . . 33
8.1.2 Theorem (NP-hardness of $A_1$ estimation [14]) . . . 34
8.2.1 Lemma (Exact degeneracy extraction [14]) . . . 35
8.2.2 Lemma (Paturi [31]) . . . 36
8.2.3 Lemma (Approximate degeneracy extraction [14]) . . . 36
8.2.4 Theorem (#P-hardness of $A_1$ estimation [14]) . . . 36
8.3.1 Theorem (Interpolation barrier) . . . 37
8.3.2 Theorem (Generic extrapolation barrier) . . . 38
8.3.3 Theorem (Quantum algorithm for $A_1$) . . . 38
8.3.4 Theorem (Classical lower bound for $A_1$ estimation) . . . 39
8.3.5 Corollary (Quadratic quantum-classical separation) . . . 40

9.1.1 Definition (Gap class) . . . 42
9.1.2 Definition (RC-admissible fixed schedules) . . . 42
9.1.3 Lemma (Adversarial gap construction) . . . 43
9.1.4 Lemma (Velocity bound for uninformed schedules) . . . 43
9.1.5 Theorem (Separation (uniformly RC-admissible class)) . . . 43
9.1.6 Corollary (Unstructured search) . . . 43
9.2.1 Lemma ($A_1$-to-$s^*$ precision propagation) . . . 44
9.2.2 Theorem (Interpolation) . . . 44
9.2.3 Theorem (Hedging) . . . 45
9.3.1 Definition (Binary decision probe) . . . 46
9.3.2 Definition (Adaptive adiabatic protocol) . . . 46
9.3.3 Lemma (Decision-probe cost) . . . 46
9.3.4 Lemma (Phase 1 cost) . . . 46
9.3.5 Theorem (Adaptive adiabatic optimality in the decision-probe model) . . . 47
9.3.6 Theorem (Measurement lower bound) . . . 47

9.3.7 Proposition ($A_1$-blindness) . . . 47
9.4.1 Theorem (Geometric characterization) . . . 48
9.4.2 Lemma (Gap integral) . . . 48
9.4.3 Theorem (Scaling spectrum) . . . 49
Remark . . . 49
9.4.4 Proposition (Structural $\alpha = 1$) . . . 49
9.4.5 Theorem (Measure condition for the rank-one gap profile) . . . 49
9.4.6 Corollary (Grover measure constant) . . . 50
9.4.7 Theorem (Constant comparison) . . . 50
Remark . . . 50
9.5.1 Theorem (Product ancilla invariance) . . . 51
Remark . . . 51
9.5.2 Theorem (Universality of uniform superposition) . . . 51
9.5.3 Corollary . . . 51
9.5.4 Theorem (Coupled ancilla limitation) . . . 51
9.5.5 Theorem (Multi-segment rigidity) . . . 51
9.5.6 Theorem (No-go) . . . 52
9.5.7 Proposition (Rank-$k$ two-level obstruction) . . . 52
9.5.8 Proposition (Trace no-go) . . . 52
Remark . . . 52
9.5.9 Proposition (Constant-control optimality on two-level family) . . . 52
9.5.10 Proposition (Normalized-control lower bound) . . . 53
9.6.1 Proposition ($A_1$ hardness is counting hardness) . . . 53
9.6.2 Proposition (Bounded treewidth tractability) . . . 54
9.6.3 Proposition (Reverse bridge obstruction) . . . 54
9.6.4 Proposition (Unique solution does not imply easy $A_1$) . . . 54
9.6.5 Proposition (Bounded degeneracy is vacuous) . . . 54
9.6.6 Proposition (Hard optimization does not imply hard $A_1$) . . . 55
9.7.1 Theorem (Tight quantum query complexity at schedule precision) . . . 55
9.7.2 Proposition (Precision phase diagram) . . . 55
9.7.3 Theorem (ETH computational complexity) . . . 55
9.7.4 Corollary (Quantum pre-computation cost) . . . 56
9.7.5 Proposition (Two-level worst-case reduction) . . . 56
9.7.6 Theorem (Bit-runtime information law) . . . 56

# List of Algorithms

# List of Figures

6.1 Schematic gap profile for $H(s)$. The solid curve shows the true spectral gap $g(s)$, which equals 1 at $s = 0$, dips to $g_{\min}$ at $s = s^*$, and recovers to $\Delta$ at $s = 1$. The left arm is steep (slope $A_1(A_1 + 1)/A_2$); the right arm is shallower (slope controlled by $\Delta$). Dashed lines show the piecewise lower bounds from Theorem 6.3.1: linear on the left, constant $g_{\min}$ in the window, and linear on the right (reaching $\Delta/30$ at $s = 1$). The right bound is below $g_{\min}$ at $s^*$ but remains $O(g_{\min})$. . . . . . . . 21

# Chapter 1

# Introduction

## Chapter 2

# Physics and Computation

Chapter 3

# Quantum Computation

## Chapter 4

# Adiabatic Quantum Computation

# Chapter 5

# Adiabatic Quantum Optimization

In the circuit model, unstructured optimization is a solved problem. Given a black-box cost function on $N = 2^n$ bit-strings, Grover's algorithm and its generalizations find a minimizer in $O(\sqrt{N/d_0})$ queries, where $d_0$ is the number of optima [1, 2]. The algorithm works without any prior knowledge of the cost function's structure: amplitude amplification gathers the needed information adaptively, one oracle query at a time. No spectral parameter must be computed in advance, no schedule must be tuned to a gap profile, and no pre-computation threatens to match the cost of the search itself.

Adiabatic quantum computation is polynomially equivalent to the circuit model [3], so a matching speedup is achievable in principle. But the adiabatic approach operates under a different constraint: the evolution Hamiltonian $H(s)$ interpolates continuously between an initial Hamiltonian $H_0$ and the problem Hamiltonian $H_z$, and the runtime is controlled by the spectral gap of $H(s)$ along the entire path. The gap structure of the interpolated Hamiltonian — where the avoided crossing occurs, how narrow it is, how fast the gap reopens — introduces obstacles that the circuit model avoids entirely. Matching the Grover speedup in this setting requires understanding and controlling these spectral features, which depend on the cost function through the full degeneracy structure of $H_z$.

The adiabatic version of Grover's algorithm, due to Roland and Cerf [4], finds a single marked item among $N = 2^n$ by slowly interpolating between a uniform superposition and a problem Hamiltonian that penalizes all unmarked items. The crossing between the two lowest energy levels occurs at $s = 1/2$, its position independent of the Hamiltonian's spectrum. The minimum spectral gap scales as $1/\sqrt{N}$, and a schedule that slows near the crossing achieves the optimal $O(\sqrt{N})$ runtime.

Consider a cost function encoded in an $n$-qubit Hamiltonian diagonal in the computational basis, with $M$ distinct energy levels, arbitrary degeneracies, and a spectral gap that may vary with the number of qubits. The ground states encode solutions to a combinatorial optimization problem. Can the adiabatic approach still match the $\Theta(\sqrt{N})$ lower bound for unstructured search [5]?

The bound applies directly to our setup: Farhi et al. proved that when $H_0$ is a rank-one projector onto the uniform superposition, no schedule can find the ground state in time $o(\sqrt{N/d_0})$, regardless of the cost function. Their proof constructs $N$ equivalent Hamiltonians related by Fourier shifts and applies a continuous-time analogue of the BBBV argument [6]. Partial answers exist: Žnidarič and Horvat [7] showed via analytical and heuristic arguments that the minimum gap scales as $\sqrt{d_0/2^n}$ for 3-SAT instances and identified the crossing position, but did not rigorously bound the runtime. Hen [8] proved a quadratic speedup for a random Hamiltonian whose energy distribution ensures a crossing position independent of the spectrum, avoiding the central difficulty.

The answer in full generality is yes. The spectrum of the interpolated Hamiltonian is far richer: instead of a two-level system plus a degenerate bulk, there are $M$ interacting energy levels in a symmetric subspace, with avoided crossings between higher excited states that obscure the gap between the two lowest. The position of the ground-state avoided crossing depends nontrivially on the degeneracy structure of the problem Hamiltonian. And the minimum gap, while still scaling as $\Theta(1/\sqrt{N})$ up to spectral factors, occurs at a position that must be known to exponential precision for the schedule to be correct.

With a general diagonal problem Hamiltonian, $H(s)$ has a single avoided crossing at position $s^* = A_1/(A_1 + 1)$, where $A_1$ is a spectral parameter determined by the degeneracy structure. The minimum spectral gap at the crossing scales as $\Theta(\sqrt{d_0/(NA_2)})$, and the gap grows linearly on both sides. Chapter 6 establishes the gap bounds outside the crossing window. The optimal runtime follows in Chapter 7. That computing $s^*$ is itself NP-hard — the subject of Chapter 8 — is what gives the result its edge.

## 5.1 The Problem

Consider an $n$-qubit Hamiltonian $H_z$ that is diagonal in the computational basis:

$$H_z = \sum_{z\in\{0,1\}^n} E_z |z\rangle\langle z|, \tag{5.1.1}$$

where $E_z$ is the energy assigned to bit-string $z$. Since $H_z$ acts diagonally, it encodes a classical cost function: the energy $E_z$ is the cost of configuration $z$, and the ground states are the optimal solutions. Without loss of generality, we rescale and shift so that all eigenvalues lie in $[0, 1]$.

Suppose $H_z$ has $M$ distinct energy levels with eigenvalues

$$0 \le E_0 < E_1 < \cdots < E_{M-1} \le 1. \tag{5.1.2}$$

For each level $k$, the set of bit-strings at that energy is

$$\Omega_k = \{z \in \{0,1\}^n : H_z |z\rangle = E_k |z\rangle\}, \tag{5.1.3}$$

with degeneracy $d_k = |\Omega_k|$. The degeneracies partition the full Hilbert space: $\sum_{k=0}^{M-1} d_k = 2^n = N$. The spectral gap of the problem Hamiltonian is $\Delta = E_1 - E_0$, the energy difference between the ground state and the first excited level.

NP-hard optimization problems — MaxCut, QUBO — encode directly as ground states of the 2-local Ising Hamiltonian [9, 10]:

$$H_\sigma = \sum_{\langle i,j\rangle} J_{ij}\sigma_z^i\sigma_z^j + \sum_{j=1}^{n} h_j\sigma_z^j, \tag{5.1.4}$$

where $J_{ij}, h_j \in \{-m, -m+1, \ldots, m\}$ for some constant positive integer $m$. Since each eigenvalue is an integer linear combination of at most $\binom{n}{2} + n$ couplings bounded by $m$, the eigenvalues lie in $\{-L, -L+1, \ldots, L\}$ for $L = O(mn^2)$, giving at most $2L+1 \in \text{poly}(n)$ distinct energy levels. After normalization to unit operator norm, consecutive eigenvalues differ by at least $1/(2L) \ge 1/\text{poly}(n)$, so the spectral gap satisfies $\Delta \ge 1/\text{poly}(n)$.

Unstructured search fits this framework: $M = 2$ energy levels, a single ground state ($d_0 = 1$) with energy $E_0 = 0$, and $N - 1$ excited states ($d_1 = N - 1$) at energy $E_1 = 1$. The ground state is the "marked item." Classical search requires $\Theta(N)$ queries; Grover's circuit algorithm requires $\Theta(\sqrt{N})$ [1, 6].

The adiabatic Hamiltonian interpolates between a rank-one projector and $H_z$. The initial Hamiltonian is

$$H_0 = -|\psi_0\rangle\langle\psi_0|, \qquad |\psi_0\rangle = |+\rangle^{\otimes n} = \frac{1}{\sqrt{N}}\sum_{z\in\{0,1\}^n}|z\rangle. \tag{5.1.5}$$

Every computational basis state receives equal amplitude, so $|\psi_0\rangle$ introduces no bias toward any particular solution.

The adiabatic Hamiltonian is the linear interpolation

$$H(s) = -(1-s)|\psi_0\rangle\langle\psi_0| + sH_z, \qquad s \in [0,1]. \tag{5.1.6}$$

At $s = 0$, the ground state is $|\psi_0\rangle$ with energy $-1$, and all other states have energy 0. At $s = 1$, the Hamiltonian is $H_z$ itself, and its ground states encode the solutions. The adiabatic theorem guarantees that if the schedule $s(t)$ traverses $[0, 1]$ slowly enough, the evolved state remains close to the instantaneous ground state throughout, arriving at the end in a state with high overlap with the ground space of $H_z$.

A rank-one $H_0$ produces exactly one avoided crossing between the two lowest energy levels. That single crossing is the structural reason the spectral analysis in Chapters 5–7 is possible at all. At $s = 0$, the spectrum has a non-degenerate ground state at $-1$ and an $(N-1)$-fold degenerate level at 0. As $s$ increases, the degeneracy splits according to $H_z$. But because $H_0 = -|\psi_0\rangle\langle\psi_0|$ has rank one, all coupling between eigenstates of $sH_z$ factors through $|\psi_0\rangle$: the matrix element $\langle k| H_0 |j\rangle = -\sqrt{d_k d_j}/N$ is nonzero for all pairs, yet the perturbation has only one degree of freedom, so eigenvalues repel through a single channel. Generic AQC Hamiltonians may exhibit multiple crossings requiring qualitatively different techniques [11, 12]. Here, there is one.

The standard alternative to the rank-one projector is the transverse-field driver $H_0 = -\sum_{j=1}^{n}\sigma_x^j$, which is the default in quantum annealing hardware and in much of the AQC literature [11]. It couples every pair of computational basis states that differ in a single qubit, producing a dense web of avoided crossings throughout the interpolation. For random instances of NP-complete problems, Altshuler, Krovi, and Roland [13] showed that the resulting spectrum exhibits Anderson localization: exponentially many avoided crossings with exponentially small gaps, a regime where no known analytical technique yields tight gap bounds. The rank-one projector avoids this entirely. Because $|\psi_0\rangle\langle\psi_0|$ has a single non-zero eigenvalue, all coupling between eigenstates of $sH_z$ flows through one channel, producing one crossing that can be analyzed exactly. The tractability of Chapters 5–7 is a direct consequence of this choice. Whether comparable results can be obtained for the transverse-field driver remains open; the Discussion of [14] identifies this as a central challenge.

In the unstructured case, $H(s) = -(1-s)|\psi_0\rangle\langle\psi_0| + s(I - |w\rangle\langle w|)$, where $|w\rangle$ is the marked item. Up to a global energy shift of $s$, this is the Roland-Cerf Hamiltonian [4]. The spectrum has $N-2$ states at energy $s$ (degenerate, orthogonal to both $|\psi_0\rangle$ and $|w\rangle$) and two states whose energies depend on $s$ and undergo an avoided crossing near $s = 1/2$.

## 5.2 Spectral Parameters

In the Roland-Cerf setting, the crossing position ($s^* = 1/2$), its width, and the minimum gap are all determined by a single quantity: $N$. For a general problem Hamiltonian $H_z$ with $M$ energy levels and arbitrary degeneracies, no single number suffices. The crossing position depends on the full eigenvalue structure of $H_z$ — not just $E_0$ and $E_1$, but all $M$ levels and their degeneracies. We need quantities that distill this $M$-dimensional information into numbers that directly control the algorithm's behavior: where the crossing occurs, how sharp the gap minimum is, and how fast the gap reopens. The relevant information is captured by a family of spectral parameters that aggregate the degeneracy structure weighted by inverse energy gaps.

**Definition 5.2.1** (Spectral parameters)**.** *For the problem Hamiltonian $H_z$ with eigenvalues $E_0 < E_1 < \cdots < E_{M-1}$ and degeneracies $d_k$, define*

$$A_p = \frac{1}{N}\sum_{k=1}^{M-1}\frac{d_k}{(E_k - E_0)^p}, \qquad p \in \mathbb{N}. \tag{5.2.1}$$

Each excited level contributes its degeneracy $d_k$ weighted by the inverse $p$-th power of its distance to the ground energy. Higher values of $p$ emphasize levels closer to the ground state: $A_1$ weights each level by $1/(E_k - E_0)$, giving most influence to levels just above the ground energy, while $A_2$ weights by $1/(E_k - E_0)^2$, amplifying this emphasis so that a level at energy $E_0 + \varepsilon$ contributes $O(1/\varepsilon^2)$ to $A_2$ but only $O(1/\varepsilon)$ to $A_1$. $A_1$ controls where the crossing occurs; $A_2$ controls how sharp the crossing is. The normalization by $N = 2^n$ makes $A_p$ an average over the full Hilbert space.

When $M = 2$, $d_0 = 1$, $d_1 = N-1$, $E_0 = 0$, $E_1 = 1$:

$$A_p = \frac{N-1}{N} \approx 1 \quad \text{for all } p, \tag{5.2.2}$$

since $E_1 - E_0 = 1$. The spectral parameters are trivial in this case, which is precisely why the Roland-Cerf analysis is simple.

For a general Ising Hamiltonian with $\Delta \geq 1/\mathrm{poly}(n)$ and $M \in \mathrm{poly}(n)$, the bound $A_1 \leq (1 - d_0/N)/\Delta$ gives $A_1 = O(\mathrm{poly}(n))$, while $A_2 \geq 1 - d_0/N$ ensures $A_2 = \Theta(1)$ at minimum.

$A_1$ determines the crossing position: $s^* = A_1/(A_1+1)$. The parameter $A_2$ enters the minimum spectral gap: $g_{\min} = \Theta(\sqrt{d_0/(NA_2)})$. The gap scales as $\sqrt{d_0/N}$: more ground states strengthen the coupling and widen the crossing. Both parameters appear in the runtime: $T = O((\sqrt{A_2}/(A_1(A_1+1)\Delta^2))\sqrt{N/d_0})$.

Since every eigenvalue gap satisfies $E_k - E_0 \leq 1$ and the total excited degeneracy is $\sum_{k\geq 1} d_k = N - d_0$, we have

$$A_2 \geq \frac{1}{N}\sum_{k=1}^{M-1} d_k = 1 - \frac{d_0}{N}. \tag{5.2.3}$$

For $d_0 \ll N$ (few solutions), $A_2 \geq 1 - 1/N$ is close to 1. Also, $A_1 \leq (1 - d_0/N)/\Delta$, since $(E_k - E_0)^{-1} \leq \Delta^{-1}$ for all $k \geq 1$. Since $E_k - E_0 \geq \Delta$ for all $k \geq 1$, termwise comparison gives $A_1 \geq A_2\Delta$. Since $E_k - E_0 \leq 1$, we also have $A_1 \leq A_2$. Together: $A_2\Delta \leq A_1 \leq A_2$.

The two-level approximation near the crossing is accurate only when the crossing window $\delta_s = O(\sqrt{d_0 A_2/N})$ is narrow compared to $[0, 1]$. Since $\delta_s/s^* = O((1/\Delta)\sqrt{d_0/(A_2 N)})$, this requires the spectral parameters to be polynomially bounded relative to $N$.

**Definition 5.2.2** (Spectral condition)**.** *The problem Hamiltonian $H_z$ satisfies the spectral condition if there exists a constant $c \ll 1$ such that*

$$\frac{1}{\Delta}\sqrt{\frac{d_0}{A_2 N}} < c. \tag{5.2.4}$$

The quantity on the left is the ratio of the crossing width parameter to the spectral gap, up to constant factors. When it is small, the two-level approximation near the crossing is accurate (the higher levels do not interfere), and the crossing window occupies a negligible fraction of $[0, 1]$. The appendix of [14] shows that $c \approx 0.02$ suffices. When the condition fails, the crossing window is no longer narrow, higher energy levels interfere with the two-level dynamics, and the gap bounds of this chapter no longer apply. The failure reflects a change in spectral structure: the eigenvalue equation still holds, but the truncation to a quadratic in $\delta$ (Eq. (5.4.3)) requires $|\delta| \ll s\Delta$, which fails when many excited levels crowd near the ground energy. The multi-crossing regime discussed above — exemplified by the transverse-field driver on random NP-complete instances [13] — is precisely the setting where the spectral condition breaks down. The condition therefore marks a boundary between the single-crossing regime, where the framework of Chapters 5–7 applies and the Grover speedup is achievable, and the multi-crossing regime, where the spectral landscape is currently intractable [12].

For any $H_z$ with $\Delta > (1/c)\sqrt{d_0/N}$, the condition holds, using $A_2 \geq 1 - d_0/N$. For the Ising Hamiltonian with $\Delta \geq 1/\text{poly}(n)$ and $d_0$ not scaling with $N$, the left side is exponentially small in $n$, so the condition is easily satisfied. With $\Delta = 1$ and $d_0 = 1$ (unstructured search), the left side is $1/\sqrt{N}$, well below any constant $c$ for $N \geq 2$.

## 5.3 Symmetry Reduction

The Hilbert space of $H(s)$ has dimension $N = 2^n$, exponentially large in the number of qubits. Direct spectral analysis is intractable. But the problem Hamiltonian $H_z$ has only $M$ distinct energy levels, and the initial state $|\psi_0\rangle$ treats all bit-strings at the same energy identically. This permutation symmetry within each degenerate subspace reduces the eigenvalue problem from $N$ dimensions to $M$.

For each energy level $k$, define the symmetric state

$$|k\rangle = \frac{1}{\sqrt{d_k}} \sum_{z \in \Omega_k} |z\rangle\,, \qquad 0 \leq k \leq M-1. \tag{5.3.1}$$

These $M$ states are orthonormal: $\langle j\rangle\, k = \delta_{jk}$. They span the $M$-dimensional symmetric subspace

$$\mathcal{H}_S = \text{span}\left\{|k\rangle : 0 \leq k \leq M-1\right\}. \tag{5.3.2}$$

In this basis, the problem Hamiltonian has $M$ non-degenerate eigenvalues:

$$H_z = \sum_{k=0}^{M-1} E_k \,|k\rangle\langle k| \quad \text{on } \mathcal{H}_S, \tag{5.3.3}$$

and the initial state decomposes as

$$|\psi_0\rangle = \sum_{k=0}^{M-1} \sqrt{\frac{d_k}{N}}\,|k\rangle\,. \tag{5.3.4}$$

Since $|\psi_0\rangle \in \mathcal{H}_S$ and both $H_z$ and $|\psi_0\rangle\langle\psi_0|$ map $\mathcal{H}_S$ to itself, the adiabatic Hamiltonian $H(s)$ leaves $\mathcal{H}_S$ invariant. The time evolution starting from $|\psi_0\rangle$ remains in $\mathcal{H}_S$ for all $s$.

The complement $\mathcal{H}_S^\perp$ has dimension $N-M$ and is spanned by states orthogonal to $|\psi_0\rangle$ within each degenerate subspace. For each level $k$, order the bit-strings in $\Omega_k$ as $z_k^{(1)}, \ldots, z_k^{(d_k)}$ and define the Fourier basis

$$|k^{(\ell)}\rangle = \frac{1}{\sqrt{d_k}} \sum_{\ell'=1}^{d_k} \exp\left[\frac{i2\pi\ell\ell'}{d_k}\right] |z_k^{(\ell')}\rangle\,, \qquad 1 \leq \ell \leq d_k - 1. \tag{5.3.5}$$

Note that $|k^{(0)}\rangle = |k\rangle$ is the symmetric state already in $\mathcal{H}_S$. The remaining $d_k - 1$ states for each level $k$ form a basis for $\mathcal{H}_S^\perp$:

$$\mathcal{H}_S^\perp = \text{span}\left\{|k^{(\ell)}\rangle : 0 \leq k \leq M-1,\ 1 \leq \ell \leq d_k - 1\right\}. \tag{5.3.6}$$

Each $|k^{(\ell)}\rangle$ is an eigenstate of $H(s)$ with eigenvalue $sE_k$:

$$H(s)\,|k^{(\ell)}\rangle = -(1-s)\,|\psi_0\rangle \underbrace{\langle\psi_0\rangle\, k^{(\ell)}}_{=0} + sE_k\,|k^{(\ell)}\rangle = sE_k\,|k^{(\ell)}\rangle\,. \tag{5.3.7}$$

The inner product vanishes because $|k^{(\ell)}\rangle$ is orthogonal to $|k\rangle = |k^{(0)}\rangle$ by construction, and $|\psi_0\rangle$ is a linear combination of the $|k\rangle$ states. Of $2^n$ dimensions in the full Hilbert space, only $M$ participate in the adiabatic evolution. The remaining $N - M$ eigenstates are spectators: exact eigenstates with trivially known eigenvalues $sE_k$, invisible to the initial state. For the Ising Hamiltonian, $M = O(\mathrm{poly}(n))$. The entire dynamics lives in a polynomially-sized subspace of an exponentially large space.

Henceforth, $H(s)$ denotes its restriction to the symmetric subspace $\mathcal{H}_S$:

$$H(s) = -(1-s)\,|\psi_0\rangle\,\langle\psi_0| + s\sum_{k=0}^{M-1} E_k\,|k\rangle\,\langle k|\,. \tag{5.3.8}$$

This is a rank-one perturbation of the diagonal matrix $sH_z$ — the setting of the Golub eigenvalue interlacing results [15].

**Lemma 5.3.1** (Eigenvalue equation)**.** *Let $H(s)$ be the adiabatic Hamiltonian restricted to $\mathcal{H}_S$ as in Eq. (5.3.8). Then $\lambda(s)$ is an eigenvalue of $H(s)$ if and only if*

$$\frac{1}{1-s} = \frac{1}{N}\sum_{k=0}^{M-1}\frac{d_k}{sE_k - \lambda(s)}. \tag{5.3.9}$$

*Proof.* Let $|\psi\rangle = \sum_{k=0}^{M-1}\alpha_k\,|k\rangle$ be an eigenstate of $H(s)$ with eigenvalue $\lambda$, and set $\gamma = \langle\psi_0\rangle\,\psi$. Acting with $H(s)$ on $|\psi\rangle$:

$$H(s)\,|\psi\rangle = s\sum_{k=0}^{M-1}E_k\alpha_k\,|k\rangle - (1-s)\gamma\,|\psi_0\rangle = \lambda\sum_{k=0}^{M-1}\alpha_k\,|k\rangle\,. \tag{5.3.10}$$

Comparing coefficients of $|k\rangle$ and using $\langle\psi_0\rangle\,k = \sqrt{d_k/N}$ gives

$$\alpha_k = \frac{(1-s)\gamma\sqrt{d_k/N}}{sE_k - \lambda}. \tag{5.3.11}$$

Since $\gamma = \langle\psi_0\rangle\,\psi = (1/\sqrt{N})\sum_k \alpha_k\sqrt{d_k}$, substituting Eq. (5.3.11) yields

$$1 = \frac{1-s}{N}\sum_{k=0}^{M-1}\frac{d_k}{sE_k-\lambda}, \tag{5.3.12}$$

which is equivalent to Eq. (5.3.9). Each step is reversible: given a solution $\lambda$ of Eq. (5.3.9), the coefficients in Eq. (5.3.11) define an eigenstate (after normalization), provided $\gamma \neq 0$. The case $\gamma = 0$ corresponds to $\lambda = sE_k$ for some $k$, which are the eigenvalues in $\mathcal{H}_S^{\perp}$ already accounted for. □

Viewed as a function of $\lambda$, the right-hand side of Eq. (5.3.9) is a sum of $M$ terms, each decreasing with a vertical asymptote at $\lambda = sE_k$. Between consecutive poles $sE_{k-1}$ and $sE_k$, the function decreases monotonically from $+\infty$ to $-\infty$, producing exactly one root per interval. Below the lowest pole $sE_0$, there is one additional root. The total count is $M$ eigenvalues in $\mathcal{H}_S$, consistent with the dimension.

The two lowest eigenvalues are $\lambda_0(s) < sE_0$ (ground state) and $\lambda_1(s) \in (sE_0, sE_1)$ (first excited state). The spectral gap is $g(s) = \lambda_1(s) - \lambda_0(s) > 0$. However, this ordering information alone does not yield a useful quantitative upper bound on $g(s)$ uniformly over $s \in [0,1]$. Extracting tight bounds requires analyzing the eigenvalue equation in the vicinity of the crossing.

For $M = 2$, Eq. (5.3.9) becomes

$$\frac{1}{1-s} = \frac{1}{N}\cdot\frac{1}{-\lambda} + \frac{N-1}{N}\cdot\frac{1}{s-\lambda}, \tag{5.3.13}$$

where we set $E_0 = 0$ and $E_1 = 1$. Clearing denominators produces the quadratic $N\lambda^2 - N(2s-1)\lambda - s(1-s) = 0$, whose two roots give the ground and first excited energies:

$$\lambda_{\pm}(s) = \frac{2s-1}{2} \pm \frac{1}{2}\sqrt{(2s-1)^2 + \frac{4s(1-s)}{N}}. \tag{5.3.14}$$

At $s = 0$, the ground energy is $\lambda_- = -1$ and the first excited energy is $\lambda_+ = 0$, consistent with the spectrum of $H(0) = -\,|\psi_0\rangle\,\langle\psi_0|$. The gap $g(s) = \lambda_+(s) - \lambda_-(s)$ simplifies to

$$g(s) = \sqrt{(2s-1)^2 + \frac{4s(1-s)}{N}}, \tag{5.3.15}$$

which is minimized at $s = 1/2$ exactly, giving $g_{\min} = 1/\sqrt{N}$. This is the Roland-Cerf gap. The general theory of the next section reproduces this scaling as a special case.

## 5.4 The Avoided Crossing

The eigenvalue equation (Lemma 5.3.1) characterizes the spectrum of $H(s)$ implicitly, but yields explicit formulas for $s^*$, $\delta_s$, and $g_{\min}$ when analyzed near the ground-state energy. Near the crossing, the ground and first excited states behave like a two-level system, with the higher levels acting as a perturbation controlled by the spectral condition.

The two lowest eigenvalues have the form $\lambda(s) = sE_0 + \delta(s)$, where $\delta(s)$ is a correction to the trivial energy $sE_0$. Writing the eigenvalue as a perturbation of the nearest pole isolates the ground-state contribution and converts the implicit equation into an explicit power series — a standard technique for rank-one updates of diagonal eigenvalue problems [15]. Substituting into Eq. (5.3.9):

$$-\frac{d_0}{N\delta} + \frac{1}{N}\sum_{k=1}^{M-1}\frac{d_k}{s(E_k - E_0) - \delta} = \frac{1}{1-s}. \tag{5.4.1}$$

The first term has a pole at $\delta = 0$; the sum has poles at $\delta = s(E_k - E_0)$ for $k \geq 1$. When $|\delta| \ll s\Delta$ (guaranteed by the spectral condition), the sum can be expanded in powers of $\delta/(s(E_k - E_0))$:

$$\frac{1}{N}\sum_{k=1}^{M-1}\frac{d_k}{s(E_k - E_0) - \delta} = \frac{1}{s}\left(A_1 + \frac{\delta}{s}A_2 + \frac{\delta^2}{s^2}A_3 + \cdots\right). \tag{5.4.2}$$

Truncating at the $A_2$ term and rearranging Eq. (5.4.1) gives a quadratic in $\delta$ whose two roots are the corrections $\delta_0^+(s)$ and $\delta_0^-(s)$ for the first excited and ground states, respectively:

$$\delta_0^{\pm}(s) = \frac{s(A_1+1)}{2A_2(1-s)}\left[(s - s^*) \pm \sqrt{(s^* - s)^2 + \frac{4A_2 d_0}{N(A_1+1)^2}(1-s)^2}\right], \tag{5.4.3}$$

Here $\delta_0^+(s) > 0$ corresponds to the first excited state and $\delta_0^-(s) < 0$ to the ground state: the superscript indicates the sign of the correction relative to $sE_0$. The crossing position is

$$s^* = \frac{A_1}{A_1 + 1}. \tag{5.4.4}$$

The problem Hamiltonian has $M$ eigenvalues and $M$ degeneracies — $2M$ free parameters. Yet the crossing position depends on a single weighted average. That is what makes a closed-form schedule possible despite arbitrary spectral complexity. For Ising Hamiltonians with $\Delta \geq 1/\mathrm{poly}(n)$, $A_1$ is always polynomially bounded above; in the hard-search regime $d_0 \ll N$, one also has $A_1 = \Omega(1)$, so $s^*$ stays away from 0. In the limit $A_1 \to \infty$ (many levels near the ground state), $s^* \to 1$; when $A_1$ is small, $s^*$ is closer to 0.

The crossing position marks a balance in the eigenvalue equation: $A_1/s^* = 1/(1 - s^*)$, where the left side is the aggregate spectral pull of the excited levels toward $sE_0$ and the right side is the projector strength. At $s = s^*$, the linear coefficient in the quadratic for $\delta$ (Eq. (5.4.3)) vanishes, and the two roots $\delta_0^{\pm}$ are symmetric about zero. The gap is determined entirely by the constant term $d_0/N$: the ground-state degeneracy is what opens the minimum gap.

How good is the truncation? The actual roots $\delta_{\pm}(s)$ of the full equation differ from $\delta_0^{\pm}(s)$ by a relative error controlled by the spectral condition. The following result, whose proof uses the intermediate value theorem on the full equation after bounding the remainder using $A_3$ and the spectral condition, makes this precise. The technique was developed for optimal spatial search via continuous-time quantum walks [16], where the same rank-one perturbation structure arises with a graph Laplacian replacing the diagonal Hamiltonian; the adaptation to the AQO setting appears in [14].

**Lemma 5.4.1** (Validity of approximation)**.** *Let $H_z$ satisfy the spectral condition (Definition 5.2.2) with constant $c \approx 0.02$, and define*

$$\delta_s = \frac{2}{(A_1+1)^2}\sqrt{\frac{d_0 A_2}{N}}. \tag{5.4.5}$$

*Then for any $s \in \mathcal{I}_{s^*} = [s^* - \delta_s,\ s^* + \delta_s]$, there exists a constant $\eta \ll 1$ such that the two lowest eigenvalues of $H(s)$ satisfy*

$$\delta_+(s) \in \left((1-\eta)\,\delta_0^+(s),\ (1+\eta)\,\delta_0^+(s)\right), \tag{5.4.6}$$

$$\delta_-(s) \in \left((1+\eta)\,\delta_0^-(s),\ (1-\eta)\,\delta_0^-(s)\right), \tag{5.4.7}$$

*where $\delta_0^{\pm}(s)$ are given by Eq. (5.4.3).*

The proof evaluates the full equation (5.4.1) at $\delta_0^{\pm}(1 \pm \eta)$ and shows, using the spectral condition to bound the truncated Taylor remainder, that the full equation changes sign between these points. The intermediate value theorem then guarantees a root in the interval. The spectral condition enters through the bound $|\delta_0^{\pm}(s)|/(s\Delta) \leq \kappa c < 1$, where $\kappa$ is a constant depending on $c$, ensuring the geometric series in the Taylor expansion converges. The constant $c \approx 0.02$ is sufficient for $\eta \leq 0.1$. The complete calculation appears in the appendix of [14].

Since both corrections are approximated to within $1 \pm \eta$, the spectral gap $g(s) = \delta_+(s) - \delta_-(s)$ is within a factor of $1 \pm 2\eta$ of $\delta_0^+(s) - \delta_0^-(s)$, which evaluates to

$$g(s) = (1 \pm 2\eta) \cdot \frac{s(A_1+1)}{A_2(1-s)} \sqrt{(s^* - s)^2 + \frac{4A_2 d_0}{N(A_1+1)^2}(1-s)^2}. \tag{5.4.8}$$

At $s = s^*$, the first term under the square root vanishes, leaving only the second:

$$g_{\min} = g(s^*) \geq (1 - 2\eta) \cdot \frac{2A_1}{A_1+1} \sqrt{\frac{d_0}{NA_2}}. \tag{5.4.9}$$

The gap scales as $\sqrt{d_0/N}$ with corrections from the spectral structure. The factor $2A_1/(A_1+1)$ captures the position of the crossing: a crossing near the boundary ($s^* \to 0$ or $s^* \to 1$) reduces the gap. The factor $\sqrt{d_0/N}$ is the Grover-like contribution: more solutions (larger $d_0$) increase the gap and reduce the runtime. The factor $1/\sqrt{A_2}$ encodes the spectral structure beyond the simplest two-level case.

An exact algebraic identity connects $s^*$, $\delta_s$, and the leading-order minimum gap. Writing $\hat{g} = \frac{2A_1}{A_1+1}\sqrt{\frac{d_0}{NA_2}}$ for the leading-order expression, direct substitution gives

$$\frac{s^*(A_1+1)^2}{A_2} \cdot \delta_s = \hat{g}, \tag{5.4.10}$$

and by Eq. (5.4.9), $g_{\min} \geq (1 - 2\eta)\hat{g}$. This relation will be used in Chapter 7 to verify the runtime calculation.

Three regions partition $[0, 1]$ based on the crossing:

$$\mathcal{I}_{s^{\leftarrow}} = [0,\, s^* - \delta_s), \qquad \mathcal{I}_{s^*} = [s^* - \delta_s,\, s^* + \delta_s], \qquad \mathcal{I}_{s^{\rightarrow}} = (s^* + \delta_s,\, 1]. \tag{5.4.11}$$

**Lemma 5.4.2** (Gap within the crossing window). *Let $H_z$ satisfy the spectral condition with constant $c$, and define*

$$\kappa' = \frac{(1+2\eta)(1+2c)}{(1-2\eta)(1-2c)} \sqrt{1 + (1-2c)^2}. \tag{5.4.12}$$

*Then for any $s \in \mathcal{I}_{s^*}$,*

$$g_{\min} \leq g(s) \leq \kappa' \cdot g_{\min}. \tag{5.4.13}$$

*Proof.* The lower bound is immediate from the definition of $g_{\min}$ as the minimum over $\mathcal{I}_{s^*}$. For the upper bound, start from Eq. (5.4.8) with $|s - s^*| \leq \delta_s$:

$$g(s) \leq \frac{s(A_1+1)}{A_2(1-s)} \sqrt{\delta_s^2 + \frac{4A_2 d_0}{N(A_1+1)^2}(1-s)^2}. \tag{5.4.14}$$

Factoring out $(A_1+1)\delta_s(1-s)$ under the square root and using $s/s^* \leq 1 + \delta_s/s^*$:

$$g(s) \leq \frac{s^*(A_1+1)^2}{A_2}\delta_s \cdot \frac{s}{s^*} \cdot \sqrt{\frac{1}{(1-s)^2(A_1+1)^2} + 1}. \tag{5.4.15}$$

The first factor equals $\hat{g}$ by Eq. (5.4.10). The spectral condition gives $\delta_s/(1-s^*) \leq 2c$ and $\delta_s/s^* \leq 2c$. To see the first, compute

$$\frac{\delta_s}{1-s^*} = \frac{2}{1+A_1}\sqrt{\frac{d_0 A_2}{N}} = \frac{2A_2\Delta}{1+A_1} \cdot \frac{1}{\Delta}\sqrt{\frac{d_0}{A_2 N}} \leq 2s^* c \leq 2c, \tag{5.4.16}$$

where we used $A_2\Delta/(1+A_1) \leq A_1/(1+A_1) = s^*$. The bound $\delta_s/s^* \leq 2c$ follows similarly. Substituting into the upper bound:

$$g(s) \leq (1+2\eta)\hat{g} \cdot (1+2c)\sqrt{1+(1-2c)^2} \leq \kappa' \cdot g_{\min}, \tag{5.4.17}$$

where the factor $(1 + 2\eta)$ comes from the upper approximation in Eq. (5.4.8), and the last step uses $\hat{g} \leq g_{\min}/(1 - 2\eta)$. □

Inside $\mathcal{I}_{s^*}$, the gap is $\Theta(g_{\min})$; outside, it is strictly larger, as the next section establishes. The avoided crossing is localized.

Specializing to unstructured search, with $A_1 = A_2 = (N-1)/N$:

$$s^* = \frac{(N-1)/N}{(N-1)/N+1} = \frac{N-1}{2N-1} \approx \frac{1}{2}, \tag{5.4.18}$$

$$g_{\min} = \frac{2(N-1)/(2N-1)}{\sqrt{N\cdot(N-1)/N}} = \frac{2(N-1)}{(2N-1)\sqrt{N-1}} \approx \frac{1}{\sqrt{N}}, \tag{5.4.19}$$

$$\delta_s = \frac{2N^2}{(2N-1)^2}\sqrt{\frac{N-1}{N^2}} \approx \frac{1}{2\sqrt{N}}. \tag{5.4.20}$$

The crossing is at $s^* \approx 1/2$, the minimum gap scales as $1/\sqrt{N}$, and the window width scales as $1/\sqrt{N}$. These agree asymptotically with the exact quadratic solution in Eq. (5.3.15), confirming the general theory reproduces the known scaling. The small discrepancy between $s^* = (N-1)/(2N-1)$ and the exact minimum at $s = 1/2$ is a higher-order effect of the two-level truncation, vanishing as $O(1/N)$.

## 5.5 Gap Structure

The adiabatic schedule requires the gap everywhere, not just near the crossing. The local adaptive schedule speeds up where the gap is large and slows where it is small, so the runtime depends on the gap profile across the full interval $[0,1]$. Inside $\mathcal{I}_{s^*}$, the gap is $\Theta(g_{\min})$. Outside it, the gap grows linearly — but proving this requires different techniques for the two sides.

**Lemma 5.5.1** (Gap to the left of the crossing)**.** *For any $s \in \mathcal{I}_{s^\leftarrow} = [0,\, s^* - \delta_s)$, the spectral gap of $H(s)$ satisfies*

$$g(s) \geq \frac{A_1(A_1+1)}{A_2}(s^* - s). \tag{5.5.1}$$

Why does this hold? The variational principle bounds the ground energy from above: an explicit ansatz $|\phi\rangle$ gives $\lambda_0(s) \leq \langle\phi| H(s) |\phi\rangle$, while the eigenvalue equation gives $\lambda_1(s) \geq sE_0$ from below. The ansatz is

$$|\phi\rangle = \frac{1}{\sqrt{A_2 N}} \sum_{k=1}^{M-1} \frac{\sqrt{d_k}}{E_k - E_0} |k\rangle, \tag{5.5.2}$$

which concentrates amplitude on levels close to the ground energy, yielding a tight upper bound on $\lambda_0(s)$. A second route uses concavity: since $\lambda_0(s) = \min_{|\psi\rangle} \langle\psi| H(s) |\psi\rangle$ is the pointwise minimum of functions linear in $s$, it is concave. The tangent to a concave function lies above it, so the tangent to $\lambda_0$ at $s^*$ gives a linear upper bound that, combined with $\lambda_1(s) \geq sE_0$, reproduces Eq. (5.5.1). Chapter 6 develops both approaches.

**Lemma 5.5.2** (Gap to the right of the crossing)**.** *Assume $A_1 \geq 1/2$ (equivalently $s^* \geq 1/3$). Let $k = 1/4$, $a = 4k^2\Delta/3$, and*

$$s_0 = s^* - \frac{k\, g_{\min}(1-s^*)}{a - k\, g_{\min}}. \tag{5.5.3}$$

*Then for all $s \geq s^*$, the spectral gap of $H(s)$ satisfies*

$$g(s) \geq \frac{\Delta}{30} \cdot \frac{s - s_0}{1 - s_0}. \tag{5.5.4}$$

This bound is linear in $s - s_0$, with slope proportional to $\Delta$. The idea, developed in Chapter 6, is different from the left bound: place a line $\gamma(s) = sE_0 + \beta(s)$ between the two lowest eigenvalues and use the Sherman-Morrison formula [17] to bound the resolvent norm $\|R_{H(s)}(\gamma)\|$, giving $g(s) \geq 2/\|R_{H(s)}(\gamma)\|$. The constants $k = 1/4$ and $a = 4k^2\Delta/3$ are tuned to make the resulting function $f(s)$ monotonically decreasing on $[s^*, 1]$, yielding the clean bound $\Delta/30$.

At the window boundary, both bounds match $g_{\min}$ in order. At $s = s^* - \delta_s$, the left bound gives

$$g(s^* - \delta_s) \geq \frac{A_1(A_1+1)}{A_2} \cdot \delta_s = \frac{2A_1}{A_1+1}\sqrt{\frac{d_0}{NA_2}} = \hat{g}, \tag{5.5.5}$$

which satisfies $\hat{g} = \Theta(g_{\min})$ by Eq. (5.4.9). At $s = s^*$ (right boundary start), $\beta(s^*) \geq k\, g_{\min}$, so $g(s^*) \geq 2k\, g_{\min}/(1 + f(s^*)) = O(g_{\min})$ since $f(s^*) = \Theta(1)$. The gap profile is therefore continuous across region boundaries: it dips to $g_{\min}$ at $s^*$ and rises linearly on both sides.

With the gap profile in hand, the runtime follows from the optimal local adaptive schedule [18, 4], which has $ds/dt \propto g(s)^2$: the evolution slows quadratically as the gap decreases. The total runtime is

$$T \propto \int_0^1 \frac{ds}{g(s)^2}, \tag{5.5.6}$$

split across the three regions. In the left and right regions, linear gap growth makes $1/g(s)^2 \propto 1/(s-s^*)^2$, giving logarithmic contributions. Inside the window, the gap is approximately constant at $g_{\min}$, and the contribution is $2\delta_s/g_{\min}^2$. The window dominates everything else. The algorithm's bottleneck is a $\Theta(1/\sqrt{N})$-wide interval around $s^*$:

$$\frac{\delta_s}{g_{\min}^2} \propto \frac{\sqrt{A_2}}{A_1(A_1+1)\Delta^2}\sqrt{\frac{N}{d_0}}, \tag{5.5.7}$$

yielding the optimal runtime [14]. For the Ising Hamiltonian with $A_1, A_2 = O(\mathrm{poly}(n))$ and $\Delta \geq 1/\mathrm{poly}(n)$, this gives $T = \widetilde{O}(\sqrt{N/d_0})$, matching the Grover lower bound up to polylogarithmic factors. Chapter 7 carries out this calculation rigorously.

## 5.6 The Central Questions

What remains is to close the argument: prove the gap bounds outside the window (Chapter 6), derive the optimal runtime (Chapter 7), and confront the hardness of the pre-computation (Chapter 8).

Given the complete gap profile, the optimal runtime is

$$T = O\left(\frac{1}{\varepsilon} \cdot \frac{\sqrt{A_2}}{A_1(A_1+1)\Delta^2} \cdot \sqrt{\frac{N}{d_0}}\right), \tag{5.6.1}$$

where $\varepsilon$ is the target error. For Ising Hamiltonians, this is $\widetilde{O}(\sqrt{N/d_0})$, matching the lower bound of Farhi, Goldstone, and Gutmann [5]. Adiabatic quantum optimization achieves the Grover speedup. Chapter 7 derives this rigorously.

The local adaptive schedule requires knowing $s^*$ to precision $O(\delta_s) = O(2^{-n/2})$, which requires knowing $A_1$ to comparable precision. Approximating $A_1$ to additive accuracy $1/\mathrm{poly}(n)$ is NP-hard: two queries to such an oracle suffice to solve 3-SAT. Computing $A_1$ exactly, or to accuracy $O(2^{-\mathrm{poly}(n)})$, is #P-hard: polynomial interpolation extracts all degeneracies $d_k$ from $O(\mathrm{poly}(n))$ exact queries. There is an exponential gap between the precision needed ($O(2^{-n/2})$) and the precision at which the problem is already NP-hard ($1/\mathrm{poly}(n)$). Chapter 8 proves both results.

In the circuit model, Grover's algorithm achieves $\widetilde{O}(\sqrt{N/d_0})$ without pre-computing any spectral parameter: the oracle queries gather the needed information adaptively during execution. The adiabatic framework requires the schedule to be fixed before the evolution begins, necessitating the NP-hard pre-computation. This asymmetry is not an artifact of the analysis but a genuine difference between the two computational models. This is optimality with limitations: the adiabatic speedup exists but is contingent on solving a hard problem first [14]. Chapter 9 characterizes this information-runtime tradeoff precisely, proving a separation theorem for uninformed schedules, a smooth interpolation for partial information, and an adaptive measurement protocol that circumvents the classical hardness.

In the unstructured case, the limitation vanishes: $A_1 = (N-1)/N \approx 1$ is trivially known, so $s^* \approx 1/2$ requires no hard computation. The complexity arises only for problem Hamiltonians with rich spectral structure, where the degeneracies $d_k$ and energy gaps $E_k - E_0$ are not known in advance. The Ising Hamiltonian encoding an NP-hard problem is precisely such a case.

# Chapter 6

# Spectral Analysis

Chapter 5 established the crossing window $\mathcal{I}_{s^*}$ where the spectral gap satisfies $g(s) = \Theta(g_{\min})$, and stated two bounds for the regions outside: a linear lower bound to the left (Lemma 5.5.1) and a linear lower bound to the right (Lemma 5.5.2). This chapter proves both lemmas.

The two proofs use different techniques, reflecting different spectral structures on each side of the crossing. To the left of $s^*$, the ground energy $\lambda_0(s)$ sits below $sE_0$ while the first excited energy $\lambda_1(s)$ sits above it. The variational principle bounds how far below $sE_0$ the ground energy can be, yielding a linear gap bound. To the right of $s^*$, the eigenvalues of $sH_z$ crowd the interval $[sE_0, sE_1]$, and the variational approach no longer applies. Instead, a resolvent identity combined with the Sherman-Morrison formula for rank-one perturbations tracks the gap through this congested region. The resulting piecewise linear profile — steep on the left, shallower on the right, flat in the window — feeds directly into the runtime calculation of Chapter 7.

## 6.1 Gap to the Left of the Crossing

The eigenvalue equation (Lemma 5.3.1) places the ground state energy at $\lambda_0(s) < sE_0$ and the first excited energy at $\lambda_1(s) \in (sE_0, sE_1)$. The gap $g(s) = \lambda_1(s) - \lambda_0(s)$ is therefore positive, but this ordering alone does not provide a useful quantitative bound for the runtime integral. We need a tight lower bound that captures the linear growth of the gap as $s$ decreases away from $s^*$.

The strategy is to tighten the upper bound on $\lambda_0(s)$. Two approaches give the same result. The first uses the variational principle: for any normalized state $|\phi\rangle$, the ground energy satisfies $\lambda_0(s) \leq \langle\phi| H(s) |\phi\rangle$, so a well-chosen ansatz produces a quantitative upper bound. The second uses concavity: since $\lambda_0(s) = \min_{|\psi\rangle} \langle\psi| H(s) |\psi\rangle$ is the pointwise minimum of affine functions in $s$, it is concave, and any tangent line lies above it. The variational approach is more direct — it produces the bound in a single calculation — so we present it here.

**Lemma 6.1.1** (Gap to the left of the crossing)**.** *For any $s \in \mathcal{I}_{s^\leftarrow} = [0,\, s^* - \delta_s)$, the spectral gap of $H(s)$ satisfies*

$$g(s) \geq \frac{A_1(A_1+1)}{A_2}\,(s^* - s)\,. \tag{6.1.1}$$

*Proof.* We upper-bound $\lambda_0(s)$ via the variational principle and lower-bound $\lambda_1(s)$ from the eigenvalue equation.

The ansatz must live in the span of $\{|k\rangle : k \geq 1\}$, orthogonal to the ground-state component $|0\rangle$, and should concentrate amplitude on levels close to $E_0$ where the energy expectation is lowest. The natural weighting is the inverse energy gap: levels near $E_0$ receive more amplitude. Requiring unit norm fixes the overall scale, giving

$$|\phi\rangle = \frac{1}{\sqrt{A_2 N}} \sum_{k=1}^{M-1} \frac{\sqrt{d_k}}{E_k - E_0}\,|k\rangle\,. \tag{6.1.2}$$

This weighting arises naturally in first-order perturbation theory: the correction to the ground state $|E_0\rangle$ of $sH_z$ due to the perturbation $-(1-s)\,|\psi_0\rangle\langle\psi_0|$ has coefficients proportional to $\langle E_k\rangle\,\psi_0/(E_k - E_0) = \sqrt{d_k/N}/(E_k - E_0)$, which is exactly the form above up to normalization. Normalization is immediate:

$$\langle\phi\rangle\,\phi = \frac{1}{A_2 N} \sum_{k=1}^{M-1} \frac{d_k}{(E_k - E_0)^2} = \frac{A_2}{A_2} = 1. \tag{6.1.3}$$

To compute $\langle\phi| H(s) |\phi\rangle$, decompose $H(s) = -(1-s)|\psi_0\rangle\langle\psi_0| + s(H_z - E_0) + sE_0$. Each term contributes separately.

The projector term gives

$$-(1-s)|\langle\psi_0\rangle\,\phi|^2 = -(1-s)\left(\frac{1}{\sqrt{A_2 N}}\sum_{k=1}^{M-1}\frac{d_k}{(E_k - E_0)\sqrt{N}}\right)^2 = -(1-s)\frac{A_1^2}{A_2}, \tag{6.1.4}$$

where $\langle\psi_0\rangle\,\phi = A_1/\sqrt{A_2}$ follows from $\langle\psi_0\rangle\,k = \sqrt{d_k/N}$ and the definition of $A_1$.

The shifted diagonal term gives

$$s\langle\phi|(H_z - E_0)|\phi\rangle = \frac{s}{A_2 N}\sum_{k=1}^{M-1}\frac{d_k}{(E_k - E_0)^2}\cdot(E_k - E_0) = \frac{s}{A_2 N}\sum_{k=1}^{M-1}\frac{d_k}{E_k - E_0} = \frac{s\,A_1}{A_2}. \tag{6.1.5}$$

The constant term contributes $sE_0\langle\phi\rangle\,\phi = sE_0$. Combining:

$$\lambda_0(s) \le \langle\phi| H(s) |\phi\rangle = sE_0 - (1-s)\frac{A_1^2}{A_2} + s\frac{A_1}{A_2} = sE_0 + \frac{A_1}{A_2}\left(s(1+A_1) - A_1\right). \tag{6.1.6}$$

Since $s^*(1 + A_1) = A_1$, we have $s(1 + A_1) - A_1 = (1 + A_1)(s - s^*) = (s - s^*)/(1 - s^*)$, so

$$\lambda_0(s) \le sE_0 + \frac{A_1}{A_2}\cdot\frac{s - s^*}{1 - s^*}. \tag{6.1.7}$$

For $s < s^*$, the second term is negative, confirming $\lambda_0(s) < sE_0$.

For the first excited state, the eigenvalue equation (Lemma 5.3.1) confines $\lambda_1(s)$ to the interval $(sE_0, sE_1)$, so

$$\lambda_1(s) \ge sE_0. \tag{6.1.8}$$

The gap is therefore

$$g(s) = \lambda_1(s) - \lambda_0(s) \ge sE_0 - sE_0 - \frac{A_1}{A_2}\cdot\frac{s - s^*}{1 - s^*} = \frac{A_1}{A_2}\cdot\frac{s^* - s}{1 - s^*}. \tag{6.1.9}$$

Since $1/(1 - s^*) = A_1 + 1$, we obtain $g(s) \ge A_1(A_1 + 1)(s^* - s)/A_2$. □

At the left boundary of the crossing window, $s = s^* - \delta_s$, the bound gives

$$g(s^* - \delta_s) \ge \frac{A_1(A_1 + 1)}{A_2}\cdot\delta_s = \hat{g}, \tag{6.1.10}$$

using $A_1(A_1 + 1)\delta_s/A_2 = \hat{g}$ from Eq. (5.4.10). Since $g_{\min} = (1 \pm O(\eta))\hat{g}$ from Eq. (5.4.9), the gap at the window boundary is $\Theta(g_{\min})$, so the three-region decomposition is tight: the left bound meets the window bound at the boundary rather than leaving a gap between them.

An alternative derivation uses concavity. Since $\lambda_0(s) = \min_{|\psi\rangle}\langle\psi| H(s) |\psi\rangle$ is the pointwise minimum of affine functions in $s$, it is concave. The Hellmann-Feynman theorem [19] gives the second derivative explicitly:

$$\ddot{\lambda}_0(s) = -2\sum_{j\ge 1}\frac{|\langle\phi_j(s)|\dot{H}|\phi_0(s)\rangle|^2}{\lambda_j(s) - \lambda_0(s)} \le 0,$$

where $\dot{H} = H_z + |\psi_0\rangle\langle\psi_0|$ and $|\phi_j(s)\rangle$ are the instantaneous eigenstates. Concavity implies any tangent lies above the function: the tangent to $\lambda_0$ at $s^*$ gives $\lambda_0(s) \le \lambda_0(s^*) + \lambda_0'(s^*)(s - s^*)$, an upper bound of the same form as (6.1.7), though the variational approach gives slightly sharper constants.

When $M = 2$ ($d_0 = 1$, $d_1 = N - 1$, $E_0 = 0$, $E_1 = 1$), the ansatz reduces to $|\phi\rangle = |1\rangle$, and the bound becomes

$$g(s) \ge \frac{(N-1)/N\cdot(2N-1)/N}{(N-1)/N}\left(\frac{1}{2} - s\right) = \frac{2N-1}{N}\left(\frac{1}{2} - s\right) \approx 2\left(\frac{1}{2} - s\right). \tag{6.1.11}$$

The exact gap $g(s) = \sqrt{(2s-1)^2 + 4s(1-s)/N}$ at $s = 1/4$ equals $\sqrt{1/4 + 3/(4N)} \approx 1/2$, while the bound gives $(2N - 1)/(4N) \approx 1/2$. The bound is tight near $s^*$ and only becomes loose as $s$ approaches 0, where the true gap approaches 1 while the bound continues growing.

## 6.2 Gap to the Right of the Crossing

The variational principle cannot bound the gap to the right of $s^*$. It bounds ground energies from above, not excited energies from below, and what we need on the right is a lower bound on $\lambda_1(s) - \lambda_0(s)$ that captures the linear reopening of the gap.

The obstacle is structural. On the left, the first excited eigenvalue $\lambda_1(s)$ is bounded below by $sE_0$ from the eigenvalue equation, giving a clean reference point. On the right, $\lambda_1(s)$ lies between $sE_0$ and $sE_1$, but so do eigenvalues from the higher levels of $sH_z$, which undergo their own avoided crossings with the first excited state. Tracking $\lambda_1(s)$ through this congested region requires a tool that bounds the distance from a given point to the spectrum without identifying individual eigenvalues. The eigenvalue equation (Lemma 5.3.1) characterizes the full spectrum implicitly — each eigenvalue satisfies a transcendental equation — but it does not yield a closed-form bound on any individual eigenvalue that captures the gap's linear dependence on $s - s^*$.

The resolvent provides exactly this. For a self-adjoint operator $A$ with spectrum $\sigma(A)$ and any $\lambda \notin \sigma(A)$, the resolvent

$$R_A(\lambda) = (\lambda I - A)^{-1} \tag{6.2.1}$$

is a bounded operator whose norm equals the inverse distance from $\lambda$ to the spectrum:

$$\|R_A(\lambda)\| = \frac{1}{\operatorname{dist}(\lambda,\, \sigma(A))}. \tag{6.2.2}$$

This follows from the spectral theorem: in the eigenbasis of $A$ with eigenvalues $\{\lambda_j\}$, the resolvent is diagonal with entries $1/(\lambda - \lambda_j)$, and its operator norm is the maximum absolute value $\max_j |1/(\lambda - \lambda_j)| = 1/\min_j |\lambda - \lambda_j|$. If a point $\gamma$ lies between two consecutive eigenvalues $\lambda_0$ and $\lambda_1$, then $\operatorname{dist}(\gamma, \sigma(A)) = \min(\gamma - \lambda_0, \lambda_1 - \gamma) \le g/2$, since the minimum of two non-negative numbers summing to $g$ is at most $g/2$. Therefore $\|R_A(\gamma)\| = 1/\operatorname{dist}(\gamma, \sigma(A)) \ge 2/g$, and the useful contrapositive is

$$g(s) \ge \frac{2}{\|R_{H(s)}(\gamma)\|}. \tag{6.2.3}$$

The spectral gap problem has become a norm problem: bounding the gap from below reduces to bounding the resolvent norm from above.

This resolvent approach to rank-one perturbations has precedent in the spatial search literature. Childs and Goldstone [20] showed that a continuous-time quantum walk on the complete graph finds a marked vertex in $O(\sqrt{N})$ time by analyzing the resolvent of the graph Laplacian perturbed by a rank-one oracle projector — the same algebraic structure as our adiabatic Hamiltonian $H(s) = sH_z - (1-s)\,|\psi_0\rangle\,\langle\psi_0|$, with the Laplacian replaced by the diagonal problem Hamiltonian. Chakraborty, Novo, and Roland [16] extended this to general graphs, proving optimality of spatial search for almost all graphs using the Sherman-Morrison identity to bound the resolvent of rank-one perturbations. Their technique transfers directly to the adiabatic setting: the algebraic steps are identical, with the spectral parameters $A_1$, $A_2$ replacing the graph-theoretic quantities.

Spatial search via continuous-time quantum walks solves the following problem: given a graph $G$ on $N$ vertices with a subset $S$ of marked vertices, find a marked vertex by evolving the initial state $|s\rangle = (1/\sqrt{N}) \sum_v |v\rangle$ under the Hamiltonian $H_{\text{search}} = -\gamma L - \sum_{v \in S} |v\rangle\,\langle v|$, where $L$ is the graph Laplacian and $\gamma > 0$ is a tunable parameter [20]. The oracle term $-\sum_{v\in S} |v\rangle\,\langle v|$ is a rank-one projector when $|S| = 1$ (or more generally a low-rank perturbation), and the Laplacian $L$ plays the role of the diagonal Hamiltonian $sH_z$: its eigenvalues are the graph's spectrum, and the spectral gap of $L$ determines the time scale of the walk. The mapping is: $L \leftrightarrow sH_z$, the oracle projector $\leftrightarrow (1-s)\,|\psi_0\rangle\,\langle\psi_0|$, the algebraic connectivity of $G \leftrightarrow$ the spectral gap $\Delta$ of $H_z$, and the effective resistance at the marked vertex $\leftrightarrow$ the spectral parameter $A_2$. The resolvent bound proceeds identically in both settings: place a line $\gamma(s)$ between the two lowest eigenvalues, apply the Sherman-Morrison formula to decompose the resolvent of the rank-one perturbation into the known resolvent of the diagonal operator plus a correction, and bound the correction using the spectral parameters. The reason this works is structural: rank-one perturbations of diagonal operators admit Sherman-Morrison inversion regardless of the dimension or the specific eigenvalue distribution, reducing the spectral gap problem to bounding a single rational function of the parameters.

The constants $k = 1/4$ and $f(s^*) = 4$ are not accidents of this particular Hamiltonian. They are artifacts of the line-placement optimization — balancing the denominator's positivity against the numerator's growth in the function $f(s)$ — and depend only on the rank-one structure, not on whether the underlying operator is a graph Laplacian or a problem Hamiltonian. Any future application of this technique to a new rank-one perturbation will face the same optimization, with the same constants serving as a starting point.

Since $H(s) = sH_z - (1-s)\left|\psi_0\right\rangle\left\langle\psi_0\right|$ is a rank-one perturbation of $sH_z$, we can invert its resolvent explicitly. The Sherman-Morrison identity [17] states that for an invertible operator $A$ and vectors $\left|u\right\rangle, \left\langle v\right|$,

$$(A + \left|u\right\rangle\left\langle v\right|)^{-1} = A^{-1} - \frac{A^{-1}\left|u\right\rangle\left\langle v\right|A^{-1}}{1 + \left\langle v\right|A^{-1}\left|u\right\rangle}, \tag{6.2.4}$$

provided $1 + \left\langle v\right|A^{-1}\left|u\right\rangle \neq 0$. Applying this to the resolvent of $H(s)$ decomposes it into the resolvent of $sH_z$ (whose spectrum is known explicitly) and a correction from the rank-one term $-(1-s)\left|\psi_0\right\rangle\left\langle\psi_0\right|$. The triangle inequality then yields an upper bound on $\|R_{H(s)}(\gamma)\|$.

Choose a line $\gamma(s)$ between $\lambda_0(s)$ and $\lambda_1(s)$ for all $s \geq s^*$, apply the Sherman-Morrison decomposition, bound each piece using the spectral parameters $A_1$ and $A_2$, and convert the resulting bound on $\|R_{H(s)}(\gamma)\|$ into a linear lower bound on $g(s)$.

The simplest choice for $\gamma(s)$ is a line starting at $sE_0$ when $s = s^*$ and ending between $E_0$ and $E_1$ at $s = 1$: take $\beta(s) = a(s-s^*)/(1-s^*)$ with $a < \Delta$ and set $\gamma(s) = sE_0+\beta(s)$. With $a = \Delta/6$, the function $f(s)$ controlling the resolvent bound can be shown to satisfy $f(s) \leq 1$ for all $s \geq s^*$, giving $g(s) \geq \beta(s) = (\Delta/6)(s-s^*)/(1-s^*)$. This bound has a problem: at the window boundary $s = s^* + \delta_s$, it gives $g(s^* + \delta_s) \geq (\Delta/6)\cdot\delta_s/(1-s^*) = (\Delta A_2)/(6A_1)\cdot g_{\min}$. Since $\Delta A_2 \leq A_1$, this is at most $g_{\min}/6$, and for Hamiltonians with $\Delta A_2 \ll A_1$, it can be polynomially smaller than $g_{\min}$. At $s = s^*$ itself, the bound gives $g(s^*) \geq 0$, missing the true gap entirely.

The failure has a geometric explanation. At $s^*$, the ground energy $\lambda_0(s^*)$ is not at $s^*E_0$ but rather $g_{\min}/2$ below it. The line $\gamma(s)$ passes through $s^*E_0$ at $s = s^*$, so it sits between the two eigenvalues but with zero margin below. The resolvent norm at a point equidistant from two eigenvalues has norm $2/g$, but at a point touching one eigenvalue, the norm diverges. The line must start with $O(g_{\min})$ separation from both eigenvalues at $s^*$.

The fix is to shift the line's origin from $s^*$ to a point $s_0 < s^*$ so that $\beta(s^*) = k\,g_{\min}$ for a constant $k < 1$. With $\beta(s) = a(s-s_0)/(1-s_0)$, the constraint $\beta(s^*) = k\,g_{\min}$ determines

$$s_0 = s^* - \frac{k\,g_{\min}(1-s^*)}{a - k\,g_{\min}}. \tag{6.2.5}$$

The line now passes through $\gamma(s^*) = s^*E_0 + k\,g_{\min}$, which lies between $\lambda_0(s^*)$ and $\lambda_1(s^*)$ when $k$ is chosen appropriately. The price is that $s_0 < s^*$ introduces additional terms in the monotonicity analysis for $f(s)$, requiring a careful choice of $a$.

**Lemma 6.2.1** (Gap to the right of the crossing)**.** *Assume $A_1 \geq 1/2$. Let $k = 1/4$, $a = 4k^2\Delta/3 = \Delta/12$, and $s_0$ as in Eq. (6.2.5). Then for all $s \geq s^*$, the spectral gap of $H(s)$ satisfies*

$$g(s) \geq \frac{\Delta}{30}\cdot\frac{s-s_0}{1-s_0}. \tag{6.2.6}$$

*Proof.* Set $\gamma(s) = sE_0 + \beta(s)$ with $\beta(s) = a(s-s_0)/(1-s_0)$. We bound $\|R_{H(s)}(\gamma)\|$ from above using the Sherman-Morrison formula.

Since $H(s) = sH_z - (1-s)\left|\psi_0\right\rangle\left\langle\psi_0\right|$, the resolvent of $H(s)$ at $\gamma$ satisfies, via Eq. (6.2.4) and the triangle inequality,

$$\|R_{H(s)}(\gamma)\| \leq \|R_{sH_z}(\gamma)\| + (1-s)\frac{\|R_{sH_z}(\gamma)\left|\psi_0\right\rangle\left\langle\psi_0\right|R_{sH_z}(\gamma)\|}{1 + (1-s)\left\langle\psi_0\right|R_{sH_z}(\gamma)\left|\psi_0\right\rangle}. \tag{6.2.7}$$

The unperturbed resolvent $R_{sH_z}(\gamma)$ is diagonal in the $\left|k\right\rangle$ basis with entries $1/(\gamma - sE_k) = 1/(\beta - s(E_k - E_0))$ for $k \geq 1$ and $1/\beta$ for $k = 0$. The nearest eigenvalue of $sH_z$ to $\gamma$ is $sE_0$, at distance $\beta$, so $\|R_{sH_z}(\gamma)\| = 1/\beta$.

We bound the numerator and denominator of the second term separately. Both require that $\beta(s) \leq s(E_k - E_0)/2$ for all $k \geq 1$, which ensures the Taylor expansion in powers of $\beta/(s(E_k - E_0))$ converges rapidly. Since $\beta(s) \leq a = \Delta/12$ and $s(E_k - E_0) \geq s^*\Delta \geq \Delta/3$ (using $s^* = A_1/(A_1+1) \geq 1/3$, which holds when $A_1 \geq 1/2$), we have $\beta \leq \Delta/12 < \Delta/6 \leq s(E_k - E_0)/2$. The condition $A_1 \geq 1/2$ requires that the spectral gaps $E_k - E_0$ are not too large relative to $d_0$; when $A_1 < 1/2$, the crossing occurs at $s^* < 1/3$ and the ground-state degeneracy $d_0$ is large enough that random sampling finds a solution with constant probability, making the adiabatic approach unnecessary.

**Numerator bound.** The squared norm of $R_{sH_z}(\gamma)\left|\psi_0\right\rangle$ expands as

$$\|R_{sH_z}(\gamma)\left|\psi_0\right\rangle\|^2 = \frac{d_0}{N\beta^2} + \frac{1}{N}\sum_{k=1}^{M-1}\frac{d_k}{(s(E_k - E_0) - \beta)^2}. \tag{6.2.8}$$

Using $s(E_k - E_0) - \beta \geq s(E_k - E_0)/2$, each term in the sum is at most $4d_k/(Ns^2(E_k - E_0)^2)$, giving

$$\|R_{sH_z}(\gamma)\,|\psi_0\rangle\,\langle\psi_0|\,R_{sH_z}(\gamma)\| \leq \|R_{sH_z}(\gamma)\,|\psi_0\rangle\|^2 \leq \frac{d_0}{N\beta^2} + \frac{4A_2}{s^2}. \tag{6.2.9}$$

**Denominator bound.** Expanding the expectation value:

$$\begin{aligned} 1 + (1-s)\,\langle\psi_0|\,R_{sH_z}(\gamma)\,|\psi_0\rangle &= 1 + \frac{(1-s)d_0}{N\beta} - \frac{1-s}{N}\sum_{k=1}^{M-1}\frac{d_k}{s(E_k - E_0) - \beta} \\ &= 1 + \frac{(1-s)d_0}{N\beta} - \frac{1-s}{s}\sum_{k=1}^{M-1}\frac{d_k}{N(E_k - E_0)}\sum_{\ell=0}^{\infty}\left(\frac{\beta}{s(E_k - E_0)}\right)^{\ell}. \end{aligned} \tag{6.2.10}$$

Using $\beta/(s(E_k - E_0)) \leq 1/2$ to bound the geometric series by $1 + 2\beta/(s(E_k - E_0))$:

$$1 + (1-s)\,\langle\psi_0|\,R_{sH_z}(\gamma)\,|\psi_0\rangle \geq 1 + \frac{(1-s)d_0}{N\beta} - (1-s)\left(\frac{A_1}{s} + \frac{2A_2\beta}{s^2}\right). \tag{6.2.11}$$

**Collecting terms.** Substituting the bounds (6.2.9) and (6.2.11) into (6.2.7) and factoring:

$$\|R_{H(s)}(\gamma)\| \leq \frac{1}{\beta}\left(1 + f(s)\right), \tag{6.2.12}$$

and

$$f(s) = \frac{\frac{d_0}{N}\,s^2(1-s) + 4A_2\beta^2(1-s)}{\frac{d_0}{N}\,s^2(1-s) + \beta\,s\,\frac{s-s^*}{1-s^*} - 2A_2\beta^2(1-s)}. \tag{6.2.13}$$

To obtain this form, multiply numerator and denominator of the second term in (6.2.7) by $\beta$, then multiply by $s^2(1-s)$ to clear fractions. The key step is rewriting the denominator's constant-plus-linear terms. Using $A_1 = s^*/(1-s^*)$:

$$1 - \frac{(1-s)A_1}{s} + \frac{(1-s)d_0}{N\beta} = \frac{s-s^*}{s(1-s^*)} + \frac{(1-s)d_0}{N\beta}, \tag{6.2.14}$$

since $1 - A_1(1-s)/s = (s - A_1(1-s))/s = (s - s^*(1-s)/(1-s^*))/s = (s(1-s^*) - s^*(1-s))/(s(1-s^*)) = (s-s^*)/(s(1-s^*))$. Multiplying through by $\beta s^2(1-s)$ and collecting the Taylor-bounded terms into the $A_2\beta^2$ contributions gives Eq. (6.2.13). The fraction $d_0/N$ measures the density of ground states in the computational basis.

The numerator of $f(s)$ measures the rank-one perturbation's effect on the resolvent: the $d_0/N$ term comes from the $|0\rangle$ component of $|\psi_0\rangle$ (the ground-state overlap), while the $A_2$ term comes from the excited components. The denominator captures the spectral rigidity: the term $\beta\,s(s-s^*)/(1-s^*)$ grows as $\gamma$ moves away from the crossing, stabilizing the resolvent against the perturbation. Near $s^*$, the denominator is small (the gap is small), so $f(s^*)$ is $O(1)$. As $s$ increases, the denominator grows and $f(s) \to 0$.

From (6.2.12) and (6.2.3), the spectral gap satisfies

$$g(s) \geq \frac{2\beta(s)}{1 + f(s)} \geq \frac{2\beta(s)}{1 + \max_{s \geq s^*} f(s)}. \tag{6.2.15}$$

If $f$ is monotonically decreasing on $[s^*, 1]$, then $\max_{s \geq s^*} f(s) = f(s^*)$, and the bound becomes $g(s) \geq 2\beta(s)/(1 + f(s^*))$, which is linear in $s - s_0$.

**Monotonicity of $f$.** We show $f'(s) < 0$ for $s \in [s^*, 1]$. Writing $f = u/v$, the sign of $f'$ is determined by $u'v - uv'$. After expanding and cancelling common terms, the expression reduces to three contributions: two are manifestly negative, while a third — positive and proportional to $(d_0/N)\,s_0$ — arises from having shifted the line's origin below $s^*$. The proof amounts to showing the negative terms dominate. Write $f = u/v$ with

$$\begin{aligned} u &= \frac{d_0}{N}\,s^2(1-s) + 4A_2\beta^2(1-s), \\ v &= \frac{d_0}{N}\,s^2(1-s) + \beta\,s\,\frac{s-s^*}{1-s^*} - 2A_2\beta^2(1-s). \end{aligned} \tag{6.2.16}$$

Then $f' = (u'v - uv')/v^2$, so the sign of $f'$ is determined by $u'v - uv'$.

Computing $u'$ and $v'$ using $\beta' = a/(1-s_0)$:

$$u' = \frac{4aA_2\beta}{1-s_0}(2+s_0-3s) + \frac{d_0}{N}\,s(2-3s), \tag{6.2.17}$$
$$v' = \frac{a(3s^2-2s(s^*+s_0)+s^*s_0)}{(1-s_0)(1-s^*)} - \frac{2aA_2\beta}{1-s_0}(2+s_0-3s) + \frac{d_0}{N}\,s(2-3s).$$

Expanding $u'v$ and $uv'$ and taking the difference, two terms cancel exactly: the $(d_0/N)^2s^3(2-3s)(1-s)$ term and the $8aA_2^2\beta^3(1-s)(2+s_0-3s)/(1-s_0)$ term. The remaining expression has three terms [14]:

$$\begin{aligned} u'v - uv' = &-\frac{4aA_2\beta^2}{(1-s_0)(1-s^*)}\Big(s^2(1+s_0-s^*) - 2s\,s_0 + s^*s_0\Big) \\ &+ \frac{12aA_2\frac{d_0}{N}\,\beta}{1-s_0}\,s(1-s)^2\,s_0 \\ &- \frac{\frac{d_0}{N}\,s^2a}{(1-s_0)(1-s^*)}\Big(-s^2(s^*+s_0-1) + 2s\,s_0s^* - s^*s_0\Big). \end{aligned} \tag{6.2.18}$$

The first and third terms are negative; the second is positive (it is the only term involving $(d_0/N)\,s_0$, which arises from the shift of $s_0$ below $s^*$). We must show the first negative term dominates the positive one.

Factor out $-4aA_2\beta/(1-s_0)$ from the sum of the first two terms:

$$-\frac{4aA_2\beta}{1-s_0}\left(\frac{\beta}{1-s^*}\Big(s^2(1+s_0-s^*) - 2s\,s_0 + s^*s_0\Big) - \frac{3d_0}{N}\,s_0\,s(1-s)^2\right). \tag{6.2.19}$$

The quadratic $s^2(1+s_0-s^*) - 2s\,s_0 + s^*s_0$ is a convex function of $s$ (the leading coefficient $1+s_0-s^* > 0$ since $s_0 < s^*$), minimized at some $s_m < s^*$, and positive for $s \geq s^*$: at $s = s^*$, it evaluates to $s^*(1-s^*)(s^*-s_0) > 0$. The cubic $s(1-s)^2$ is maximized at $s = 1/3 \leq s^*$. Therefore, on $[s^*, 1]$, the bracket in (6.2.19) is bounded below by its value at $s = s^*$:

$$\frac{a(s^*-s_0)^2}{1-s_0} - \frac{3d_0}{N}\,s_0(1-s^*)^2. \tag{6.2.20}$$

Using $s_0 \leq s^*$ and $s^* - s_0 = k\,g_{\min}(1-s^*)/(a - k\,g_{\min})$, this is positive whenever

$$a < \frac{4}{3}k^2\frac{A_1}{A_2}. \tag{6.2.21}$$

Since $\Delta A_2 \leq A_1$ (because $A_2 \leq \sum_{k\geq 1} d_k/(N(E_k-E_0)^2) \leq A_1/\Delta$), the choice $a = (4/3)k^2\Delta$ satisfies (6.2.21). With this choice, $u'v - uv' < 0$ on $[s^*, 1]$, so $f$ is monotonically decreasing.

**Evaluating $f(s^*)$.** At $s = s^*$, $\beta(s^*) = k\,g_{\min}$. The term $\beta\,s(s-s^*)/(1-s^*)$ vanishes, so

$$f(s^*) = \frac{\frac{d_0}{N}\,s^{*2}(1-s^*) + 4A_2k^2g_{\min}^2(1-s^*)}{\frac{d_0}{N}\,s^{*2}(1-s^*) - 2A_2k^2g_{\min}^2(1-s^*)}. \tag{6.2.22}$$

Replacing $g_{\min}$ by its leading-order expression $\hat{g} = 2s^*\sqrt{d_0/(NA_2)}$ from Eq. (5.4.9) (valid up to a $(1 \pm O(\eta))$ factor that does not affect the final constant), we have $A_2k^2\hat{g}^2 = 4k^2s^{*2}d_0/N$. Substituting:

$$f(s^*) = \frac{1+16k^2}{1-8k^2}. \tag{6.2.23}$$

For $k = 1/4$: $f(s^*) = (1+1)/(1-1/2) = 4$, so $1 + f(s^*) = 5$.

**Final bound.** From (6.2.15):

$$g(s) \geq \frac{2\beta(s)}{1+f(s^*)} = \frac{2a}{1+f(s^*)}\cdot\frac{s-s_0}{1-s_0}. \tag{6.2.24}$$

The prefactor evaluates to

$$\frac{2a}{1+f(s^*)} = \frac{2\cdot(4/3)k^2\Delta}{1+(1+16k^2)/(1-8k^2)} = \frac{4}{3}k^2\cdot\frac{1-8k^2}{1+4k^2}\cdot\Delta. \tag{6.2.25}$$

The function $P(k) = (4/3)k^2(1-8k^2)/(1+4k^2)$ is maximized at $k_{\text{opt}} = \frac{1}{2}\sqrt{\sqrt{3/2}-1} \approx 0.237$, where $P(k_{\text{opt}}) = \frac{1}{3}(5-2\sqrt{6}) \approx 0.034$. For $k = 1/4$:

$$P(1/4) = \frac{4}{3}\cdot\frac{1}{16}\cdot\frac{1/2}{5/4} = \frac{1}{30}. \tag{6.2.26}$$

Therefore $g(s) \geq (\Delta/30)(s-s_0)/(1-s_0)$. $\square$

Specializing to $M = 2$ and $\Delta = 1$, the bound gives $g(s) \geq (1/30)(s-s_0)/(1-s_0)$, where $s_0 = 1/2 - O(1/\sqrt{N})$ is close to $s^* \approx 1/2$ for large $N$. Near $s = 3/4$, the exact gap from Eq. (5.3.15) is $g(3/4) = \sqrt{1/4 + 3/(4N)} \approx 1/2$, while the bound gives approximately $(1/30)(1/4)/(1/2) = 1/60$. The bound is conservative by a factor of approximately 30 but correctly captures the linear growth. This constant is the price of a clean, uniform bound valid for all problem Hamiltonians satisfying the spectral condition.

## 6.3 The Complete Gap Profile

Combining the results of this chapter with those of Chapter 5, the spectral gap $g(s)$ is bounded below across all of $[0, 1]$.

**Theorem 6.3.1** (Complete gap profile)**.** *Let $H_z$ satisfy the spectral condition (Definition 5.2.2) and assume $A_1 \geq 1/2$ (equivalently $s^* \geq 1/3$). The spectral gap of $H(s) = -(1-s)\,|\psi_0\rangle\,\langle\psi_0| + sH_z$ satisfies, for all $s \in [0, 1]$:*

$$g(s) \geq \begin{cases} \dfrac{A_1(A_1+1)}{A_2}\,(s^* - s)\,, & s \in \mathcal{I}_{s^\leftarrow} = [0,\, s^* - \delta_s)\,, \\ g_{\min}, & s \in \mathcal{I}_{s^*} = [s^* - \delta_s,\, s^* + \delta_s]\,, \\ \dfrac{\Delta}{30} \cdot \dfrac{s - s_0}{1 - s_0}, & s \in \mathcal{I}_{s^\rightarrow} = (s^* + \delta_s,\, 1]\,, \end{cases} \tag{6.3.1}$$

*where $s_0 = s^* - k\,g_{\min}(1 - s^*)/(a - k\,g_{\min})$ with $k = 1/4$ and $a = \Delta/12$.*

*Proof.* The three cases follow from Lemma 5.4.2 (window, proved in Chapter 5), Lemma 6.1.1 (left), and Lemma 6.2.1 (right). The right bound holds for all $s \geq s^*$ and therefore covers $\mathcal{I}_{s^\rightarrow}$. The window bound $g(s) \geq g_{\min}$ is tighter than the right bound at $s^*$ but weaker far from the crossing. □

The bounds match across region boundaries. At the left boundary $s = s^* - \delta_s$:

$$\frac{A_1(A_1+1)}{A_2} \cdot \delta_s = \hat{g} = \Theta(g_{\min}), \tag{6.3.2}$$

so the left bound at the window boundary is $\Theta(g_{\min})$, consistent with the window bound. At $s = s^*$, the right bound gives $g(s^*) \geq 2\beta(s^*)/(1 + f(s^*)) = 2k\,g_{\min}/5 = g_{\min}/10$, which is below $g_{\min}$ by a constant factor but still $O(g_{\min})$. The window bound provides the tighter estimate $g(s^*) = g_{\min}$.

The piecewise bounds are asymmetric: steep on the left, shallow on the right. The variational bound captures the true slope closely; the resolvent bound sacrifices tightness for uniform validity across a congested spectral landscape. The profile forms a broad V centered at $s^*$, with a narrow rounded minimum of width approximately $2\delta_s$. The left arm has slope $A_1(A_1+1)/A_2$, which is $O(\mathrm{poly}(n))$ for Ising Hamiltonians. The right arm has the shallower slope $\Delta/(30(1-s_0))$, controlled by the spectral gap $\Delta$ of the problem Hamiltonian. At the endpoints, $g(0) = 1$ (the initial gap between eigenvalues $-1$ and $0$ of $H_0$) and $g(1) = \Delta$ (the gap of $H_z$).

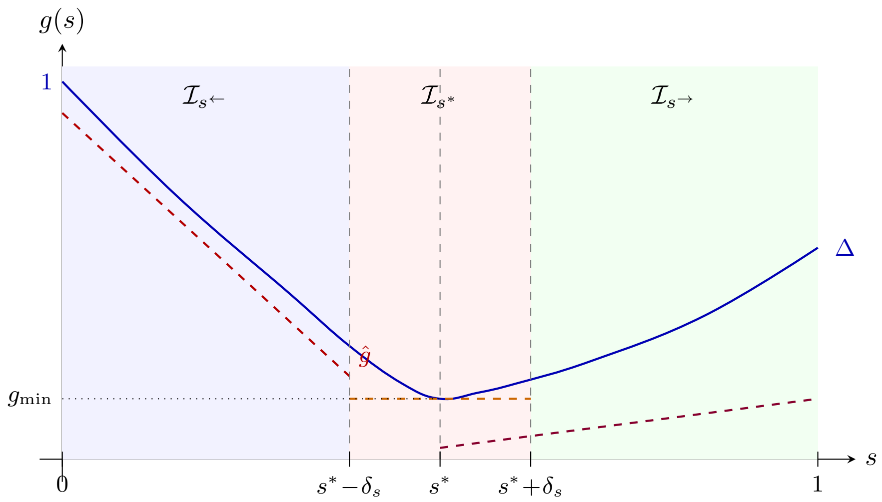


Figure 6.1: Schematic gap profile for $H(s)$. The solid curve shows the true spectral gap $g(s)$, which equals 1 at $s = 0$, dips to $g_{\min}$ at $s = s^*$, and recovers to $\Delta$ at $s = 1$. The left arm is steep (slope $A_1(A_1 + 1)/A_2$); the right arm is shallower (slope controlled by $\Delta$). Dashed lines show the piecewise lower bounds from Theorem 6.3.1: linear on the left, constant $g_{\min}$ in the window, and linear on the right (reaching $\Delta/30$ at $s = 1$). The right bound is below $g_{\min}$ at $s^*$ but remains $O(g_{\min})$.

The gap depends on four numbers: $A_1$, $A_2$, $d_0$, and $\Delta$. For any problem Hamiltonian $H_z$ satisfying the spectral condition, the piecewise profile of Theorem 6.3.1 bounds $g(s)$ across $[0, 1]$ up to constant factors. The minimum gap $g_{\min} = \Theta(\sqrt{d_0/(NA_2)})$ occurs at $s^* = A_1/(A_1 + 1)$ and is exponentially small in $n$ when $d_0 = O(1)$. The crossing position depends only on $A_1$, not on $A_2$ or $d_0$. More solutions (larger $d_0$) widen the gap; richer spectral structure (larger $A_2$) narrows it. The gap reaches $\Delta$ at $s = 1$, the spectral gap of the problem Hamiltonian itself.

For unstructured search, the exact gap $g(s) = \sqrt{(2s - 1)^2 + 4s(1 - s)/N}$ and the piecewise bound from Theorem 6.3.1 can be compared directly. The left bound has slope $(2N - 1)/N \approx 2$, matching the asymptotic slope of the exact gap, which approaches $2(1 - 1/N) \approx 2$ away from $s^*$. The window bound $g_{\min} = 1/\sqrt{N}$ is exact. The right bound has slope approximately $1/15$ near $s^*$, weaker than the true slope by a factor of 30, but sufficient for the runtime integral since the window dominates.

The window dominates the runtime integral. $\int_0^1 g(s)^{-2}\, ds$ splits across the three regions. In the left and right regions, $g(s) \sim C|s - s^*|$ for constants $C$, and

$$\int_{\delta_s}^{s^*} \frac{du}{(Cu)^2} = \frac{1}{C^2}\left(\frac{1}{\delta_s} - \frac{1}{s^*}\right) \leq \frac{1}{C^2\delta_s}, \tag{6.3.3}$$

which is $O(1/(C^2\delta_s))$. In the window, $g(s) \geq g_{\min}$ gives $\int_{s^*-\delta_s}^{s^*+\delta_s} g(s)^{-2}\, ds \leq 2\delta_s/g_{\min}^2$. The window contribution $\delta_s/g_{\min}^2 = \Theta(A_2^{3/2}/(A_1(A_1 + 1)) \cdot \sqrt{N/d_0})$ dominates the outer regions, and the full integral — including the $\Delta$-dependent right-arm contribution — yields the runtime $T = O((\sqrt{A_2}/(A_1(A_1 + 1)\Delta^2))\sqrt{N/d_0})$ that Chapter 7 derives rigorously.

# Chapter 7

# Optimal Schedule

The spectral gap of $H(s)$ is now bounded below across all of $[0, 1]$: a piecewise linear profile (Theorem 6.3.1) that dips to $g_{\min}$ at the avoided crossing $s^*$ and rises linearly on both sides, with slope $A_1(A_1 + 1)/A_2$ on the left and $\Delta/30$ on the right. Chapter 5 observed that the runtime scales as $\int_0^1 g(s)^{-2}\, ds$ (Eq. (5.5.6)), with the crossing window dominating. The exponent in that integral — and hence the speedup — depends on how the evolution rate is matched to the gap structure.

The standard adiabatic theorem, applied with a constant evolution rate, gives a runtime proportional to $\int_0^1 g(s)^{-3}\, ds$. For the gap profile of Theorem 6.3.1, the window contributes $\delta_s/g_{\min}^3$, which when $M = 2$ and $g_{\min} = 1/\sqrt{N}$ gives $T = O(N)$: no speedup over classical search. An adaptive schedule whose rate $K'(s)$ scales inversely with the instantaneous gap concentrates evolution time near the crossing, reducing the controlling integral from $\int g^{-3}\, ds$ to $\int g^{-p}\, ds$ for $p \in (1, 2)$. The resulting runtime is $T = O((\sqrt{A_2}/(A_1(A_1 + 1)\Delta^2))\sqrt{N/d_0}/\varepsilon)$, achieving the Grover speedup up to spectral factors.

## 7.1 Prior Adiabatic Theorems

The gap profile alone does not determine the runtime: the translation from spectral data to evolution time requires an adiabatic theorem, and the form of the theorem dictates what schedule the algorithm can use. Different adiabatic theorems impose different gap dependences, and the distinction is the difference between $O(N)$ and $O(\sqrt{N})$ for the running example.

The earliest rigorous bounds, due to Jansen, Ruskai, and Seiler [21], apply to a constant schedule $K'(s) = T$ and give a transition probability of order $O(1/T^2)$. Their Theorem 3 states that for a state $\psi \in P(0)$, the probability of leaving the ground space satisfies

$$(\psi, [1 - P(s)]U_\tau(s)\psi) \leq A(s)^2, \tag{7.1.1}$$

where $A(s) \leq (1/T)(\|H'\|/g^2)|_{\text{bdry}} + (1/T) \int_0^s (7\sqrt{m}\, \|H'\|^2/g^3 + \|H'\|/g^2)\, ds'$, with $m$ the multiplicity of the ground eigenvalue and the boundary term evaluated at $s = 0$ and $s$. Setting $A(s) = \varepsilon$ and solving for $T$ gives

$$T = O\left(\frac{1}{\varepsilon} \int_0^1 \frac{\|H'\|^2}{g(s)^3}\, ds\right). \tag{7.1.2}$$

With $M = 2$ and $\|H'\| = O(1)$, the integral $\int_0^1 g^{-3}\, ds$ is dominated by the $O(1/\sqrt{N})$-wide window where $g \approx 1/\sqrt{N}$: the contribution is $(1/\sqrt{N}) \cdot N^{3/2} = N$. Therefore the JRS bound gives $T = O(N/\varepsilon)$, reproducing the classical search complexity. A constant schedule treats every value of $s$ equally, spending the same physical time per unit of $s$ whether the gap is $O(1)$ or $O(1/\sqrt{N})$. The integral $\int g^{-3}\, ds$ is a consequence of this uniformity: the $g^{-3}$ dependence means the narrow crossing window contributes overwhelmingly, and no speedup is possible.

The resolution is to make the schedule depend on the gap. Roland and Cerf [4] proposed a *local* adiabatic condition: instead of demanding that the entire evolution be adiabatic with a single time scale $T$, demand that each infinitesimal step $[s, s + ds]$ be adiabatic on its own. The standard adiabatic criterion requires $|ds/dt| \leq \varepsilon\, g(s)^2/|\langle e_1(s)|H'(s)|e_0(s)\rangle|$, where $e_0$ and $e_1$ are the ground and first excited states. Inverting gives $K'(s) = dt/ds \geq |\langle e_1|H'|e_0\rangle|/(\varepsilon\, g(s)^2)$. For the running example, $|\langle e_1|H'|e_0\rangle| = O(1)$ since $H'(s) = |\psi_0\rangle\langle\psi_0| + H_z$ is constant, so $K'(s) \propto 1/g(s)^2$ and the total runtime is

$$T = \frac{C}{\varepsilon} \int_0^1 g(s)^{-2}\, ds. \tag{7.1.3}$$

The integral can be evaluated explicitly. Writing $g(s)^2 = (2s-1)^2 + 4s(1-s)/N$ and substituting $u = 2s - 1$:

$$\int_0^1 g(s)^{-2}\,ds = \frac{1}{2}\int_{-1}^{1}\frac{du}{u^2 + (1-u^2)/N} = \frac{1}{2}\int_{-1}^{1}\frac{N\,du}{1+(N-1)u^2}. \tag{7.1.4}$$

For large $N$, the substitution $v = \sqrt{N-1}\,u$ gives $\frac{N}{2\sqrt{N-1}}\int_{-\sqrt{N-1}}^{\sqrt{N-1}}\frac{dv}{1+v^2} = \frac{N}{2\sqrt{N-1}}\cdot 2\arctan\big(\sqrt{N-1}\big) = O(\sqrt{N})$, since $\arctan\big(\sqrt{N-1}\big) \to \pi/2$. Therefore $T = O(\sqrt{N}/\varepsilon)$, recovering the Grover speedup from a smooth, continuous-time evolution.

The Roland-Cerf construction requires knowing the exact gap $g(s)$ at every point. For the running example with $M = 2$ marked items, the gap has a closed form (Eq. (5.3.15)), so this requirement is met. For a general problem Hamiltonian with $M$ energy levels, the exact gap is unknown — only the piecewise bounds of Theorem 6.3.1 are available. Applying the local adiabatic condition with a lower bound $g_0(s) \le g(s)$ instead of the exact gap means the schedule slows down more than necessary (since $1/g_0^2 \ge 1/g^2$), increasing the runtime by at most a constant factor. But the error analysis requires more care: the commutator bounds of the adiabatic theorem involve derivatives of the schedule, and a non-smooth $g_0$ introduces additional terms. The adaptive schedule of section 7.3 handles these terms through the parameter $p \in (1,2)$.

Several generalizations of these ideas exist. Boixo, Knill, and Somma [22] introduced eigenpath traversal, a discrete framework that replaces continuous adiabatic evolution with a sequence of projections onto ground states of intermediate Hamiltonians $H(s_0), H(s_1), \ldots, H(s_L)$. Between consecutive segments, phase randomization — deliberately destroying coherence between the ground and excited components — suppresses the accumulation of diabatic errors across segments. Coherent errors from successive small transitions can interfere constructively, producing an overall error that grows faster than the sum of individual errors; phase randomization breaks this coherence, converting the error scaling from $O(1/g_{\min}^2)$ (the standard adiabatic bound, which reflects coherent accumulation) to $O(1/g_{\min})$ when the gap integral condition $\int g^{-p}\,ds = O(g_{\min}^{1-p})$ holds. This condition ensures that the gap profile is sufficiently concentrated near its minimum: a broad, flat gap minimum would require many more segments than a narrow, sharp one. Cunningham and Roland [23] obtained tighter constants and extended the framework to the continuous-time setting; the error bound of section 7.2 is the continuous-time version of their result. Elgart and Hagedorn [24] took a different approach: rather than adapting the schedule to the gap, they used smooth switching functions in a Gevrey class, achieving superpolynomial (but not exponential) suppression of diabatic transitions with runtime $T \ge K\,g^{-2}|\ln g|^{6\alpha}$ for Gevrey index $\alpha$. The advantage of the adaptive schedule approach is that it requires only a lower bound $g_0(s) \le g(s)$, not the exact gap or special smoothness conditions. This makes it applicable to general adiabatic quantum optimization with the piecewise bounds of Chapter 6.

## 7.2 The Adiabatic Error Bound

The Schrödinger equation $i\,d\,|\psi\rangle/dt = H(s(t))\,|\psi\rangle$ governs the evolution of a quantum state under the time-dependent Hamiltonian $H(s)$, where $s : [0,T] \to [0,1]$ parametrizes the interpolation and $T$ is the total evolution time. The density matrix formulation $d\rho/dt = -i[H,\rho]$ accommodates mixed states and simplifies the error analysis. Introduce a reparametrization $t = K(s)$, where $K : [0,1] \to \mathbb{R}^+$ is a differentiable, monotonically increasing function called the *schedule*. The chain rule transforms the evolution equation to

$$\frac{d\rho}{ds} = -iK'(s)[H(s), \rho(s)], \tag{7.2.1}$$

where $K'(s) = dK/ds > 0$ controls the instantaneous evolution rate. The total runtime is $T = K(1) = \int_0^1 K'(s)\,ds$. A large $K'(s)$ means slow evolution (long physical time per unit of $s$), allowing the state to track the ground state through a small-gap region. A small $K'(s)$ means fast evolution, appropriate where the gap is large and diabatic transitions are suppressed.

The error of the adiabatic evolution is the probability that the final state does not lie in the ground space of $H(1)$:

$$\varepsilon = 1 - \mathrm{Tr}[P(1)\rho(1)], \tag{7.2.2}$$

where $P(s)$ denotes the projector onto the ground eigenspace of $H(s)$ and $\rho(0) = P(0)$ (the system starts in the ground state of $H(0)$). The projector $P(s)$ and the ground energy $\lambda_0(s)$ are both functions of $s$, varying as the Hamiltonian interpolates from $H_0$ to $H_z$. The operator

$$(H(s) - \lambda_0(s))^+ = \sum_{j\ge 1}\frac{1}{\lambda_j(s) - \lambda_0(s)}\,|\phi_j(s)\rangle\,\langle\phi_j(s)| \tag{7.2.3}$$

is the pseudoinverse of $H(s)-\lambda_0(s)$: it acts as zero on the ground space and as $(\lambda_j-\lambda_0)^{-1}$ on the $j$-th excited eigenspace. Its operator norm is $1/g(s)$, so a small spectral gap amplifies the pseudoinverse.

**Lemma 7.2.1** (Adiabatic error bound [14, 23])**.** *Let $H(s)$ be a twice-differentiable path of Hamiltonians with a continuous ground energy $\lambda_0(s)$ and a spectral gap $g(s)>0$ for all $s\in[0,1]$. Let $K:[0,1]\to\mathbb{R}^+$ be a schedule with absolutely continuous derivative $K'$. Then the evolution (7.2.1) starting from $\rho(0)=P(0)$ satisfies*

$$\varepsilon \le \frac{1}{K'(1)}\left\|\left[P'(1),\,(H(1)-\lambda_0(1))^+\right]\right\| + \int_0^1 \frac{1}{K'}\left\|\left[P',\,(H-\lambda_0)^+\right]'\right\|ds + \int_0^1\left|\left(\frac{1}{K'}\right)'\right|\left\|\left[P',\,(H-\lambda_0)^+\right]\right\|ds. \tag{7.2.4}$$

*Proof.* Since $\rho(0)=P(0)$, the error is $\varepsilon=\mathrm{Tr}[P(0)\rho(0)]-\mathrm{Tr}[P(1)\rho(1)]=|\mathrm{Tr}[P\rho]|_0^1$, so it suffices to track $\mathrm{Tr}[P(s)\rho(s)]$. Differentiating:

$$\frac{d}{ds}\mathrm{Tr}[P\rho]=\mathrm{Tr}[P'\rho]+\mathrm{Tr}[P\rho']. \tag{7.2.5}$$

The second term vanishes. Substituting the evolution equation (7.2.1): $\mathrm{Tr}[P\rho']=-iK'\,\mathrm{Tr}[P[H,\rho]]$. Since $HP=\lambda_0P$, the cyclic property gives $\mathrm{Tr}[P[H,\rho]]=\mathrm{Tr}[PH\rho-P\rho H]=\lambda_0\,\mathrm{Tr}[P\rho]-\mathrm{Tr}[HP\rho]=0$.

For $\mathrm{Tr}[P'\rho]$, write $Q=I-P$ and use the decomposition $P'=PP'Q+QP'P$, which holds because $PP'P=0$ and $QP'Q=0$.[i] Inserting $Q=(H-\lambda_0)^+(H-\lambda_0)$ and using the identities $(H-\lambda_0)\rho P=[H,\rho]P$ and $P\rho(H-\lambda_0)=-P[H,\rho]$ (both consequences of $HP=\lambda_0P$), a cyclic rearrangement under the trace gives

$$\mathrm{Tr}[P'\rho]=\mathrm{Tr}\left[PP'(H-\lambda_0)^+[H,\rho]\right]-\mathrm{Tr}\left[(H-\lambda_0)^+P'P[H,\rho]\right]. \tag{7.2.6}$$

Since $(H-\lambda_0)^+P=P(H-\lambda_0)^+=0$ (the pseudoinverse annihilates the ground space), $PP'(H-\lambda_0)^+$ reduces to $P'(H-\lambda_0)^+$ and $(H-\lambda_0)^+P'P$ reduces to $(H-\lambda_0)^+P'$, so the two terms combine into a commutator:

$$\mathrm{Tr}[P'\rho]=\mathrm{Tr}\left[\left[P',\,(H-\lambda_0)^+\right][H,\rho]\right]=i(K')^{-1}\,\mathrm{Tr}\left[\left[P',\,(H-\lambda_0)^+\right]\rho'\right], \tag{7.2.7}$$

where the last equality substitutes $[H,\rho]=i(K')^{-1}\rho'$ from (7.2.1).

Integrating from 0 to 1 gives $\mathrm{Tr}[P\rho]\big|_0^1=i\int_0^1(K')^{-1}\,\mathrm{Tr}[[P',\,(H-\lambda_0)^+]\,\rho']\,ds$. Integration by parts — with $u=(K')^{-1}[P',\,(H-\lambda_0)^+]$ and $dv=\rho'\,ds$ — transfers the derivative from $\rho$ onto $u$:

$$\begin{aligned}\mathrm{Tr}[P\rho]\big|_0^1 &= i(K'(1))^{-1}\,\mathrm{Tr}\left[\left[P'(1),\,(H(1)-\lambda_0(1))^+\right]\rho(1)\right]\\ &\quad -i\int_0^1\mathrm{Tr}\left[\left((K')^{-1}\left[P',\,(H-\lambda_0)^+\right]'+\left((K')^{-1}\right)'\left[P',\,(H-\lambda_0)^+\right]\right)\rho\right]ds.\end{aligned} \tag{7.2.8}$$

The boundary term at $s=0$ vanishes. Since $\rho(0)=P(0)$, the commutator trace expands as

$$\mathrm{Tr}\left[\left[P',\,(H-\lambda_0)^+\right]P\right]=\mathrm{Tr}[P'(H-\lambda_0)^+P]-\mathrm{Tr}[(H-\lambda_0)^+P'P].$$

For the first summand, $(H-\lambda_0)^+P=0$ (the pseudoinverse annihilates the ground-space projector), so $\mathrm{Tr}[P'(H-\lambda_0)^+P]=0$. For the second, cyclicity of the trace gives $\mathrm{Tr}[(H-\lambda_0)^+P'P]=\mathrm{Tr}[P(H-\lambda_0)^+P']=0$ by the same identity. Taking absolute values and bounding $|\mathrm{Tr}[A\rho]|\le\|A\|$ for any density matrix $\rho$ yields (7.2.4). □

The error bound depends on $H(s)$ only through the commutator $[P',(H-\lambda_0)^+]$ and its derivative. The following bounds express these in terms of the Hamiltonian derivatives $H'$, $H''$ and the spectral gap $g$, using the Riesz integral representation of the spectral projector introduced by Kato [19].

**Lemma 7.2.2** (Projector derivative bounds [14])**.** *Under the conditions of Lemma 7.2.1:*

$$\|P'(s)\|\le\frac{2\|H'(s)\|}{g(s)}, \tag{7.2.9}$$

$$\left\|\left[P'(s),\,(H(s)-\lambda_0(s))^+\right]\right\|\le\frac{4\|H'(s)\|}{g(s)^2}, \tag{7.2.10}$$

$$\left\|\left[P'(s),\,(H(s)-\lambda_0(s))^+\right]'\right\|\le\frac{40\|H'(s)\|^2}{g(s)^3}+\frac{4\|H''(s)\|}{g(s)^2}. \tag{7.2.11}$$

[i] Differentiating $P^2=P$ gives $P'P+PP'=P'$. Left-multiplying by $P$: $PP'P+PP'=PP'$, so $PP'P=0$. Then $QP'Q=P'-PP'-P'P+PP'P=P'-P'=0$.

*Proof of* (7.2.9). Let $\Gamma$ be a circle in the complex plane centered at $\lambda_0(s)$ with radius $g(s)/2$. The Riesz integral representation gives

$$P(s) = \frac{1}{2\pi i} \oint_\Gamma R_{H(s)}(z)\, dz, \tag{7.2.12}$$

where $R_{H(s)}(z) = (zI - H(s))^{-1}$ is the resolvent. Differentiating with respect to $s$:

$$P'(s) = \frac{1}{2\pi i} \oint_\Gamma R_{H(s)}(z)\, H'(s)\, R_{H(s)}(z)\, dz, \tag{7.2.13}$$

using the resolvent identity $R'_H = R_H H' R_H$. On the contour $\Gamma$, every point $z$ lies at distance exactly $g(s)/2$ from $\lambda_0(s)$ and at distance at least $g(s)/2$ from every other eigenvalue (since the nearest eigenvalue is $\lambda_1(s)$ at distance $g(s)$ from $\lambda_0(s)$). Therefore $\|R_{H(s)}(z)\| = 1/\mathrm{dist}(z, \sigma(H(s))) \le 2/g(s)$ on $\Gamma$. Bounding the integral:

$$\|P'(s)\| \le \frac{1}{2\pi} \oint_\Gamma \|R_H(z)\| \cdot \|H'(s)\| \cdot \|R_H(z)\|\, |dz| \le \frac{1}{2\pi} \left(\frac{2}{g}\right)^2 \|H'\| \cdot \pi g = \frac{2\|H'\|}{g}. \tag{7.2.14}$$

□

Bound (7.2.10) follows from (7.2.9): $\|[A, B]\| \le 2\|A\| \cdot \|B\|$ gives $\|[P', (H - \lambda_0)^+]\| \le 2 \cdot 2\|H'\|/g \cdot 1/g = 4\|H'\|/g^2$.

Bound (7.2.11) requires two intermediate results. Write $\widetilde{H} = H - \lambda_0$ for the shifted Hamiltonian. Its pseudoinverse satisfies

$$(\widetilde{H}^+)' = -\widetilde{H}^+ \widetilde{H}' \widetilde{H}^+ + P' \widetilde{H}^+ + \widetilde{H}^+ P', \tag{7.2.15}$$

where $\widetilde{H}' = H' - \lambda'_0$. To see this, split the difference quotient $(\widetilde{H}^+(s + h) - \widetilde{H}^+(s))/h$ using $Q = \widetilde{H}^+ \widetilde{H}$ and $P = I - Q$. The $Q$-part gives $\lim_{h\to 0} \widetilde{H}^+(s)(\widetilde{H}(s) - \widetilde{H}(s + h))\widetilde{H}^+(s + h)/h = -\widetilde{H}^+ \widetilde{H}' \widetilde{H}^+$, while the $P$-part, after adding and subtracting $P(s + h)\widetilde{H}^+(s + h)$ and $\widetilde{H}^+(s)P(s)$, yields $P' \widetilde{H}^+ + \widetilde{H}^+ P'$. Bounding the norm and using $|\lambda'_0| = |\langle \phi_0 | H' | \phi_0 \rangle| \le \|H'\|$ (Hellmann-Feynman):

$$\|(\widetilde{H}^+)'\| \le \frac{\|H'\| + |\lambda'_0|}{g^2} + \frac{4\|H'\|}{g^2} \le \frac{6\|H'\|}{g^2}. \tag{7.2.16}$$

The second intermediate result bounds $P''$. Differentiating $P' = (2\pi i)^{-1} \oint_\Gamma R_H H' R_H\, dz$ gives

$$P'' = \frac{1}{2\pi i} \oint_\Gamma (2R_H H' R_H H' R_H + R_H H'' R_H)\, dz, \tag{7.2.17}$$

where the two $R_H H' R_H H' R_H$ terms arise from differentiating each resolvent factor. Bounding by $\|R_H(z)\| \le 2/g$ on $\Gamma$ and integrating over the contour of length $\pi g$:

$$\|P''\| \le \frac{1}{2\pi} \left(\frac{2}{g}\right)^3 2\|H'\|^2 \cdot \pi g + \frac{1}{2\pi} \left(\frac{2}{g}\right)^2 \|H''\| \cdot \pi g = \frac{8\|H'\|^2}{g^2} + \frac{2\|H''\|}{g}. \tag{7.2.18}$$

Now expand $[P', (H - \lambda_0)^+]' = [P'', (H - \lambda_0)^+] + [P', ((H - \lambda_0)^+)']$ and bound each commutator:

$$\|[P'', (H - \lambda_0)^+]\| \le \frac{2\|P''\|}{g} \le \frac{16\|H'\|^2}{g^3} + \frac{4\|H''\|}{g^2}, \tag{7.2.19}$$

and, using (7.2.9) and (7.2.16):

$$\|[P', ((H - \lambda_0)^+)']\| \le 2\|P'\| \cdot \|(\widetilde{H}^+)'\| \le 2 \cdot \frac{2\|H'\|}{g} \cdot \frac{6\|H'\|}{g^2} = \frac{24\|H'\|^2}{g^3}. \tag{7.2.20}$$

Summing gives $40\|H'\|^2/g^3 + 4\|H''\|/g^2$. A block-matrix decomposition of the commutator with respect to $P$ and $Q = I - P$, tracking cross terms exactly rather than using submultiplicativity, replaces the coefficient 40 by $\approx 4.77$ [14]; the asymptotic scaling is unchanged.

The simplest schedule is constant: $K'(s) = T$, evolving at a uniform rate regardless of the gap. Substituting the derivative bounds into the error bound (7.2.4) with $(1/K')' = 0$ gives the constant-rate result.

**Theorem 7.2.3** (Constant-rate runtime)**.** *Under the conditions of Lemma 7.2.1, a constant schedule $K'(s) = T$ achieves error at most $\varepsilon$ provided*

$$T \ge \frac{1}{\varepsilon} \left( \frac{4\|H'(1)\|}{g(1)^2} + \int_0^1 \frac{40\|H'(s)\|^2}{g(s)^3}\, ds + \int_0^1 \frac{4\|H''(s)\|}{g(s)^2}\, ds \right). \tag{7.2.21}$$

*Proof.* With constant $K'$, the third term in (7.2.4) vanishes. Substituting bounds (7.2.10) and (7.2.11) into the remaining two terms:

$$\varepsilon \leq \frac{1}{T}\left(\frac{4\|H'(1)\|}{g(1)^2} + \int_0^1 \frac{40\|H'(s)\|^2}{g(s)^3}\,ds + \int_0^1 \frac{4\|H''(s)\|}{g(s)^2}\,ds\right). \tag{7.2.22}$$

Setting the right side equal to $\varepsilon$ and solving for $T$ gives (7.2.21). □

Since $H'' = 0$ for the linear interpolation $H(s) = -(1-s)\,|\psi_0\rangle\langle\psi_0| + sH_z$, and $H'(s) = |\psi_0\rangle\langle\psi_0| + H_z$ is constant with $\|H'\| = O(1)$, the dominant term in (7.2.21) is $\int_0^1 g(s)^{-3}\,ds$. From the gap profile of Theorem 6.3.1, the crossing window contributes

$$\int_{s^*-\delta_s}^{s^*} g(s)^{-3}\,ds \leq \frac{\delta_s}{g_{\min}^3} = \frac{A_2}{A_1(A_1+1)} \cdot g_{\min}^{-2}, \tag{7.2.23}$$

using $\delta_s = A_2 g_{\min}/(A_1(A_1+1))$ from Eq. (5.4.10). This gives $T_{\text{constant}} = O(\delta_s/(\varepsilon\, g_{\min}^3))$.

Specializing to $M = 2$ and $g_{\min} = 1/\sqrt{N}$: the exact gap $g(s) = \sqrt{(2s-1)^2 + 4s(1-s)/N}$ (Eq. (5.3.15)) satisfies $\int_0^1 g(s)^{-3}\,ds = O(N)$ since the integral is dominated by the $O(1/\sqrt{N})$ window where $g \approx 1/\sqrt{N}$. Therefore $T_{\text{constant}} = O(N/\varepsilon)$, matching the classical search complexity. A constant-rate schedule provides no quantum speedup: it spends the same physical time per unit of $s$ whether the gap is $O(1)$ or $O(1/\sqrt{N})$, wasting time far from the crossing while still moving too quickly near $s^*$.

## 7.3 The Adaptive Schedule

The constant schedule's failure stems from treating all values of $s$ equally. The error bound (7.2.4) indicates a remedy: make $K'(s)$ large where $g(s)$ is large (slow evolution, low error contribution per unit of $s$) and small where $g(s)$ is small (fast physical evolution, but over a narrow interval of $s$). The natural ansatz is $K'(s)$ proportional to $1/g(s)^p$ for some parameter $p \geq 1$. The total runtime becomes $T \propto \int_0^1 g(s)^{-p}\,ds$, and the error terms involve $\int g^{q-3}\,ds$ for various $q$ depending on $p$.

The parameter $p$ controls the trade-off between error reduction and runtime. The schedule $K'(s) \propto 1/g_0(s)^p$ generalizes the Roland-Cerf local condition (which corresponds to $p = 2$) to arbitrary exponents. At $p = 1$, the runtime integral $\int g_0^{-1}\,ds$ is $O(\log(1/g_{\min}))$ (optimal), but the error integral $\int g_0^{-2}\,ds$ diverges for a piecewise linear gap profile, so the error cannot be controlled. At $p = 2$, the runtime integral $\int g_0^{-2}\,ds = O(1/g_{\min})$ matches Roland-Cerf and the error integral $\int g_0^{-1}\,ds = O(\log(1/g_{\min}))$ converges, but bounding the schedule derivative term requires the exact gap (not just a lower bound), limiting the applicability. For $p \in (1,2)$, both integrals scale as $O(g_{\min}^{1-p})$ and $O(g_{\min}^{p-2})$ respectively, and their product is $O(g_{\min}^{-1})$ regardless of the specific $p$. The error analysis requires only $g_0 \leq g$ (not $g_0 = g$), and the constant $c$ in (7.3.2) absorbs the $p$-dependent prefactors. For the piecewise linear gap profile of Theorem 6.3.1, any $p \in (1,2)$ balances the integrals; the specific choice affects only the constants, not the asymptotic scaling.

The adaptive rate theorem, extending the eigenpath traversal framework of [23] to the continuous-time setting, formalizes this trade-off.

**Theorem 7.3.1** (Adaptive rate [14])**.** *Let $H(s)$ satisfy the conditions of Lemma 7.2.1, and let $g_0 : [0,1] \to \mathbb{R}^+$ be an absolutely continuous function satisfying $g_0(s) \leq g(s)$ for all $s$. Suppose there exist $1 < p < 2$ (the endpoints are excluded: at $p = 1$ the $B_1$ integral diverges logarithmically, and at $p = 2$ the schedule variation term requires the exact gap) and constants $B_1, B_2 \geq 1$ such that*

$$\int_0^1 \frac{ds}{g_0(s)^p} \leq B_1\, g_{\min}^{1-p} \qquad \textit{and} \qquad \int_0^1 \frac{ds}{g_0(s)^{3-p}} \leq B_2\, g_{\min}^{p-2}. \tag{7.3.1}$$

*Assume additionally that $g_0(1) \geq g_{\min}$, that there exists $b \in (0,1]$ with $g_0(s) \geq b\, g_{\min}$ for all $s \in [0,1]$, and that $\sup_{s\in[0,1]} |g_0'(s)| < \infty$. Define*

$$c = \sup_{s\in[0,1]} \left(4\|H'(s)\| + 40\|H'(s)\|^2 B_2 + 4\|H''(s)\| + 6p\,|g_0'(s)|\,\|H'(s)\|\,B_2\right). \tag{7.3.2}$$

*The last term uses $|g_0'(s)|$ rather than $|g'(s)|$: since the schedule is defined in terms of $g_0$, the derivative $(K'^{-1})' \propto (g_0^p)'$ involves $g_0'$. Then the schedule*

$$K'(s) = \frac{1}{\varepsilon} \cdot \frac{c}{g_0(s)^p \cdot g_{\min}^{2-p}} \tag{7.3.3}$$

*achieves error at most $\varepsilon$, with total runtime*

$$T = \int_0^1 K'(s)\, ds \le \frac{c\, B_1}{\varepsilon\, g_{\min}}. \tag{7.3.4}$$

*Proof.* Let $\varepsilon_0$ denote the actual error. Substituting (7.3.3) into the error bound (7.2.4): $(K')^{-1} = \varepsilon\, g_0^p\, g_{\min}^{2-p}/c$, and $|((K')^{-1})'| = (\varepsilon\, g_{\min}^{2-p}/c) \cdot p\, g_0^{p-1}\, |g_0'|$. The three terms become

$$\varepsilon_0 \le \frac{\varepsilon}{c}\, g_{\min}^{2-p} \Big( g_0(1)^p \, \big\| [P'(1), (H(1) - \lambda_0(1))^+] \big\| \\ + \int_0^1 g_0^p \, \Big\| \big[P', (H-\lambda_0)^+\big]' \Big\|\, ds + \int_0^1 p\, g_0^{p-1} |g_0'|\, \big\| [P', (H-\lambda_0)^+] \big\|\, ds \Big). \tag{7.3.5}$$

**Boundary term.** Using bound (7.2.10) with $g_0 \le g$:

$$g_{\min}^{2-p}\, g_0(1)^p \cdot \frac{4\|H'(1)\|}{g(1)^2} \le 4\|H'(1)\|\, g_{\min}^{2-p}\, g_0(1)^{p-2} \le 4\|H'\|, \tag{7.3.6}$$

since $g_0(1) \ge g_{\min}$ and $p - 2 < 0$ imply $g_0(1)^{p-2} \le g_{\min}^{p-2}$.

**Commutator derivative integral.** Using bound (7.2.11) and splitting:

$$g_{\min}^{2-p} \int_0^1 g_0^p \cdot \frac{40\|H'\|^2}{g^3}\, ds \le 40\|H'\|^2\, g_{\min}^{2-p} \int_0^1 \frac{ds}{g_0^{3-p}} \le 40\|H'\|^2 B_2, \tag{7.3.7}$$

where $g_0^p/g^3 \le g_0^p/g_0^3 = 1/g_0^{3-p}$ since $g_0 \le g$, and the $B_2$ condition (7.3.1) absorbs $g_{\min}^{2-p} \cdot g_{\min}^{p-2} = 1$. Similarly, the $H''$ sub-term contributes

$$g_{\min}^{2-p} \int_0^1 g_0^p \cdot \frac{4\|H''\|}{g^2}\, ds \le 4\|H''\|\, g_{\min}^{2-p} \int_0^1 \frac{ds}{g_0^{2-p}} \le 4\|H''\|, \tag{7.3.8}$$

since $g_0 \ge b\, g_{\min}$ and $p - 2 < 0$ imply $g_0^{p-2} \le b^{p-2} g_{\min}^{p-2}$, giving $\int g_0^{p-2}\, ds = O(g_{\min}^{p-2})$ with the constant $b^{p-2}$ absorbed into the $O$-notation.

**Schedule variation integral.** Using bound (7.2.10):

$$\begin{aligned} g_{\min}^{2-p} \int_0^1 p\, g_0^{p-1} |g_0'| \cdot \frac{4\|H'\|}{g^2}\, ds &\le 4p\, \|H'\|\, g_{\min}^{2-p} \int_0^1 \frac{g_0^{p-1}\, |g_0'|}{g_0^2}\, ds \\ &= 4p\, \|H'\|\, g_{\min}^{2-p} \int_0^1 g_0^{p-3}\, |g_0'|\, ds. \end{aligned} \tag{7.3.9}$$

Using $\sup |g_0'| < \infty$, we have $\int g_0^{p-3} |g_0'|\, ds \le \sup |g_0'| \cdot \int g_0^{p-3}\, ds \le \sup |g_0'| \cdot B_2\, g_{\min}^{p-2}$. The resulting bound is $4p \sup |g_0'|\, \|H'\|\, B_2$. The constant $c$ in (7.3.2) uses the factor $6p$ rather than $4p$; this is a valid overestimate that simplifies the expression without affecting the asymptotic result.

**Collecting.** Summing all contributions:

$$\varepsilon_0 \le \frac{\varepsilon}{c} \left( 4\|H'\| + 40\|H'\|^2 B_2 + 4\|H''\| + 6p \sup |g_0'|\, \|H'\|\, B_2 \right) \le \frac{\varepsilon}{c} \cdot c = \varepsilon. \tag{7.3.10}$$

**Runtime.** The total evolution time is

$$T = \int_0^1 K'\, ds = \frac{c}{\varepsilon}\, g_{\min}^{p-2} \int_0^1 \frac{ds}{g_0^p} \le \frac{c}{\varepsilon}\, g_{\min}^{p-2} \cdot B_1\, g_{\min}^{1-p} = \frac{c\, B_1}{\varepsilon\, g_{\min}}. \tag{7.3.11}$$

□

Three terms compose the error: a boundary term that depends on $g_0(1)$ and is $O(1)$; an integral that pairs $g_0^p$ from the schedule with $g^{-3}$ from the derivative bounds, producing $\int g_0^{p-3}\, ds$; and a schedule variation term from the non-constant $K'$. The parameter $p$ balances the two integrals: $B_1$ bounds $\int g_0^{-p}\, ds$ (the runtime cost), while $B_2$ bounds $\int g_0^{p-3}\, ds$ (the error cost). Their product with $g_{\min}^{-1}$ gives the final runtime.

**Corollary 7.3.2.** *If $\int_0^1 g(s)^{-p}\, ds = O(g_{\min}^{1-p})$ for all $p > 1$, and $\|H'\|$, $\|H''\|$, $|\lambda_0'|$, $|g'|$ are all $O(1)$, then $T = O(1/(\varepsilon\, g_{\min}))$.*

The runtime scales inversely with the minimum gap, which is optimal for quantum search [5]. The running example satisfies these conditions.

The integral $\int_0^1 g(s)^{-p}\,ds$ is dominated by the $O(1/\sqrt{N})$-wide window where $g \approx 1/\sqrt{N}$: the window's contribution is $(1/\sqrt{N})\cdot N^{p/2} = N^{(p-1)/2}$, while outside the window $g = \Omega(|s-1/2|)$ and the integral converges. For any $p > 1$, this gives $O(g_{\min}^{1-p})$.

**Lemma 7.3.3** (Grover gap integral)**.** *For the exact gap $g(s) = \sqrt{(2s-1)^2 + 4s(1-s)/N}$ of the running example ($M = 2$, $d_0 = 1$, $d_1 = N-1$),*

$$\int_0^1 g(s)^{-p}\,ds = O\left(N^{(p-1)/2}\right) = O\left(g_{\min}^{1-p}\right) \qquad \text{for all } p > 1. \tag{7.3.12}$$

*Proof.* The gap is symmetric about $s = 1/2$ and achieves its minimum $g_{\min} = 1/\sqrt{N}$ there. Split the integral at $1/2 - 1/\sqrt{N}$. In the window $[1/2 - 1/\sqrt{N},\, 1/2]$, bound $g \geq g_{\min}$:

$$\int_{1/2-1/\sqrt{N}}^{1/2} g^{-p}\,ds \leq \frac{1}{\sqrt{N}} \cdot N^{p/2} = N^{(p-1)/2}. \tag{7.3.13}$$

Outside the window, $g(s) \geq c|s-1/2|$ for a constant $c > 0$ (the gap grows linearly away from the minimum). The change of variable $u = g(s)$, with $|ds/du| = O(1)$ since $|g'(s)| \leq 2$, gives

$$\int_0^{1/2-1/\sqrt{N}} g^{-p}\,ds \leq C\int_{1/\sqrt{N}}^{O(1)} u^{-p}\,du = O\left(N^{(p-1)/2}\right). \tag{7.3.14}$$

Combining and using the symmetry about $1/2$ gives the result. □

The other conditions of Corollary 7.3.2 are immediate: $\|H'\| = \||\psi_0\rangle\langle\psi_0| + H_z\| \leq 2$, $H'' = 0$, $|\lambda_0'| \leq \|H'\| \leq 2$ by the Hellmann-Feynman theorem, and $|g'(s)| \leq 2$ (from $|g'| = |4(1-1/N)(1/2-s)/g| \leq 2$, since the numerator is at most $2g$). Therefore $T = O(\sqrt{N}/\varepsilon)$ for the running example with an adaptive schedule, compared to $T = O(N/\varepsilon)$ with a constant schedule. The adaptive schedule recovers the full Grover speedup.

The schedule $K'(s) \propto 1/g(s)^p$ concentrates the evolution time near the crossing: at $s = 1/2$, where $g \approx 1/\sqrt{N}$, the schedule rate is $K' \propto N^{p/2}$, while far from $1/2$, where $g = O(1)$, it is $K' = O(1)$. The algorithm spends $O(\sqrt{N})$ physical time traversing the window and $O(1)$ time traversing the rest of $[0,1]$.

## 7.4 Runtime of Adiabatic Quantum Optimization

Applying Theorem 7.3.1 to the adiabatic Hamiltonian $H(s) = -(1-s)|\psi_0\rangle\langle\psi_0| + sH_z$ with the gap profile of Theorem 6.3.1 requires three steps: construct a continuous lower bound $g_0(s)$ from the piecewise bounds, compute $B_1$ and $B_2$, and evaluate the constant $c$.

The piecewise bounds of Theorem 6.3.1 are valid in their respective regions but are not continuous at the boundaries $s^* - \delta_s$ and $s^*$: the left bound exceeds the window bound at $s^* - \delta_s$, and the right bound is smaller than $g_{\min}$ at $s^*$. The adaptive rate theorem requires $g_0$ to be absolutely continuous on $[0,1]$. Shrinking the left and window bounds by a constant factor $b$ makes all three pieces meet continuously at the boundaries.

Define

$$g_0(s) = \begin{cases} b\,\dfrac{A_1(A_1+1)}{A_2}\,(s^*-s)\,, & s \in [0,\, s^*-\delta_s), \quad (\text{i.e., } b\,\frac{A_1}{A_2}\cdot\frac{s^*-s}{1-s^*}) \\ b\,g_{\min}, & s \in [s^*-\delta_s,\, s^*), \\ \dfrac{\Delta}{30}\cdot\dfrac{s-s_0}{1-s_0}, & s \in [s^*,\, 1], \end{cases} \tag{7.4.1}$$

where $s_0$ is given by Eq. (6.2.5) and the shrinking factor is

$$b = k\cdot\frac{2}{1+f(s^*)} = \frac{1}{4}\cdot\frac{2}{1+4} = \frac{1}{10}, \tag{7.4.2}$$

using $k = 1/4$ and $f(s^*) = 4$ from Eq. (6.2.23).

Each piece of $g_0$ lies below the corresponding gap bound from Theorem 6.3.1: the left and window pieces are shrunk by $b = 1/10$, and the right piece equals the original bound. The function $g_0$ is continuous at both boundaries. At $s = s^* - \delta_s$, the left piece gives $b \cdot A_1(A_1+1)\delta_s/A_2$. Using $\delta_s = A_2 g_{\min}/(A_1(A_1+1))$ from

Eq. (5.4.10), this equals $b\,g_{\min} = g_{\min}/10$, matching the window piece. At $s = s^*$, the window piece gives $b\,g_{\min} = g_{\min}/10$, and the right piece gives $(\Delta/30)(s^* - s_0)/(1 - s_0)$. Using $s^* - s_0 = k\,g_{\min}(1 - s^*)/(a - k\,g_{\min})$ and $1 - s_0 = (1 - s^*) \cdot a/(a - k\,g_{\min})$ from Eq. (6.2.5):

$$\frac{\Delta}{30} \cdot \frac{s^* - s_0}{1 - s_0} = \frac{\Delta}{30} \cdot \frac{k\,g_{\min}}{a} = \frac{\Delta}{30} \cdot \frac{g_{\min}/4}{\Delta/12} = \frac{g_{\min}}{10}, \tag{7.4.3}$$

again matching the window piece. The parameters $b$, $k$, and $a$ are coupled precisely so that $g_0$ is continuous: the shrinking factor $b = 1/10$ absorbs both the ratio $k = 1/4$ from the right-side resolvent bound and the value $f(s^*) = 4$ from the monotonicity analysis of Chapter 6.

The integral $\int_0^1 g_0^{-p}\,ds$ splits across the three regions. In the left region, $g_0(s) = b\,A_1(A_1 + 1)(s^* - s)/A_2$, so

$$\begin{aligned} \int_0^{s^*-\delta_s} g_0^{-p}\,ds &= \left(\frac{A_2}{b\,A_1(A_1+1)}\right)^p \int_{\delta_s}^{s^*} \frac{du}{u^p} = \frac{1}{b^p}\left(\frac{A_2}{A_1(A_1+1)}\right)^p \cdot \frac{1}{(p-1)\,\delta_s^{p-1}} \\ &= \frac{1}{b^p(p-1)} \cdot \frac{A_2}{A_1(A_1+1)} \cdot g_{\min}^{1-p}, \end{aligned} \tag{7.4.4}$$

where the last step uses $\delta_s^{p-1} = (A_2 g_{\min}/(A_1(A_1+1)))^{p-1}$. In the window, $g_0 = b\,g_{\min}$ is constant:

$$\int_{s^*-\delta_s}^{s^*} g_0^{-p}\,ds = \frac{\delta_s}{b^p\,g_{\min}^p} = \frac{1}{b^p} \cdot \frac{A_2}{A_1(A_1+1)} \cdot g_{\min}^{1-p}. \tag{7.4.5}$$

Combining the left and window contributions with $b^{-p} = 10^p$: $(1/(p-1)+1)/b^p = p \cdot 10^p/(p-1)$, giving $(p/(p-1)) \cdot 10^p \cdot A_2/(A_1(A_1+1)) \cdot g_{\min}^{1-p}$.

In the right region, $g_0(s) = (\Delta/30)(s - s_0)/(1 - s_0)$, so

$$\begin{aligned} \int_{s^*}^{1} g_0^{-p}\,ds &= \left(\frac{30(1-s_0)}{\Delta}\right)^p \int_{s^*-s_0}^{1-s_0} \frac{du}{u^p} = \left(\frac{30(1-s_0)}{\Delta}\right)^p \cdot \frac{1}{(p-1)(s^*-s_0)^{p-1}} \\ &= \frac{1}{p-1}\left(\frac{30}{\Delta}\right)^p \left(\frac{a}{k}\right)^{p-1} (1-s_0) \cdot g_{\min}^{1-p}, \end{aligned} \tag{7.4.6}$$

using $s^* - s_0 = k\,g_{\min}(1 - s^*)/(a - k\,g_{\min})$ and $1 - s_0 = a(1 - s^*)/(a - k\,g_{\min})$. With $a = (4/3)k^2\Delta$ and $k = 1/4$: $a/k = \Delta/3$, so $(30/\Delta)^p(\Delta/3)^{p-1} = 30^p/(3\Delta)$, and $(1 - s_0) \le 1/(1 + A_1)$. The right contribution is $3 \cdot 10^p/((p-1)\Delta(1 + A_1)) \cdot g_{\min}^{1-p}$.

Since $\Delta A_2 \le A_1$ (from $A_2 \le A_1/\Delta$, which follows because $A_2 = (1/N)\sum d_k/(E_k - E_0)^2 \le (1/\Delta) \cdot (1/N)\sum d_k/(E_k - E_0) = A_1/\Delta$), the left-plus-window term $A_2/(A_1(1 + A_1)) \le 1/(\Delta(1 + A_1))$. Combining all three:

$$\int_0^1 g_0^{-p}\,ds \le \frac{(p+3)\cdot 10^p}{(p-1)(1+A_1)\Delta} \cdot g_{\min}^{1-p}, \qquad \text{so} \quad B_1 = O\!\left(\frac{1}{\Delta(1+A_1)}\right). \tag{7.4.7}$$

The integral $\int_0^1 g_0^{p-3}\,ds$ has the same three-region structure, with the exponent $p$ replaced by $3 - p$. Since $p \in (1, 2)$, the conjugate exponent $3 - p$ also lies in $(1, 2)$, so the integrals converge by the same mechanism: the substitution $u = g_0(s)$ reduces each region to $\int u^{-(3-p)}\,du$, which converges at $u = 0$ precisely when $3 - p < 2$ (i.e., $p > 1$). For concreteness, the window contributes $\int_{s^*-\delta_s}^{s^*} (b\,g_{\min})^{p-3}\,ds = \delta_s\,b^{p-3}\,g_{\min}^{p-3} = b^{p-3}\,(A_2/(A_1(A_1+1)))\,g_{\min}^{p-2}$, which is $O(g_{\min}^{p-2})$ since $b^{p-3} = 10^{3-p}$ is a constant. The left and right regions contribute the same order by the same substitution as for $B_1$, with $b^{p-3}$ replacing $b^{-p}$. Combining all three gives

$$B_2 = O\!\left(\frac{1}{\Delta(1+A_1)}\right). \tag{7.4.8}$$

For the adiabatic Hamiltonian $H(s) = -(1 - s)\,|\psi_0\rangle\,\langle\psi_0| + sH_z$:

$$\|H'(s)\| = O(1), \qquad \|H''(s)\| = 0, \qquad |\lambda_0'(s)| = O(1), \tag{7.4.9}$$

since $H'(s) = |\psi_0\rangle\,\langle\psi_0| + H_z$ is constant and $\lambda_0'(s) = \langle\phi_0(s)|\,H'(s)\,|\phi_0(s)\rangle$ is bounded by $\|H'\|$ via the Hellmann-Feynman theorem. The derivative $|g_0'(s)|$ is bounded on each piece: on the left, $|g_0'| = b\,A_1(A_1 + 1)/A_2$; in the window, $g_0' = 0$; on the right, $|g_0'| = \Delta/(30(1 - s_0))$. For piecewise linear $g_0$, the product $|g_0'| \cdot B_2$ remains bounded. The window contributes nothing ($g_0' = 0$ there). On each linear piece, $|g_0'|$ is constant and factors out; the change of variable $u = g_0(s)$ reduces the integral to $\int g_0^{p-3}|g_0'|\,ds = \int_{g_{\min}/10}^{O(1)} u^{p-3}\,du = O(g_{\min}^{p-2})$, independently of the slopes. With $\|H''\| = 0$, the dominant term in (7.3.2) is $40\|H'\|^2 B_2$. Therefore

$$c = O(B_2). \tag{7.4.10}$$

**Theorem 7.4.1** (Runtime of AQO — Main Result 1 [14])**.** *Let $H_z$ satisfy the spectral condition (Definition 5.2.2) and assume $A_1 \geq 1/2$ (equivalently $s^* \geq 1/3$). For any $\varepsilon > 0$, the adaptive schedule (7.3.3) with the gap lower bound (7.4.1) prepares the ground state of $H_z$ with fidelity at least $1-\varepsilon$ in time*

$$T = O\left(\frac{1}{\varepsilon} \cdot \frac{\sqrt{A_2}}{\Delta^2 A_1(A_1+1)} \cdot \sqrt{\frac{N}{d_0}}\right).^{\text{ii}} \tag{7.4.11}$$

*Proof.* By Theorem 7.3.1, $T \leq c\, B_1/(\varepsilon\, g_{\min})$. Substituting $c = O(B_2)$, $B_1 = O(1/(\Delta(1+A_1)))$, $B_2 = O(1/(\Delta(1+A_1)))$, and $g_{\min} = (2A_1/(A_1+1))\sqrt{d_0/(NA_2)}$ from Eq. (5.4.9):

$$T = O\left(\frac{1}{\varepsilon} \cdot \frac{B_1 B_2}{g_{\min}}\right) = O\left(\frac{1}{\varepsilon} \cdot \frac{1}{\Delta^2(1+A_1)^2} \cdot \frac{A_1+1}{2A_1}\sqrt{\frac{NA_2}{d_0}}\right) = O\left(\frac{1}{\varepsilon} \cdot \frac{\sqrt{A_2}}{\Delta^2 A_1(A_1+1)} \cdot \sqrt{\frac{N}{d_0}}\right). \tag{7.4.12}$$

□

The runtime (7.4.11) decomposes into five factors. The dependence $1/\varepsilon$ is linear in the target precision: the adaptive schedule converts time directly into fidelity, unlike the standard adiabatic theorem where $T$ scales as $1/\varepsilon$ times a higher polynomial in $1/g_{\min}$. The factor $\sqrt{A_2}$ reflects the spectral spread: larger $A_2 = (1/N)\sum d_k/(E_k - E_0)^2$ means eigenvalues close to $E_0$ carry substantial degeneracy, sharpening the gap minimum and narrowing the crossing window. The denominator $A_1(A_1+1)$ captures the crossing position: larger $A_1$ pushes $s^*$ closer to 1, steepening the gap's left arm and allowing faster traversal. The factor $1/\Delta^2$ is the price of the right-side bound — a larger spectral gap $\Delta$ in $H_z$ means the gap reopens faster after the crossing, and the quadratic dependence arises because both $B_1$ and $B_2$ contribute a factor of $1/\Delta$. The factor $\sqrt{N/d_0}$ is the quantum speedup; the remaining factors are the spectral price of generality. The scaling $\sqrt{N} = \sqrt{2^n}$ is exponential in $n$, and more solutions (larger $d_0$) reduce the runtime.

For the Ising Hamiltonian $H_\sigma$ (Eq. (5.1.4)) with $A_1, A_2 = O(\mathrm{poly}(n))$ and $\Delta \geq 1/\mathrm{poly}(n)$: $T = \widetilde{O}(\sqrt{N/d_0})$, matching the lower bound of [5] up to polylogarithmic factors. When $d_0 = O(1)$ (constant number of solutions), the adiabatic algorithm achieves the Grover speedup $\sqrt{N}$.

When $M = 2$, $A_1 \approx 1$, $A_2 \approx 1$, $\Delta = 1$, and $d_0 = 1$:

$$T = O\left(\frac{1}{\varepsilon} \cdot \frac{1}{1 \cdot 2} \cdot \sqrt{N}\right) = O\left(\frac{\sqrt{N}}{\varepsilon}\right), \tag{7.4.13}$$

matching the circuit-based Grover algorithm. The adaptive adiabatic approach achieves the same quadratic speedup through a smooth interpolation between two Hamiltonians, without requiring oracle queries or amplitude amplification.

The runtime depends on how much the schedule knows about the gap. A constant rate (Theorem 7.2.3) treats every $s$ equally: the narrow crossing window dominates, and $T = O(N/\varepsilon)$. The Roland-Cerf local schedule (section 7.1) sets $K'(s) \propto 1/g(s)^2$ and achieves $T = O(\sqrt{N}/\varepsilon)$, but requires the exact gap $g(s)$ at every point. What distinguishes the adaptive schedule of Theorem 7.3.1 is that it matches the $O(\sqrt{N}/\varepsilon)$ scaling using only a piecewise linear lower bound $g_0(s) \leq g(s)$ — the bounds constructed in Chapter 6. This generalization from exact gap to lower bound is what makes the result applicable to arbitrary problem Hamiltonians satisfying the spectral condition, at the cost of the spectral prefactors $\sqrt{A_2}/(\Delta^2 A_1(A_1+1))$ in (7.4.11). The discrete-time eigenpath traversal of [22] achieves the same $O(1/g_{\min})$ scaling.

A general framework due to Guo and An [25] places the adaptive schedule in broader context. They consider arbitrary time-dependent Hamiltonians $H(u(s)) = (1-u(s))H_0 + u(s)H_1$ and introduce a *measure condition*: the Lebesgue measure of the set $\{s : \Delta(u(s)) \leq x\}$ is $O(x)$ as $x \to 0$, where $\Delta(u(s))$ is the instantaneous spectral gap. Under this condition, they prove that a power-law schedule with exponent $p = 3/2$ achieves $O(1/\Delta_*)$ runtime, a quadratic improvement in gap dependence over the standard $O(1/\Delta_*^2)$ bound. They further show via variational analysis that $p = 3/2$ is optimal for linear gap profiles and that linear schedules are never optimal when the gap is non-constant. The gap profile of Theorem 6.3.1 satisfies their measure condition: the gap has finitely many local minima (exactly one, at $s^*$) and reopens linearly on both sides, so the set where $g(s) \leq x$ has width $O(x)$. The general framework therefore applies to the AQO setting, but the concrete spectral bounds of Chapter 6 — the explicit slopes, the crossing position, the window width — are what make the runtime formula (7.4.11) explicit rather than existential. Chapter 9 develops the connection to Guo and An's framework further, particularly the role of the measure condition in the information-runtime tradeoff.

To run the adaptive schedule, one must know $g_0(s)$, which requires knowing $s^*$, $\delta_s$, and $g_{\min}$. All three depend on the spectral parameter $A_1$. In the crossing window $[s^* - \delta_s, s^*)$, the schedule is constant: $K' = c/(\varepsilon\, b^p\, g_{\min}^2)$.

[ii] The published paper [14] states $A_1^2$ in Theorem 1. The expression $A_1(A_1+1)$ follows from the proof derivation in Appendix A-IV of the same paper. For Ising Hamiltonians with $A_1 = O(\mathrm{poly}(n))$, the distinction is absorbed by the $O(\cdot)$ notation, since $A_1(A_1+1) = A_1^2 + A_1 = \Theta(A_1^2)$.

This rate does not depend on $A_1$ beyond $g_{\min}$. But the window's location is $[s^* - \delta_s, s^*)$, and $s^* = A_1/(A_1+1)$ must be known to accuracy $O(\delta_s) = O(2^{-n/2})$ to ensure the slow phase occurs at the right place. Outside the window, the schedule depends linearly on the distance from $s^*$, so a small error in $s^*$ introduces a proportionally small error in $K'$, absorbed by the polynomial factors. But the window itself is exponentially narrow in $n$: placing it incorrectly causes the algorithm to evolve rapidly through the crossing, destroying the ground-state fidelity.

Imprecision in $A_2$ and $d_0$ costs only polynomial slowdown. Replacing $A_2$ with the general lower bound $1 - d_0/N$ (Eq. (5.2.3)) and setting $d_0 = 1$ (the worst-case search regime) introduces at most a poly$(n)$ slowdown in the runtime, since these parameters enter only through the ratio $\sqrt{A_2/d_0}$ and the bound $B_1$. The critical parameter is $A_1$: it must be computed to additive accuracy $O(\delta_s) = O(2^{-n/2})$ before the evolution begins. How hard is this computation? The precision needed is exponential in $n$, while the problem Hamiltonian $H_z$ is specified by poly$(n)$ bits. Approximating $A_1$ to the far coarser precision $1/\text{poly}(n)$ is already NP-hard; computing it exactly is #P-hard. Chapter 8 proves both results.

# Chapter 8

# Hardness of Optimality

The optimal schedule of the previous chapter achieves a quadratic speedup over classical brute-force search, but the schedule must be fixed before evolution begins. It depends on the spectral parameter $A_1$ — the weighted sum of inverse gaps that determines where the avoided crossing occurs — and this parameter must be known to additive accuracy $O(2^{-n/2})$. Given the $N = 2^n$ diagonal entries of the problem Hamiltonian $H_z$, the brute-force approach to computing $A_1 = (1/N)\sum_{k=1}^{M-1} d_k/(E_k - E_0)$ — enumerating all eigenvalues, sorting, and summing — takes $O(N)$ time, precisely the cost of classical unstructured search. If the pre-computation is as expensive as the problem itself, the quadratic speedup becomes conditional: the adiabatic algorithm is fast, provided someone has already done the slow part.

The runtime of Theorem 7.4.1,

$$T = O\left(\frac{1}{\varepsilon} \cdot \frac{\sqrt{A_2}}{\Delta^2\, A_1(A_1+1)} \cdot \sqrt{\frac{N}{d_0}}\right),$$

makes this dependence explicit. The adaptive schedule places a slow phase in the window $[s^*-\delta_s,\, s^*)$ centered at the crossing position $s^* = A_1/(A_1+1)$, where the spectral gap reaches its minimum, and accelerates elsewhere. The parameters $A_2$ and $d_0$ enter only through the ratio $\sqrt{A_2/d_0}$. Using conservative bounds ($A_2 \geq 1 - d_0/N$ from Eq. (5.2.3), and $d_0 = 1$ for worst-case search) changes only polynomial prefactors in the hard-search regime $d_0 \ll N$. The critical parameter is $A_1$: it determines where the crossing occurs, and the window width $\delta_s = O(\sqrt{d_0 A_2/N}) = O(2^{-n/2})$ sets the required precision. An error larger than $\delta_s$ in the crossing position causes the algorithm to evolve rapidly through the gap minimum, destroying the ground-state fidelity. Throughout this chapter, we write $A_1(H)$ to make the dependence on the Hamiltonian explicit when multiple Hamiltonians are under consideration.

The hardness of computing $A_1$ is not the only obstacle to adiabatic optimization for hard problems. Even if $A_1$ were known exactly, the single-crossing framework of Chapters 5–7 applies only to the rank-one projector $H_0 = -\left|\psi_0\right\rangle\left\langle\psi_0\right|$. For the transverse-field driver (Chapter 5), the multi-crossing regime renders the single-crossing analysis inapplicable, and knowing $A_1$ does not help because the schedule would need to navigate exponentially many crossings rather than one. The information-theoretic barrier (computing $A_1$ is hard) and the spectral-structural barrier (the single-crossing framework does not apply) are complementary: the first limits the adiabatic approach with the rank-one driver when the problem Hamiltonian has rich spectral structure, while the second limits alternative drivers even when spectral information is available.

NP-hardness holds at $1/\mathrm{poly}(n)$: two queries to an $A_1$-oracle suffice to solve 3-SAT (section 8.1), and #P-hardness at $2^{-\mathrm{poly}(n)}$: polynomial interpolation extracts all degeneracies from polynomially many queries (section 8.2). The algorithmically relevant precision $2^{-n/2}$ sits between — close enough to matter, far enough that neither proof extends. At this precision, a quantum algorithm achieves $O(2^{n/2})$ queries while any classical algorithm requires $\Omega(2^n)$, yielding a Grover-type quadratic separation (section 8.3).

## 8.1 NP-Hardness of Estimating $A_1$

The Hamiltonian $H_z$ encodes an optimization problem whose ground energy $E_0$ determines whether a solution exists. For a 3-SAT instance, $E_0 = 0$ when a satisfying assignment exists and $E_0 \geq 1/\mathrm{poly}(n)$ otherwise. Distinguishing these two cases is the local Hamiltonian promise problem, known to be NP-hard [26]. The spectral parameter $A_1$ is not obviously related to this decision problem — it aggregates information about all energy levels, not just the ground energy. A modified Hamiltonian $H'$ creates a bridge: comparing $A_1(H')$ with $A_1(H)$ reveals whether $E_0$ vanishes.

Define the $(n+1)$-qubit Hamiltonian

$$H' = H \otimes \frac{I + \sigma_z}{2}. \tag{8.1.1}$$

The operator $(I+\sigma_z)/2$ is the projector onto $|0\rangle$ for the ancilla qubit: it has eigenvalue 1 on $|0\rangle$ and eigenvalue 0 on $|1\rangle$. On the $|0\rangle$ branch, $H'$ has the same spectrum as $H$: eigenvalues $E_k$ with degeneracies $d_k$. On the $|1\rangle$ branch, $H'$ annihilates every state, contributing $2^n$ eigenvalues at energy 0. The ground energy of $H'$ is therefore always zero, regardless of $E_0(H)$. This invariance is the mechanism: $A_1(H')$ measures the spectrum from a fixed reference point $E_0' = 0$, while $A_1(H)$ measures from the variable reference $E_0(H)$. When $E_0(H) > 0$, the two measurements diverge, and the divergence is detectable.

**Lemma 8.1.1** (Disambiguation [14])**.** *Let $\varepsilon, \mu_1, \mu_2 \in (0,1)$. Suppose $\mathcal{C}_\varepsilon$ is a procedure that accepts the description of a Hamiltonian $H$ and outputs $\widetilde{A}_1(H)$ with $|\widetilde{A}_1(H) - A_1(H)| \leq \varepsilon$. Let $H$ be an $n$-qubit diagonal Hamiltonian with eigenvalues $0 \leq E_0 < E_1 < \cdots < E_{M-1} \leq 1$ and $M \in poly(n)$, such that either* (i) $E_0 = 0$ *or* (ii) $\mu_1 \leq E_0 \leq 1 - \mu_2$. *Then two calls to $\mathcal{C}_\varepsilon$ suffice to decide between* (i) *and* (ii)*, provided*

$$\varepsilon < \frac{\mu_1}{6(1-\mu_1)} - \frac{d_0}{6N} \cdot \frac{1}{\mu_1 \mu_2}. \tag{8.1.2}$$

*Proof.* Call $\mathcal{C}_\varepsilon$ on $H$ and on $H'$ defined by Eq. (8.1.1), obtaining estimates $\widetilde{A}_1(H)$ and $\widetilde{A}_1(H')$. The test statistic is $\widetilde{A}_1(H) - 2\widetilde{A}_1(H')$, where the factor 2 compensates for the doubling of the Hilbert space ($H'$ acts on $2^{n+1}$ states, so $A_1(H')$ carries a normalization factor $1/2^{n+1}$ instead of $1/2^n$).

**Case (i):** $E_0 = 0$**.** The ground energy of $H'$ is 0 with degeneracy $d_0 + 2^n$, and the excited levels of $H'$ are $E_1, \ldots, E_{M-1}$ with degeneracies $d_1, \ldots, d_{M-1}$. Since $E_0 = 0$, both $A_1(H)$ and $A_1(H')$ sum over the same gaps $E_k - 0 = E_k$:

$$A_1(H) = \frac{1}{2^n} \sum_{k=1}^{M-1} \frac{d_k}{E_k}, \qquad A_1(H') = \frac{1}{2^{n+1}} \sum_{k=1}^{M-1} \frac{d_k}{E_k}.$$

Therefore $A_1(H) - 2A_1(H') = 0$, and by the triangle inequality the test statistic satisfies $|\widetilde{A}_1(H) - 2\widetilde{A}_1(H')| \leq 3\varepsilon$.

**Case (ii):** $\mu_1 \leq E_0 \leq 1 - \mu_2$**.** The ground energy of $H'$ is still 0 (from the $|1\rangle$ branch), but now $E_0, E_1, \ldots, E_{M-1}$ are all excited levels. Thus

$$A_1(H') = \frac{1}{2^{n+1}} \sum_{k=0}^{M-1} \frac{d_k}{E_k}.$$

Decompose $A_1(H)$ using the partial fraction identity $d_k/(E_k - E_0) = d_k/E_k + d_k E_0/(E_k(E_k - E_0))$:

$$\begin{aligned} A_1(H) &= \frac{1}{2^n} \sum_{k=1}^{M-1} \frac{d_k}{E_k - E_0} = \frac{1}{2^n} \sum_{k=1}^{M-1} \frac{d_k}{E_k} + \frac{E_0}{2^n} \sum_{k=1}^{M-1} \frac{d_k}{E_k(E_k - E_0)} \\ &= \frac{1}{2^n} \sum_{k=0}^{M-1} \frac{d_k}{E_k} - \frac{d_0}{2^n E_0} + \frac{E_0}{2^n} \sum_{k=1}^{M-1} \frac{d_k}{E_k(E_k - E_0)}. \end{aligned} \tag{8.1.3}$$

The first sum equals $2A_1(H')$. For the remainder sum, $E_k \leq 1$ and $E_k - E_0 \leq 1 - E_0$, so the product $E_k(E_k - E_0)$ is at most $1 - E_0$. Each fraction $d_k/(E_k(E_k - E_0))$ is therefore bounded from below:

$$\frac{E_0}{2^n} \sum_{k=1}^{M-1} \frac{d_k}{E_k(E_k - E_0)} \geq \frac{E_0}{1 - E_0} \cdot \frac{1}{2^n} \sum_{k=1}^{M-1} d_k = \frac{E_0}{1 - E_0} \left(1 - \frac{d_0}{N}\right).$$

Combining with Eq. (8.1.3):

$$\begin{aligned} A_1(H) - 2A_1(H') &\geq \frac{E_0}{1 - E_0} \left(1 - \frac{d_0}{N}\right) - \frac{d_0}{N E_0} \\ &= \frac{E_0}{1 - E_0} - \frac{d_0}{N} \cdot \frac{1 - E_0 + E_0^2}{E_0(1 - E_0)}. \end{aligned} \tag{8.1.4}$$

Since $1 - E_0 + E_0^2 \leq 1$ and $E_0(1-E_0) \geq \mu_1\mu_2$ on the given range, the fraction $(1 - E_0 + E_0^2)/(E_0(1-E_0))$ is at most $1/(\mu_1\mu_2)$. The first term $E_0/(1-E_0)$ is increasing in $E_0$, so it is at least $\mu_1/(1-\mu_1)$. Therefore

$$A_1(H) - 2A_1(H') \geq \frac{\mu_1}{1-\mu_1} - \frac{d_0}{N} \cdot \frac{1}{\mu_1\mu_2},$$

and the test statistic satisfies

$$\widetilde{A}_1(H) - 2\widetilde{A}_1(H') \geq \frac{\mu_1}{1-\mu_1} - \frac{d_0}{N\mu_1\mu_2} - 3\varepsilon.$$

The two cases are distinguished when $3\varepsilon$ from case (i) is separated from the lower bound in case (ii), requiring $6\varepsilon < \mu_1/(1-\mu_1) - d_0/(N\mu_1\mu_2)$. □

The disambiguation succeeds whenever the positive correction $E_0/(1-E_0)$ from the partial fraction identity dominates the negative term $-d_0/(NE_0)$, which happens as long as $d_0/N$ is small relative to $\mu_1^2\mu_2$. For the Ising Hamiltonians of interest, $d_0/N$ is exponentially small in $n$, so the condition is easily satisfied.

**Theorem 8.1.2** (NP-hardness of $A_1$ estimation [14])**.** *Computing $A_1(H)$ to additive accuracy*

$$\varepsilon < \frac{1}{72(n-1)}$$

*for a 3-local Hamiltonian $H$ on $n$ qubits is NP-hard.*

*Proof.* We reduce 3-SAT to ground-energy disambiguation, following the construction of [27, 14]. Let $\varphi$ be a 3-SAT formula on $n_{\text{var}}$ Boolean variables $x_0, \ldots, x_{n_{\text{var}}-1}$ with $m$ clauses, each of the form $a_k \vee b_k \vee c_k$ where each literal is some $x_l$ or $\bar{x}_l$. If $n_{\text{var}} + m < 15$, solve by brute force. Otherwise, define the single-qubit projectors

$$P_{x_l} = \frac{I - \sigma_z^{(l)}}{2}, \qquad P_{\bar{x}_l} = \frac{I + \sigma_z^{(l)}}{2},$$

which project onto the $|1\rangle$ and $|0\rangle$ states of qubit $l$, respectively. For each clause $k$ $(0 \leq k < m)$, introduce an auxiliary qubit at index $n_{\text{var}} + k$ and define

$$\begin{aligned} H_k = {} & P_{\bar{a}_k} + P_{\bar{b}_k} + P_{\bar{c}_k} + P_{\bar{x}_{n_{\text{var}}+k}} \\ & + P_{a_k}P_{b_k} + P_{a_k}P_{c_k} + P_{b_k}P_{c_k} \\ & + P_{\bar{a}_k}P_{x_{n_{\text{var}}+k}} + P_{\bar{b}_k}P_{x_{n_{\text{var}}+k}} + P_{\bar{c}_k}P_{x_{n_{\text{var}}+k}}. \end{aligned} \tag{8.1.5}$$

Direct computation on the computational basis shows that the minimum eigenvalue of $H_k$ is 3 when clause $k$ is satisfied and 4 when it is not; the maximum eigenvalue is 6. The combined Hamiltonian on $2n_{\text{var}} + 2m$ qubits is

$$H = \frac{1}{6m}\sum_{k=0}^{m-1} H_k + \frac{1}{2n_{\text{var}} + 2m}\sum_{j=n_{\text{var}}+m}^{2n_{\text{var}}+2m-1} P_{x_j} - \frac{1}{2}I. \tag{8.1.6}$$

The first sum normalizes the clause energies to $[1/2, 1]$; the second sum adds $n_{\text{var}} + m$ free qubits whose projectors prefer $|0\rangle$; the identity shift places the eigenvalues in $[0,1]$. When all clauses are satisfied, there exists an assignment making every $H_k$ achieve its minimum, giving $E_0 = 0$. When some clause is unsatisfied, the minimum of $\sum H_k/(6m)$ increases by at least $1/(6m)$, giving $E_0 \geq 1/(6m)$.

Apply Lemma 8.1.1 with $\mu_1 = 1/(6m)$ and $\mu_2 = 1/2$. The number of eigenvalues is $N = 2^{2n_{\text{var}}+2m}$ and the ground-state degeneracy satisfies $d_0 \leq 2^{n_{\text{var}}+m}$, so $d_0/N \leq 2^{-(n_{\text{var}}+m)}$. Substituting into Eq. (8.1.2), the right-hand side satisfies

$$\frac{1}{6} \cdot \frac{1}{6m-1} - \frac{12m}{6} \cdot \frac{d_0}{N} \geq \frac{1}{36(n_{\text{var}} + m - 1)} - \frac{2m}{2^{n_{\text{var}}+m}}, \tag{8.1.7}$$

since $1/(6(6m-1)) \geq 1/(36(n_{\text{var}} + m - 1))$ for $n_{\text{var}} \geq 1$ and $d_0/N \leq 2^{-(n_{\text{var}}+m)}$. For $n_{\text{var}} + m \geq 15$, the second term satisfies $2m/2^{n_{\text{var}}+m} \leq 1/(72(n_{\text{var}} + m - 1))$, so the disambiguation succeeds whenever

$$\varepsilon < \frac{1}{72(n_{\text{var}} + m - 1)}.$$

The Hamiltonian $H'$ from Eq. (8.1.1) acts on $n = 2n_{\text{var}} + 2m + 1$ qubits and is 3-local (since $H$ is 2-local and the tensor product with $(I + \sigma_z)/2$ adds one ancilla). Since $n_{\text{var}} + m \leq n$, the precision bound $\varepsilon < 1/(72(n-1))$ follows. □

When $M = 2$ (Grover search), the spectral parameter $A_1 = (N-1)/N$ is trivially known from the problem description: there are only two energy levels, and the degeneracies are determined by the number of marked items. The NP-hardness arises from Hamiltonians encoding combinatorial problems with polynomially many energy levels and exponentially small ground-energy gaps, where $A_1$ depends on the full degeneracy structure in a non-trivial way.

**Remark.** The disambiguation technique extends beyond 3-SAT. The MaxCut decision problem — given a graph $G = (V, E)$ and integer $k$, does $G$ have a cut of size at least $k$? — also reduces to $A_1$ estimation. The construction adds a weighted edge to $G$, creating an auxiliary Hamiltonian $H'$ whose $A_1$ value differs from a reference by at least $1/(|E|(|E|-1))$ between the two cases. This yields NP-hardness at precision $2/(5n^4)$ with a 2-local Hamiltonian, sharpening the locality requirement from 3-local to 2-local at the cost of a slightly tighter precision bound.

## 8.2 #P-Hardness of Computing $A_1$ Exactly

NP-hardness captures the decision problem: is $E_0 = 0$? But $A_1$ encodes more than a single bit. The spectral parameter is a weighted sum over all energy levels, and its exact value determines every degeneracy $d_k$. Extracting these degeneracies solves counting problems — $d_0$ for an NP-complete Hamiltonian counts the number of satisfying assignments — and counting is harder than deciding: it is #P-complete [28].

The extraction uses a parametrized family of Hamiltonians that shifts the spectrum continuously, turning $A_1$ into a rational function whose poles carry the degeneracies as residues. For a parameter $x > 0$, define the $(n+1)$-qubit Hamiltonian

$$H'(x) = H \otimes I - \frac{x}{2} I \otimes \frac{I + \sigma_z^{(n+1)}}{2}. \tag{8.2.1}$$

On the $|0\rangle$ branch of the ancilla, the eigenvalues are $E_k - x/2$ with degeneracies $d_k$. On the $|1\rangle$ branch, the eigenvalues are $E_k$ with degeneracies $d_k$. The ground energy is $E_0 - x/2$ (from the $|0\rangle$ branch, for $x > 0$). The gaps relative to this ground energy are $\Delta_k = E_k - E_0$ (extending the notation $\Delta = E_1 - E_0$ from earlier chapters to all levels) for the $|0\rangle$ branch and $\Delta_k + x/2$ for the $|1\rangle$ branch.

Computing $A_1(H'(x))$ from these gaps and defining $f(x) = 2A_1(H'(x)) - A_1(H)$ isolates the $|1\rangle$-branch contribution [14]:

$$f(x) = \frac{1}{N} \sum_{k=0}^{M-1} \frac{d_k}{\Delta_k + x/2}. \tag{8.2.2}$$

This function is a sum of $M$ simple poles at $x = -2\Delta_k$. Each pole has residue $2d_k/N$, encoding the degeneracy of the corresponding energy level. The function $f$ is a partial-fraction decomposition of the entire degeneracy spectrum. The extraction problem reduces to recovering these residues from evaluations of $f$.

**Lemma 8.2.1** (Exact degeneracy extraction [14])**.** *Suppose $\mathcal{C}$ is a procedure that computes $A_1(H)$ exactly for any $n$-qubit diagonal Hamiltonian $H$. Let $H_\sigma$ be an Ising Hamiltonian (Equation 5.1.4) with integer eigenvalues and known spectral gaps $\Delta_k = E_k - E_0$. Then $O(poly(n))$ calls to $\mathcal{C}$ suffice to compute all degeneracies $d_0, d_1, \ldots, d_{M-1}$.*

*Proof.* Each evaluation of $f(x_i)$ requires two calls to $\mathcal{C}$: one for $A_1(H)$ and one for $A_1(H'(x_i))$. Evaluate $f$ at $M$ distinct positive odd integers $x_i \in \{1, 3, \ldots, 2M-1\}$. These values avoid the poles: for each $k$, $\Delta_k + x_i/2 \geq 0 + 1/2 > 0$ since $\Delta_k \geq 0$ and $x_i \geq 1$. The total cost is $2M = O(\text{poly}(n))$ oracle calls.

Define the reconstruction polynomial

$$P(x) = \prod_{k=0}^{M-1} \left(\Delta_k + \frac{x}{2}\right) f(x) = \frac{1}{N} \sum_{k=0}^{M-1} d_k \prod_{\ell \neq k} \left(\Delta_\ell + \frac{x}{2}\right). \tag{8.2.3}$$

Multiplying $f(x)$ by the product of all denominators clears the poles, yielding a polynomial of degree at most $M-1$ in $x$. Since the gaps $\Delta_k$ are known integers, the values $P(x_i) = \prod_k (\Delta_k + x_i/2) \cdot f(x_i)$ are computable from the oracle outputs. The $M$ values $P(x_1), \ldots, P(x_M)$ determine $P$ uniquely by Lagrange interpolation [29]: a polynomial of degree at most $M-1$ is determined by $M$ distinct evaluations.

The degeneracies are recovered by evaluating $P$ at the poles. Setting $x = -2\Delta_k$ kills every factor $(\Delta_\ell + x/2)$ except the $k$-th, giving

$$d_k = \frac{N \cdot P(-2\Delta_k)}{\prod_{\ell \neq k} (\Delta_\ell - \Delta_k)}, \qquad k \in \{0, \ldots, M-1\}. \tag{8.2.4}$$

The denominator is nonzero because the eigenvalues are distinct. The entire computation (oracle calls, Lagrange interpolation, pole evaluation) runs in $O(\text{poly}(n))$ time. □

Extracting $d_0$ from an Ising Hamiltonian encoding a 3-SAT formula counts the number of satisfying assignments, solving #3-SAT. Since #3-SAT is #P-complete [28], an exact $A_1$ oracle would solve every problem in #P in polynomial time. The degeneracies also determine the output probability of an IQP circuit [30]: from the $d_k$ and $\Delta_k$, one computes $|\langle 0^n|C_{\text{IQP}}|0^n\rangle|^2 = |N^{-1}\sum_k d_k\, e^{i\Delta_k}|^2$, which is itself #P-hard. The NP-hardness of section 8.1 uses a 3-local Hamiltonian (the ancilla qubit raises the locality by one). The #P-hardness holds for 2-local Ising Hamiltonians, since the parametrized construction in Eq. (8.2.1) preserves 2-locality when $H$ is 2-local.

The exact oracle is unrealistic. A robust version of Lemma 8.2.1 must tolerate additive noise $\varepsilon$ in the oracle outputs. Paturi's amplification lemma controls how pointwise bounds on a polynomial propagate across an interval.

**Lemma 8.2.2** (Paturi [31])**.** *Let $P(x)$ be a polynomial of degree at most $M$ satisfying $|P(i)| \leq c$ for all integers $i \in \{0, 1, \ldots, M\}$. Then $|P(x)| \leq c \cdot 2^M$ for all $x \in [0, M]$.*

Paturi's lemma bounds the growth of a polynomial between its sample points: a polynomial bounded by $c$ at $M+1$ integer points can exceed $c$ by at most a factor $2^M$ on the interval. When applied to the difference between the exact and approximate reconstruction polynomials, it yields a controlled error on the interpolation interval. The oracle noise $\varepsilon$ propagates to $f$ as $|\tilde{f}(x_i) - f(x_i)| \leq 3\varepsilon$ (three oracle calls contribute), then to the polynomial samples as $|\tilde{P}(x_i) - P(x_i)| \leq 3\varepsilon \prod_k(\Delta_k + x_i/2)$. The product is at most $B^M$ where $B = \Delta_{\max} + M = \text{poly}(n)$, so each sample has error at most $3\varepsilon B^M$.

**Lemma 8.2.3** (Approximate degeneracy extraction [14])**.** *Under the same hypotheses as Lemma 8.2.1, but with an oracle $\mathcal{C}_\varepsilon$ satisfying $|\widetilde{A}_1(H) - A_1(H)| \leq \varepsilon$: for sufficiently small $\varepsilon \in O(2^{-\text{poly}(n)})$, all degeneracies $d_k$ can be computed exactly by $O(\text{poly}(n))$ calls to $\mathcal{C}_\varepsilon$.*

*Proof sketch.* The approximate polynomial $\tilde{P}$ is the Lagrange interpolant through the noisy values $(\tilde{P}(x_1), \ldots, \tilde{P}(x_M))$. Its difference $D = \tilde{P} - P$ is a polynomial of degree at most $M - 1$ bounded by $3\varepsilon B^M$ at the sample points. By Paturi's lemma (Lemma 8.2.2), $|D(x)| \leq 3\varepsilon B^M \cdot 2^{M-1}$ on the interpolation interval. At the pole evaluation points $x^* = -2\Delta_k$, which lie outside the interval $[1, 2M-1]$, the error is bounded by the Lagrange basis amplification:

$$|D(x^*)| \leq 3\varepsilon B^M \cdot \Lambda_M(x^*),$$

where $\Lambda_M(x^*) = \sum_j \prod_{i\neq j} |x^* - x_i|/|x_j - x_i|$ is the Lebesgue function. For extrapolation outside the interval, $\Lambda_M(x^*)$ grows exponentially in $M$, but since $M = \text{poly}(n)$, the total amplification is $2^{\text{poly}(n)}$. Dividing by $\prod_{\ell\neq k} |\Delta_\ell - \Delta_k|$ (also at most $2^{\text{poly}(n)}$ for integer gaps) and multiplying by $N = 2^n$, the degeneracy error satisfies

$$|d_k - \tilde{d}_k| \leq 3\varepsilon \cdot 2^{\text{poly}(n)}.$$

For $\varepsilon = O(2^{-\text{poly}(n)})$ with a sufficiently large polynomial, this is less than $1/2$. Since degeneracies are positive integers, rounding $\tilde{d}_k$ to the nearest integer recovers $d_k$ exactly. □

The proof extends to probabilistic oracles. If $\mathcal{C}_\varepsilon$ succeeds with probability at least $3/4$, then $O(\text{poly}(n))$ queries produce enough correct sample points to reconstruct $P$ despite corrupted evaluations. The Berlekamp-Welch algorithm recovers a polynomial of degree $d$ from $k$ partially corrupted evaluations, provided at least $\max\{d+1, (k+d)/2\}$ evaluations are correct [30]. By the Chernoff bound, querying $k = O(\text{poly}(n))$ times ensures that at least $(k + M - 2)/2$ evaluations are correct with high probability. Combining this with Lemma 8.2.3:

**Theorem 8.2.4** (#P-hardness of $A_1$ estimation [14])**.** *Estimating $A_1(H)$ to additive accuracy $\varepsilon = O(2^{-\text{poly}(n)})$ is #P-hard, even for 2-local Ising Hamiltonians. The result holds for both deterministic and probabilistic estimation algorithms.*

With $M = 2$, the reconstruction polynomial $P(x) = (d_0/N)(1+x/2)+(d_1/N)(x/2)$ is linear. Two evaluations determine $d_0$ and $d_1$ exactly, and the Lagrange interpolation is trivial: a line through two points. The #P-hardness arises from Hamiltonians with $M = O(n^2)$ levels, where the reconstruction polynomial has high degree and small errors amplify through the exponential Paturi factor. The error amplification from oracle noise to degeneracy error grows as $2^{O(M \log n)}$, a factor that the next section analyzes precisely.

## 8.3 The Intermediate Regime

The adiabatic algorithm requires $A_1$ to precision $O(2^{-n/2})$. NP-hardness holds at $1/\mathrm{poly}(n)$ (Theorem 8.1.2), and #P-hardness holds at $2^{-\mathrm{poly}(n)}$ (Theorem 8.2.4). The algorithmically relevant precision $2^{-n/2}$ sits strictly between these regimes. The interpolation technique does not extend to this precision: Braida et al. [14] left the intermediate regime as an open problem.

The interpolation technique extracts exact integers from approximate real evaluations. At precision $2^{-n/2}$, the error amplification inherent in polynomial extrapolation makes this extraction impossible.

NP-hardness extends to $2^{-n/2}$ by monotonicity: an oracle at precision $2^{-n/2}$ is strictly more powerful than one at $1/\mathrm{poly}(n)$ (since $2^{-n/2} < 1/\mathrm{poly}(n)$ for large $n$), so it also solves 3-SAT. But #P-hardness does not extend upward: an oracle at precision $2^{-n/2}$ is *less* powerful than one at $2^{-\mathrm{poly}(n)}$, and the interpolation technique that established the latter breaks down at the former. The error propagation has three stages: oracle noise enters the polynomial samples at rate $\varepsilon B^M$, the Lebesgue function amplifies this by a factor exponential in $M$, and the total amplification overwhelms the rounding margin when $\varepsilon = 2^{-n/2}$.

**Theorem 8.3.1** (Interpolation barrier). *The polynomial interpolation technique of section 8.2 requires oracle precision $\varepsilon = 2^{-n-O(M\log n)}$ to extract exact degeneracies, where $M = poly(n)$ is the number of distinct energy levels. At $\varepsilon = 2^{-n/2}$, the amplified error exceeds $1/2$ and rounding fails. The #P-hardness argument does not extend to precision $2^{-n/2}$.*

*Proof.* We trace the error propagation from oracle noise to degeneracy error through the construction of Lemma 8.2.1. Let $\varepsilon$ denote the oracle accuracy, and let $B = \Delta_{\max} + M = \mathrm{poly}(n)$ bound the denominator factors, where $\Delta_{\max}$ is the largest spectral gap.

**Sample-point error.** The approximate function values satisfy $|\tilde{f}(x_i) - f(x_i)| \le 3\varepsilon$. The approximate polynomial samples are $\tilde{P}(x_i) = \prod_k(\Delta_k + x_i/2)\,\tilde{f}(x_i)$, with error

$$|\tilde{P}(x_i) - P(x_i)| \le 3\varepsilon \prod_{k=0}^{M-1}\left(\Delta_k + \frac{x_i}{2}\right) \le 3\varepsilon\, B^M. \tag{8.3.1}$$

**Degeneracy error.** The approximate degeneracies are computed from Eq. (8.2.4) with $\tilde{P}$ in place of $P$. Since $\tilde{P}$ is the Lagrange interpolant through the noisy samples, its value at any point $x^*$ is $\tilde{P}(x^*) = \sum_j \tilde{P}(x_j)\prod_{i\ne j}(x^* - x_i)/(x_j - x_i)$. The error at $x^* = -2\Delta_k$ satisfies

$$|\tilde{P}(x^*) - P(x^*)| \le 3\varepsilon\, B^M \sum_{j=0}^{M-1}\prod_{i\ne j}\frac{|x^* - x_i|}{|x_j - x_i|} = 3\varepsilon\, B^M \cdot \Lambda_M(x^*), \tag{8.3.2}$$

where $\Lambda_M(x^*) = \sum_j \prod_{i\ne j}|x^* - x_i|/|x_j - x_i|$ is the Lebesgue function at $x^*$, measuring the worst-case amplification of pointwise errors by Lagrange interpolation: if each sample has error $\delta$, the interpolated value at $x^*$ has error at most $\delta \cdot \Lambda_M(x^*)$. For extrapolation outside the sample interval, this amplification is exponential in $M$. For the odd-integer nodes $x_j = 2j+1$ and evaluation point $x^* = -2\Delta_k \le 0$ (outside the interval $[1, 2M-1]$): each numerator factor $|x^* - x_i| = 2\Delta_k + 2i + 1 \le 2B + 1$. For the denominator, $\prod_{i\ne j}|x_j - x_i| = \prod_{i\ne j} 2|j-i| = 2^{M-1}\, j!\,(M-1-j)!$, since the nodes are equally spaced with spacing 2. The sum over $j$ evaluates to

$$\Lambda_M(x^*) \le \sum_{j=0}^{M-1}\frac{(2B+1)^{M-1}}{2^{M-1}\, j!\,(M-1-j)!} = \frac{(2B+1)^{M-1}}{(M-1)!}, \tag{8.3.3}$$

using the identity $\sum_j \binom{M-1}{j} = 2^{M-1}$. The denominator in Eq. (8.2.4) satisfies $\prod_{\ell\ne k}|\Delta_\ell - \Delta_k| \ge k!(M-1-k)!$ for integer gaps (since $|\Delta_\ell - \Delta_k| \ge |\ell - k|$), with minimum over $k$ at least $((M-1)/(2e))^{M-1}$ by Stirling's approximation. The total degeneracy error is therefore

$$|d_k - \tilde{d}_k| \le \frac{3\varepsilon\, N\, B^M\,(2B+1)^{M-1}}{(M-1)!\,((M-1)/(2e))^{M-1}}. \tag{8.3.4}$$

Since $B = \mathrm{poly}(n)$ and $M = \mathrm{poly}(n)$, the amplification factor is $2^{O(M\log n)}$.

**Rounding condition.** To extract exact degeneracies by rounding, we need $|d_k - \tilde{d}_k| < 1/2$. This requires

$$\varepsilon < \frac{1}{6N \cdot 2^{O(M\log n)}} = 2^{-n-O(M\log n)}. \tag{8.3.5}$$

**Evaluation at $\varepsilon = 2^{-n/2}$.** Set $\varepsilon = 2^{-n/2}$ and $M = n^c$ for some constant $c \geq 1$. The error bound from Eq. (8.3.4) evaluates to

$$|d_k - \tilde{d}_k| \leq 3 \cdot 2^{-n/2} \cdot 2^n \cdot 2^{O(n^c \log n)} = 3 \cdot 2^{n/2 + O(n^c \log n)} \gg 1.$$

Even for $c = 1$ (the most favorable case $M = n$), the exponent $n/2 + \Omega(n)$ diverges. The upper bound on the degeneracy error already exceeds $1/2$, so the rounding step cannot be guaranteed to succeed. □

The precision $\varepsilon = 2^{-n/2}$ is too coarse for interpolation but too fine for brute force: it sits in a gap that the existing proof techniques cannot reach from either side.

This amplification is not specific to the construction above. The exponential growth is intrinsic to polynomial extrapolation: any $d$ nodes, any interval, any evaluation point sufficiently far from the interval.

**Theorem 8.3.2** (Generic extrapolation barrier)**.** *Let $x_1, \ldots, x_d$ be any $d$ distinct nodes in an interval $[a, b]$, and let $x^*$ satisfy $\operatorname{dist}(x^*, [a, b]) \geq b - a$. The Lebesgue function at $x^*$ satisfies $\Lambda_d(x^*) \geq 2^{d-1}$. Consequently, any polynomial extrapolation scheme that evaluates a degree-$(d-1)$ interpolant at $x^*$ from samples with pointwise error $\delta$ can incur worst-case error at least $\delta \cdot 2^{d-1}$ at $x^*$.*

*Proof.* Assume $x^* \leq a - (b - a)$ (the case $x^* \geq b + (b - a)$ follows by symmetry). Let $x_{(1)} = \min_j x_j \geq a$ be the leftmost node. The corresponding Lagrange basis polynomial satisfies

$$|\ell_{(1)}(x^*)| = \prod_{i:\, x_i \neq x_{(1)}} \frac{|x_i - x^*|}{|x_i - x_{(1)}|} = \prod_{i:\, x_i \neq x_{(1)}} \left(1 + \frac{x_{(1)} - x^*}{x_i - x_{(1)}}\right).$$

Each factor has numerator shift $x_{(1)} - x^* \geq a - (a - (b - a)) = b - a$ and denominator $x_i - x_{(1)} \leq b - a$, so every factor is at least 2. With $d - 1$ such factors, $|\ell_{(1)}(x^*)| \geq 2^{d-1}$. Since $\Lambda_d(x^*) = \sum_j |\ell_j(x^*)| \geq |\ell_{(1)}(x^*)|$, the bound follows. For perturbed samples $y_j = P(x_j) + e_j$ with $|e_j| \leq \delta$, the extrapolation error is

$$\tilde{P}(x^*) - P(x^*) = \sum_{j=1}^{d} e_j\, \ell_j(x^*).$$

Choosing adversarial signs $e_j = \delta \operatorname{sign}(\ell_j(x^*))$ gives

$$|\tilde{P}(x^*) - P(x^*)| = \delta \sum_{j=1}^{d} |\ell_j(x^*)| = \delta\, \Lambda_d(x^*) \geq \delta \cdot 2^{d-1},$$

so the worst-case error can be at least $\delta \cdot 2^{d-1}$. □

Theorem 8.3.2 closes the door on rescuing the #P-hardness argument through better interpolation schemes. No rearrangement of nodes — equispaced, Chebyshev, or otherwise — no alternative polynomial basis, and no change of variables can reduce the amplification below $2^{d-1}$. At $d = M = \mathrm{poly}(n)$ levels, the required precision remains $\varepsilon = 2^{-\Omega(n)}$, exponentially below $2^{-n/2}$. The same structural obstacle appears in quantum computational advantage proposals: the polynomial interpolation techniques used to prove hardness of boson sampling [32] and random circuit sampling [33] face analogous amplification barriers when extending hardness from exponentially small to moderate error regimes.

The interpolation barrier does not rule out #P-hardness at $2^{-n/2}$ by other means. A proof that avoids polynomial extrapolation entirely — using direct algebraic reductions or information-theoretic arguments — might succeed. The barrier identifies where new proof techniques are needed: the challenge is to establish counting hardness without extracting exact integers from approximate real evaluations.

What can be computed at precision $2^{-n/2}$? We analyze the problem in the query model, where each query to a diagonal oracle $O_H \colon |x\rangle\,|0\rangle \mapsto |x\rangle\,|E_x\rangle$ reveals one diagonal entry of $H_z$ at unit cost. This framework cleanly separates quantum and classical capabilities. The interpolation barrier is a classical obstruction: it says that polynomial extrapolation cannot extract integers from evaluations at this precision. A quantum algorithm that avoids interpolation entirely — using amplitude estimation instead of polynomial reconstruction — circumvents the barrier.

**Theorem 8.3.3** (Quantum algorithm for $A_1$)**.** *There exists a quantum algorithm that estimates $A_1(H_z)$ to additive precision $\varepsilon$ using*

$$O\!\left(\sqrt{N} + \frac{1}{\varepsilon\, \Delta_1}\right) \tag{8.3.6}$$

*quantum queries to the diagonal oracle $O_H$, where $\Delta_1 = E_1 - E_0$ is the spectral gap of $H_z$.*

*Proof.* The algorithm has two stages.

**Stage 1: Finding $E_0$.** The Hamiltonian $H_z$ is diagonal in the computational basis, so computing $E_x$ for a given $|x\rangle$ requires one query to $O_H$. Finding the minimum of $E_x$ over all $x \in \{0,1\}^n$ is an instance of quantum minimum finding [34], which succeeds with high probability in $O(\sqrt{N})$ queries.

**Stage 2: Amplitude estimation of $A_1$.** Define the function

$$g(x) = \begin{cases} \dfrac{1}{E_x - E_0} & \text{if } E_x \neq E_0, \\ 0 & \text{if } E_x = E_0. \end{cases}$$

The spectral parameter is the mean $A_1 = (1/N)\sum_x g(x)$. Since the eigenvalues lie in $[0,1]$, the values of $g$ on non-ground states are in $[1, 1/\Delta_1]$. Rescaling to $h(x) = \Delta_1 \cdot g(x)$ yields $h(x) \in [0,1]$, and $A_1 = \mu_h/\Delta_1$ where $\mu_h = (1/N)\sum_x h(x)$.

Construct a quantum oracle $U_h$ acting as $U_h\colon\ |x\rangle|0\rangle \mapsto |x\rangle(\sqrt{1-h(x)}\,|0\rangle + \sqrt{h(x)}\,|1\rangle)$. The implementation queries $O_H$ once to obtain $E_x$, performs classical arithmetic on an ancilla to compute $h(x) = \Delta_1/(E_x - E_0)$ (or 0 for ground states), executes a controlled rotation $R_y(2\arcsin\sqrt{h(x)})$ on a flag qubit, and uncomputes the ancilla. Each application uses $O(1)$ queries to $O_H$ and $O(\mathrm{poly}(n))$ auxiliary gates.

Preparing the uniform superposition $|+\rangle^{\otimes n}$ and applying $U_h$, the probability of measuring the flag qubit in $|1\rangle$ is

$$p = \frac{1}{N}\sum_x h(x) = \mu_h.$$

Amplitude estimation [35] estimates $p$ to additive precision $\delta$ using $O(1/\delta)$ applications of $U_h$ and its inverse. Setting $\delta = \varepsilon\,\Delta_1$ ensures $|A_1 - \tilde{A}_1| = |\mu_h - \tilde{\mu}_h|/\Delta_1 \leq \varepsilon$. The number of $U_h$ applications is $O(1/(\varepsilon\,\Delta_1))$.

Combining both stages: $O(\sqrt{N})$ queries for Stage 1 and $O(1/(\varepsilon\,\Delta_1))$ queries for Stage 2, giving the total in Eq. (8.3.6). For $\varepsilon = 2^{-n/2}$ and $\Delta_1 = 1/\mathrm{poly}(n)$: $O(2^{n/2} + 2^{n/2}\,\mathrm{poly}(n)) = O(2^{n/2}\,\mathrm{poly}(n))$. □

To confirm that the quantum algorithm's $O(2^{n/2})$ queries represent a genuine advantage, we need a classical lower bound. The natural approach is information-theoretic: how many samples does a classical algorithm need to distinguish two carefully chosen instances whose $A_1$ values differ by $\varepsilon$?

**Theorem 8.3.4** (Classical lower bound for $A_1$ estimation)**.** *Any classical randomized algorithm estimating $A_1(H_z)$ to additive precision $\varepsilon$ in the query model requires $\Omega(1/\varepsilon^2)$ queries in the worst case.*

*Proof.* We construct an adversarial pair of instances that are indistinguishable without sufficiently many queries.

**Instance construction.** Fix $t = \lceil \varepsilon N \rceil$. Instance $H_0$ has a hidden set $S \subseteq \{0,1\}^n$ with $|S| = N/2$, and eigenvalues $E_x = 0$ for $x \in S$, $E_x = 1$ otherwise. Instance $H_1$ has $|S'| = N/2 + t$ ground states. The spectral parameters are $A_1(H_0) = 1/2$ and $A_1(H_1) = (N/2 - t)/N = 1/2 - t/N$, differing by $t/N \geq \varepsilon$. An algorithm estimating $A_1$ to precision $\varepsilon/2$ must distinguish the two instances.

**Information-theoretic bound.** A classical query at string $x$ reveals $E_x \in \{0,1\}$, equivalent to learning whether $x \in S$. Under a uniform prior on $S$ (or $S'$), successive queries follow a hypergeometric sampling model. Conditioned on previous outcomes, the $j$-th query is a Bernoulli trial: $x$ is a ground state with probability $p_j^{(i)} = (|S_i| - g_{j-1})/(N - j + 1)$ under hypothesis $H_i$, where $g_{j-1}$ counts ground states already found. The parameter difference $p_j^{(1)} - p_j^{(0)} = t/(N-j+1)$ is independent of $g_{j-1}$. Since both parameters are $\Theta(1)$, a Taylor expansion of the binary KL divergence $D(p\|p+\delta) = \delta^2/(p(1-p)) + O(\delta^3)$ with $\delta = t/(N-j+1)$ gives the conditional per-query divergence

$$D_j = O\!\left(\frac{t^2}{(N-j)^2}\right) = O\!\left(\frac{t^2}{N^2}\right)$$

when $q \leq N/2$. By the chain rule for KL divergence, the total information from $q$ adaptive queries is

$$D_{\mathrm{KL}}^{(q)} \leq \sum_{j=1}^{q} D_j \leq q \cdot O\!\left(\frac{t^2}{N^2}\right).$$

By Le Cam's two-point method [36], reliable hypothesis testing requires $D_{\mathrm{KL}}^{(q)} \geq \Omega(1)$ (via Pinsker's inequality: total variation distance $\leq \sqrt{D_{\mathrm{KL}}/2}$, and distinguishing requires total variation $\Omega(1)$). Therefore

$$q \geq \Omega\!\left(\frac{N^2}{t^2}\right) = \Omega\!\left(\frac{1}{\varepsilon^2}\right).$$

At $\varepsilon = 2^{-n/2}$: $q \geq \Omega(2^n)$. □

**Corollary 8.3.5** (Quadratic quantum-classical separation)**.** *In the query model, estimating $A_1(H_z)$ to precision $\varepsilon = 2^{-n/2}$ exhibits a quadratic quantum-classical separation: quantum complexity $O(2^{n/2}\,\mathrm{poly}(n))$ versus classical complexity $\Omega(2^n)$.*

*Proof.* The upper bound is Theorem 8.3.3 with $\Delta_1 = 1$ for the adversarial instance (or $\Delta_1 = 1/\mathrm{poly}(n)$ in general). The lower bound is Theorem 8.3.4. The separation ratio is $\Omega(2^{n/2}/\mathrm{poly}(n))$, matching Grover's quadratic speedup for unstructured search. □

At the precision the adiabatic algorithm needs, quantum computation offers exactly the speedup the algorithm achieves.

The quantum bound in Theorem 8.3.3 is not just an upper bound — it is tight. For $M = 2$ instances with $\Delta_1 = 1$, estimating $A_1 = (N - d_0)/N$ to precision $\varepsilon$ is equivalent to estimating the fraction $d_0/N$ to precision $\varepsilon$, which is an instance of approximate counting. The Grover iterate $G = (2\,|+\rangle\langle+| - I)(I - 2\Pi_S)$, where $\Pi_S$ projects onto the $d_0$ ground states, has eigenphases $\pm 2\theta$ with $\sin^2\theta = d_0/N$. For $d_0 \approx N/2$, the derivative $dp/d\theta = \sin 2\theta = 1$, so precision $\varepsilon$ in $A_1$ requires precision $\varepsilon$ in $\theta$. The Heisenberg limit for quantum phase estimation [37] — the quantum Cramér-Rao inequality with Fisher information $F_Q \leq 4T^2$ — gives $T \geq 1/(2\varepsilon)$ applications of $G$, each costing $O(1)$ oracle queries. Combined with the upper bound: the quantum query complexity at precision $\varepsilon = 2^{-n/2}$ is $\Theta(2^{n/2})$. The next chapter formalizes this as a theorem and connects it to the broader question of what the quadratic quantum advantage means for the information cost of the adiabatic approach.

Two complementary frameworks apply: computational complexity for the problem of estimating $A_1$ given an explicit Hamiltonian description, and query complexity for the problem given oracle access to the diagonal entries. The distinction matters because they answer different questions about the same bottleneck. Computational complexity asks: given the Hamiltonian's description (coupling constants $J_{ij}$, local fields $h_j$), can a classical computer extract $A_1$ efficiently? The input is fully specified and the difficulty lies in the computation itself. Query complexity asks: given black-box access to the diagonal entries $E_x$, how many evaluations does any algorithm — classical or quantum — need to estimate $A_1$? The input is hidden behind an oracle, and the difficulty lies in the information content. A problem can be computationally easy but query-hard (when the function evaluations are cheap but many are needed), or query-easy but computationally hard (when few evaluations suffice in principle but each requires solving a hard sub-problem). For the $A_1$ estimation problem, both frameworks yield hardness results, reinforcing the conclusion that the pre-computation cost is genuine rather than an artifact of a particular algorithmic approach.

In the computational model with an explicit Hamiltonian description, the complexity landscape across precision regimes is:

| Precision $\varepsilon$ | Hardness | Source |
|---|---|---|
| $1/\mathrm{poly}(n)$ | NP-hard | Theorem 8.1.2 |
| $2^{-n/2}$ | NP-hard | monotonicity |
| $2^{-\mathrm{poly}(n)}$ | #P-hard | Theorem 8.2.4 |

In the query model with a diagonal oracle at the algorithmically relevant precision $\varepsilon = 2^{-n/2}$:

| Model | Complexity | Source |
|---|---|---|
| Quantum | $O(2^{n/2} \cdot \mathrm{poly}(n))$ | Theorem 8.3.3 |
| Classical | $\Omega(2^n)$ | Theorem 8.3.4 |

The precision $2^{-n/2}$ coincides with the algorithmic requirement: the adiabatic schedule needs $A_1$ to precision $O(\sqrt{d_0/N})$, which is $O(2^{-n/2})$ in the worst case $d_0 = O(1)$. It is also the interpolation barrier: the proof technique that establishes #P-hardness breaks exactly at this threshold (Theorem 8.3.1), while NP-hardness extends by monotonicity. And it marks a query complexity transition: at $2^{-n/2}$, the quantum algorithm achieves $O(2^{n/2})$ queries while classical sampling requires $\Omega(2^n)$, a Grover-type quadratic gap.

Classical sampling provides independent evidence for the hardness of $A_1$ estimation at the algorithmic precision. Given a procedure that samples eigenvalues $E_x$ according to the distribution $\{d_k/N\}$, estimating the mean $A_1 = \mathbb{E}[1/(E_x - E_0)]$ to precision $\delta_s$ requires $O(1/\delta_s^2) = \widetilde{O}(2^n/d_0)$ samples by Chebyshev's inequality. This matches the formal $\Omega(2^n)$ lower bound of Theorem 8.3.4 up to logarithmic factors, providing a consistency check between the query-complexity result and concrete sampling algorithms.

The information barrier is not specific to adiabatic evolution. Consider the time-independent Hamiltonian $H = -|\psi_0\rangle\langle\psi_0| + r\,H_\sigma$, where $r > 0$ is a fixed parameter and $H_\sigma$ is the problem Hamiltonian. Evolving the initial state $|\psi_0\rangle$ under $H$ for time $t$ produces oscillations between $|\psi_0\rangle$ and the ground state of $H_\sigma$, with a success probability that depends on $r$. The oscillation frequency is set by the spectral gap of $H$, which is maximized when $r$ places the system at the avoided crossing — precisely when $r = A_1$ (up to normalization). For the success probability to be non-negligible, $r$ must be within $O(2^{-n/2})$ of $A_1$ [14]. Any continuous-time algorithm based on this Hamiltonian therefore faces the same information barrier: the parameter $A_1$ must be known to exponential precision, and computing it is NP-hard. The barrier is not an artifact of the adiabatic framework but a consequence of the spectral structure of rank-one perturbations of diagonal Hamiltonians.

The results of this chapter create a tension. The adiabatic algorithm of Theorem 7.4.1 achieves the Grover speedup $\widetilde{O}(\sqrt{N/d_0})$, matching the lower bound for unstructured search. But the algorithm's schedule requires a spectral parameter whose computation is NP-hard, even at a precision far coarser than what the algorithm needs. In the circuit model, Grover's algorithm achieves the same speedup without pre-computing any spectral parameter: oracle queries gather information adaptively during execution. The adiabatic framework demands the schedule be fixed before evolution begins.

This asymmetry raises a precise question. Does the information cost of the adiabatic approach represent a fundamental limitation, or can it be circumvented? What runtime is achievable by an adiabatic algorithm that knows nothing about the problem Hamiltonian beyond its dimension? The next chapter formalizes this as an information-runtime tradeoff, proving a separation theorem for uninformed schedules and exploring whether adaptive measurements can bypass the classical pre-computation barrier.

# Chapter 9

# Information Gap

The adiabatic algorithm of Theorem 7.4.1 achieves the Grover speedup $\widetilde{O}(\sqrt{N/d_0})$, but its schedule depends on $s^* = A_1/(A_1+1)$, whose computation is NP-hard (Theorem 8.1.2). In the circuit model, Grover's algorithm achieves the same speedup without computing any spectral parameter. The adiabatic framework demands the schedule be fixed before evolution begins. What runtime is achievable by an adiabatic algorithm that knows nothing about the problem Hamiltonian beyond its dimension?

The spectral gap $g(s)$ determines the runtime: physics. The gap in knowledge about where the spectral gap reaches its minimum determines what runtime is achievable: information theory. And whether the gap in knowledge matters at all depends on the computational model: complexity theory.

## 9.1 The Cost of Ignorance

Throughout this chapter, asymptotic notation ($O$, $\Omega$, $\Theta$) refers to the limit $N \to \infty$ (equivalently $n \to \infty$ with $N = 2^n$). The spectral parameters $d_0$, $M$, $\Delta$, $A_1$, $A_2$ and the target error $\varepsilon$ are treated as fixed positive constants independent of $n$ unless explicitly stated otherwise. When we write "$O(T_{\inf})$," the implicit constant may depend on these spectral parameters but not on $n$. A *fixed schedule* is determined before the instance is revealed: it depends only on the problem size $n$ and the target error $\varepsilon$, not on spectral properties. An *instance-independent* algorithm uses the same Hamiltonian design for all energy assignments with the same degeneracy structure.

The NP-hardness of $A_1$ is a statement about worst-case classical computation. It does not directly tell us how much runtime an adiabatic algorithm loses by not knowing $A_1$. If a fixed schedule that ignores $A_1$ still achieved $O(\sqrt{N/d_0})$, the hardness would be academic. It is not.

The separation between informed and uninformed schedules is a minimax result: a two-player game where the schedule designer moves first, then an adversary selects the worst-case gap function. To formalize this, we need a class of gap functions broad enough that the adversary can place the gap minimum anywhere in an uncertainty interval $[s_L, s_R]$.

**Definition 9.1.1** (Gap class)**.** *The gap class $\mathcal{G}(s_L, s_R, \Delta_*)$ consists of all gap functions $g : [0,1] \to \mathbb{R}_{>0}$ satisfying: the minimum $g(s^*) = \Delta_*$ is achieved at a unique point $s^* \in [s_L, s_R]$, and $g(s) > \Delta_*$ for all $s \neq s^*$.*

For the running example ($M = 2$, $d_0 = 1$, $N = 4$), $s^* = A_1/(A_1+1) = 3/7$ and $\Delta_* = g_{\min} = 1/\sqrt{4} = 1/2$. Any gap function in $\mathcal{G}(0,1,1/2)$ has its minimum somewhere in $[0,1]$ at value $1/2$; the adversary's freedom is in choosing where.

**Definition 9.1.2** (RC-admissible fixed schedules)**.** *Fix a family of Hamiltonian instances. A fixed schedule $u$ with velocity profile $v(s) = |ds/dt|$ is* RC-admissible *on an instance if it satisfies the local Roland-Cerf condition*

$$v(s) \le \frac{\varepsilon\, g(s)^2}{\|H'(s)\|} \qquad \forall s \in [0,1].$$

*It is* uniformly RC-admissible *on the family if this inequality holds for every instance in the family.*

The parameter $\Delta_*$ denotes the minimum of the abstract gap function $g$; it should not be confused with $\Delta = E_1 - E_0$ (the spectral gap of $H_z$) or with $g_{\min}$ (the minimum gap of the rank-one Hamiltonian $H(s)$). For the rank-one gap profile, $\Delta_* = g_{\min} = \Theta(\sqrt{d_0/(NA_2)})$.

The schedule induces a velocity profile $v(s) > 0$ on $[0,1]$, with total evolution time $T = \int_0^1 v(s)^{-1}\, ds$.

Within the uniformly RC-admissible class (Definition 9.1.2), the crossing velocity obeys a pointwise bound. Since $H'(s) = |\psi_0\rangle\langle\psi_0| + H_z$ satisfies $\|H'(s)\| \leq \||\psi_0\rangle\langle\psi_0|\| + \|H_z\| \leq 1 + 1 = 2$ (using the eigenvalue normalization $E_{M-1} \leq 1$ from Chapter 5), RC-admissibility gives $v(s) \leq \varepsilon\, g(s)^2/2$. At a crossing point where $g = \Delta_*$, this yields $v \leq \varepsilon\, \Delta_*^2/2$.

The crossing window has width $\delta_s = \Theta(\Delta_*)$, so a schedule must be slow throughout this window. To see this, recall from Chapter 5 that $\delta_s = \hat{g}/c_L$ (Equation 5.4.10), where $\hat{g} = \frac{2A_1}{A_1+1}\sqrt{d_0/(NA_2)}$ is the leading-order minimum gap satisfying $g_{\min} = (1 \pm O(\eta))\hat{g}$; since $c_L = A_1(A_1+1)/A_2$ is a fixed constant, $\delta_s = \Theta(g_{\min}) = \Theta(\Delta_*)$. We define $v_{\text{slow}} = \varepsilon\, \Delta_*^2/2$ as the maximum crossing velocity. In the ratio $T_{\text{unf}}/T_{\text{inf}}$, this velocity cancels: both runtimes are computed under the same Roland-Cerf condition, so $v_{\text{slow}}$ appears in both denominators, and the separation depends only on the geometric ratio $(s_R - s_L)/\Delta_*$.

**Lemma 9.1.3** (Adversarial gap construction)**.** *For any $s_{\text{adv}} \in [s_L, s_R]$ and $\Delta_* > 0$, the gap function $g_{\text{adv}}(s) = \Delta_* + (s - s_{\text{adv}})^2$ belongs to $\mathcal{G}(s_L, s_R, \Delta_*)$.*

*Proof.* The function satisfies $g_{\text{adv}}(s_{\text{adv}}) = \Delta_*$, $g_{\text{adv}}(s) > \Delta_*$ for $s \neq s_{\text{adv}}$, and $g_{\text{adv}}(s) > 0$ for all $s$. □

**Lemma 9.1.4** (Velocity bound for uninformed schedules)**.** *Let $u$ be a fixed schedule that is uniformly RC-admissible on the rank-one family in Theorem 9.1.5. Then $v(s) \leq v_{\text{slow}}$ for all $s \in [s_L, s_R]$, provided $N$ is sufficiently large that $\Delta_* < \min(1 - s_R, s_L)$.*

*Proof.* Suppose $v(s') > v_{\text{slow}}$ for some $s' \in [s_L, s_R]$. We construct a physical Hamiltonian in the rank-one family whose gap minimum occurs at $s'$, then apply RC-admissibility on that instance.

Since $s^* = A_1/(A_1 + 1)$ is a continuous, strictly increasing function of $A_1 \in (0, \infty)$ with range $(0, 1)$, there exists $A_1$ placing the crossing at $s'$. On the two-level family with solution fraction $\rho = d_0/N$, the leading-order gap minimum is $\hat{g} = 2(1 - s')\sqrt{\rho(1-\rho)}$ (Equation 5.4.9), so choosing $\rho$ to satisfy $\hat{g} = \Delta_*$ (feasible whenever $\Delta_* \leq 1 - s'$, which holds asymptotically since $\Delta_* = \Theta(2^{-n/2})$ and $s' \leq s_R < 1$) produces a problem Hamiltonian $H_z$ with crossing at $s'$ and $g_{\min} = \Theta(\Delta_*)$. The adversary in the minimax game selects this physical Hamiltonian, not merely an abstract gap function.

Uniform RC-admissibility on this Hamiltonian gives $v(s') \leq \varepsilon\, g_{\min}^2/\|H'(s')\| = \Theta(v_{\text{slow}})$; after absorbing the fixed constant factor into $v_{\text{slow}}$, this contradicts $v(s') > v_{\text{slow}}$. Because $s'$ was arbitrary in $[s_L, s_R]$, the bound holds throughout the interval. □

**Theorem 9.1.5** (Separation (uniformly RC-admissible class))**.** *Let $T_{\text{unf}}$ be the minimum time over all fixed schedules that are uniformly RC-admissible for all rank-one instances whose gap minima satisfy $s^* \in [s_L, s_R]$ and $g_{\min} = \Theta(\Delta_*)$, and let $T_{\text{inf}}$ be the corresponding optimal informed runtime (with known $s^*$) on the same rank-one family. Then*

$$\frac{T_{\text{unf}}}{T_{\text{inf}}} = \Omega\left(\frac{s_R - s_L}{\Delta_*}\right). \tag{9.1.1}$$

*Proof.* By Lemma 9.1.4, $v(s) \leq v_{\text{slow}}$ for all $s \in [s_L, s_R]$. The uninformed time satisfies

$$T_{\text{unf}} = \int_0^1 \frac{ds}{v(s)} \geq \int_{s_L}^{s_R} \frac{ds}{v(s)} \geq \frac{s_R - s_L}{v_{\text{slow}}}. \tag{9.1.2}$$

The informed schedule knows $s^*$ exactly and needs to be slow only in the crossing window of width $O(\Delta_*)$. For rank-one profiles, $\delta_s = \hat{g}/c_L = \Theta(g_{\min}) = \Theta(\Delta_*)$ by Equation 5.4.10, so Theorem 7.4.1 gives $T_{\text{inf}} = \Theta(\delta_s/v_{\text{slow}}) = \Theta(\Delta_*/v_{\text{slow}})$. The velocity factors cancel:

$$\frac{T_{\text{unf}}}{T_{\text{inf}}} = \Omega\left(\frac{s_R - s_L}{\Delta_*}\right). \tag{9.1.3}$$

□

**Corollary 9.1.6** (Unstructured search)**.** *For $n$-qubit unstructured search with $s_L, s_R$ bounded away from 0 and 1 (so that the condition of Lemma 9.1.4 holds for large $N$), $\Delta_* = \Theta(2^{-n/2})$ and $s_R - s_L = \Theta(1)$, giving $T_{\text{unf}}/T_{\text{inf}} = \Omega(2^{n/2})$.*

For the running example ($M = 2$, $d_0 = 1$, $N = 4$), the separation ratio is $(s_R - s_L)/\Delta_* = 1/(1/2) = 2 = \sqrt{N}$. Uninformed adiabatic evolution on this four-element instance takes twice as long as informed evolution, a discrepancy that grows exponentially with $n$.

The logical structure is: NP-hardness forces the gap-uninformed model for any fixed schedule with polynomial-time classical preprocessing; within the uniformly RC-admissible class, the gap-uninformed model has the $\Omega(2^{n/2})$ minimax lower bound from the adversarial geometry of Lemma 9.1.3; therefore this class of algorithms pays the penalty. The penalty comes from the geometry, not from computational complexity directly.

## 9.2 Partial Knowledge and Hedging

The separation theorem quantifies the worst case: an adversary who places the gap minimum anywhere in $[s_L, s_R]$ forces the schedule to be uniformly slow. But NP-hardness does not mean $A_1$ is completely unknown. What is the value of partial knowledge?

Suppose an algorithm has access to an estimate $A_{1,\text{est}}$ satisfying $|A_{1,\text{est}} - A_1| \leq \varepsilon$. The uncertainty propagates to the crossing position through the map $f(x) = x/(x+1)$, whose derivative is $f'(x) = 1/(x+1)^2$.

**Lemma 9.2.1** ($A_1$-to-$s^*$ precision propagation)**.** *If $|A_{1,\text{est}} - A_1| \leq \varepsilon$ with $|\varepsilon| \leq (1 + A_1)/2$, then $|s^*_{\text{est}} - s^*| \leq 2|\varepsilon|/(A_1 + 1)^2$.*

*Proof.* Direct computation gives the exact identity

$$s^*_{\text{est}} - s^* = \frac{A_1 + \varepsilon}{1 + A_1 + \varepsilon} - \frac{A_1}{1 + A_1} = \frac{\varepsilon}{(1 + A_1)(1 + A_1 + \varepsilon)}. \tag{9.2.1}$$

Under $|\varepsilon| \leq (1 + A_1)/2$, the denominator satisfies $1 + A_1 + \varepsilon \geq (1 + A_1)/2$, so

$$|s^*_{\text{est}} - s^*| \leq \frac{|\varepsilon|}{(1 + A_1) \cdot (1 + A_1)/2} = \frac{2|\varepsilon|}{(1 + A_1)^2}. \tag{9.2.2}$$

□

Given $A_1$ precision $\varepsilon$, the true crossing position lies within radius $2\varepsilon/(A_1+1)^2$ of the estimate by Lemma 9.2.1, giving an uncertainty interval of width $W(\varepsilon) = 4\varepsilon/(A_1+1)^2$. The $\varepsilon$-informed gap class is $\mathcal{G}_\varepsilon = \mathcal{G}(s_L(\varepsilon), s_R(\varepsilon), \Delta_*)$, where the endpoints are determined by the estimate and precision. Applying Theorem 9.1.5 to $\mathcal{G}_\varepsilon$ with interval width $W(\varepsilon)$ gives a lower bound; the matching upper bound comes from a schedule that is uniformly slow across the uncertainty interval and fast elsewhere.

**Theorem 9.2.2** (Interpolation)**.** *For $A_1$ precision $\varepsilon$, the optimal adiabatic runtime satisfies*

$$T(\varepsilon) = \Theta\left(T_{\text{inf}} \cdot \max\left(1, \frac{\varepsilon}{\delta_{A_1}}\right)\right), \tag{9.2.3}$$

*where $\delta_{A_1} = 2\sqrt{d_0 A_2/N}$ is the precision threshold for optimality.*

*Proof. Lower bound.* For $\varepsilon \geq \delta_{A_1}$, Theorem 9.1.5 applied to $\mathcal{G}_\varepsilon$ gives $T(\varepsilon) \geq W(\varepsilon)/v_{\text{slow}}$. Taking the ratio with $T_{\text{inf}} = \Theta(\delta_s/v_{\text{slow}})$ and using the identity

$$(A_1 + 1)^2 \cdot \delta_s = (A_1 + 1)^2 \cdot \frac{2}{(A_1 + 1)^2}\sqrt{\frac{d_0 A_2}{N}} = 2\sqrt{\frac{d_0 A_2}{N}} = \delta_{A_1} \tag{9.2.4}$$

yields $T(\varepsilon)/T_{\text{inf}} \geq \Theta(\varepsilon/\delta_{A_1})$. For $\varepsilon < \delta_{A_1}$, the trivial bound $T(\varepsilon) \geq T_{\text{inf}}$ holds regardless of precision.

*Upper bound.* For $\varepsilon \geq \delta_{A_1}$, construct a schedule with crossing velocity $v_{\text{slow}} = \Theta(\varepsilon\,\Delta_*^2)$ throughout the uncertainty interval $[s_L(\varepsilon), s_R(\varepsilon)]$ and fast velocity $v_{\text{fast}} = O(1)$ outside. The slow region has width $W(\varepsilon) = \Theta(\varepsilon/\delta_{A_1}) \cdot \delta_s$, so the total time is $T = W(\varepsilon)/v_{\text{slow}} + O(1) = \Theta(T_{\text{inf}} \cdot \varepsilon/\delta_{A_1})$, since $T_{\text{inf}} = \Theta(\delta_s/v_{\text{slow}})$. For $\varepsilon < \delta_{A_1}$, the optimal informed schedule achieves $T = O(T_{\text{inf}})$. □

The interpolation is linear: no threshold, no cliff, no phase transition. At precision $1/\text{poly}(n)$ (NP-hard), the overhead is $\Theta(2^{n/2}/\text{poly}(n))$, nearly the full exponential. At precision $2^{-n/2}$ (algorithmically relevant), the overhead is $\Theta(1)$. The space between these two precision scales is the "information gap." For the running example, the explicit precision table is:

| Precision $\varepsilon$ | $T(\varepsilon)/T_{\text{inf}}$ |
|---|---|
| $2^{-n/2}$ | $\Theta(1)$ |
| $2^{-n/4}$ | $\Theta(2^{n/4})$ |
| $1/n$ | $\Theta(2^{n/2}/n)$ |
| $1/\text{poly}(n)$ | $\Theta(2^{n/2}/\text{poly}(n))$ |
| 1 (no knowledge) | $\Theta(2^{n/2})$ |

The interpolation theorem treats $A_1$ precision as a continuous resource. A complementary question is operational: given that $s^*$ lies in a known interval $[u_L, u_R]$ but the exact position is unknown, what is the best fixed schedule? A hedging schedule distributes its slowdown across the entire uncertainty interval rather than concentrating at a single point: velocity $v_{\text{slow}}$ for $s \in [u_L, u_R]$ and $v_{\text{fast}}$ outside, subject to the normalization $(u_R - u_L)/v_{\text{slow}} + (1 - u_R + u_L)/v_{\text{fast}} = 1$.

Write $w = u_R - u_L$ for the interval width. The JRS error functional integrates $\|H'\|^2/g^3$; since $\|H'(s)\| = O(1)$ for the rank-one family, the effective integrand is $g^{-3}$, in contrast to the Roland-Cerf condition which integrates $g^{-2}$. For a piecewise-constant velocity profile, the JRS error bound (Equation 7.1.1) gives a transition probability proportional to $v \cdot \int g^{-3}\, ds$ on each segment. The total error is $v_{\text{slow}} I_{\text{slow}} + v_{\text{fast}} I_{\text{fast}}$, where $I_{\text{slow}} = \int_{u_L}^{u_R} g(u)^{-3}\, du$ and $I_{\text{fast}} = \int_{[0,1]\setminus[u_L,u_R]} g(u)^{-3}\, du$. Since the crossing lies within the slow region, $I_{\text{slow}} \gg I_{\text{fast}}$.

**Theorem 9.2.3** (Hedging)**.** *Let $R = I_{\text{slow}}/I_{\text{fast}} \gg 1$. Under normalization $T = 1$, the optimal hedging schedule for interval $[u_L, u_R]$ achieves $\text{Error}_{\text{hedge}}/\text{Error}_{\text{uniform}} \to u_R - u_L$ as $R \to \infty$, with optimal slow velocity $v_{\text{slow}} = w + \sqrt{(1-w)w/R}$.*

*Proof.* Write $w = u_R - u_L$ for the interval width. The normalization constraint $w/v_{\text{slow}} + (1-w)/v_{\text{fast}} = 1$ fixes the total time $T = 1$, so the JRS error integral of Equation 7.1.1 reduces to $E = v_{\text{slow}} I_{\text{slow}} + v_{\text{fast}} I_{\text{fast}}$. The constraint gives

$$v_{\text{fast}} = \frac{(1-w)\, v_{\text{slow}}}{v_{\text{slow}} - w}, \tag{9.2.5}$$

valid for $v_{\text{slow}} > w$. Substituting into the error:

$$E(v_{\text{slow}}) = v_{\text{slow}}\, I_{\text{slow}} + \frac{(1-w)\, v_{\text{slow}}}{v_{\text{slow}} - w}\, I_{\text{fast}}. \tag{9.2.6}$$

Differentiating with respect to $v_{\text{slow}}$ and setting to zero:

$$\frac{dE}{dv_{\text{slow}}} = I_{\text{slow}} - \frac{(1-w)\, w\, I_{\text{fast}}}{(v_{\text{slow}} - w)^2} = 0. \tag{9.2.7}$$

Solving: $(v_{\text{slow}} - w)^2 = (1-w)\, w\, I_{\text{fast}}/I_{\text{slow}} = (1-w)\, w/R$, so

$$v_{\text{slow}} = w + \sqrt{(1-w)\, w/R}. \tag{9.2.8}$$

At this optimum, $v_{\text{fast}} = (1-w)\, v_{\text{slow}}/\sqrt{(1-w)\, w/R} = \sqrt{R\, w\,(1-w)} + (1-w)$. The optimal error, substituting $v_{\text{slow}} - w = \sqrt{(1-w)\, w/R}$, is

$$E_{\text{opt}} = \left(w + \sqrt{(1-w)\, w/R}\right) I_{\text{slow}} + \left(\sqrt{R\, w\,(1-w)} + (1-w)\right) I_{\text{fast}}. \tag{9.2.9}$$

Since $R = I_{\text{slow}}/I_{\text{fast}} \gg 1$, the terms involving $\sqrt{R}$ contribute $2\sqrt{w\,(1-w)\, I_{\text{slow}}\, I_{\text{fast}}} = o(I_{\text{slow}})$, and the dominant term is $w\, I_{\text{slow}}$, while the uniform error is $E_{\text{unif}} = I_{\text{slow}} + I_{\text{fast}} \approx I_{\text{slow}}$. Therefore $E_{\text{opt}}/E_{\text{unif}} \to w = u_R - u_L$ as $R \to \infty$. ☐

For an uncertainty interval $[0.4, 0.8]$, the hedging schedule achieves error $E_{\text{opt}}/E_{\text{unif}} = 0.4$ compared to a uniform schedule at the same total runtime, a 60% reduction in transition probability. Bounded uncertainty about $s^*$ yields a constant-factor improvement proportional to the interval width, not an exponential overhead. The hedging schedule corresponds to Level 2 of the ignorance taxonomy developed in section 9.7.

## 9.3 Quantum Bypass

The separation theorem and the interpolation theorem characterize the cost of ignorance within the fixed-schedule model. An adiabatic device, however, is a physical system that can be measured during execution. The original paper [14] posed the question: "Can this limitation be overcome when one only has access to a device operating in the adiabatic setting?"

The answer is yes in an adaptive measurement model. Han, Park, and Choi [38] independently proposed a constant geometric speed (CGS) schedule that traverses the eigenstate path at uniform arc length, using eigenstate overlaps computed on the fly via the quantum Zeno Monte Carlo method to adaptively adjust the parameter velocity. Their approach improves the gap scaling from $O(\Delta_*^{-2})$ to $O(\Delta_*^{-1})$ and demonstrates numerically that the quadratic speedup persists for adiabatic unstructured search without prior spectral knowledge. The binary-search protocol below differs in mechanism: it uses branch probes to locate the crossing before executing the informed schedule, and in the ideal binary decision-probe model it achieves $O(T_{\text{inf}})$.

NP-hardness conflates two distinct tasks: *computing* $s^*$ from the classical description of $H_z$ is hard, but *detecting* $s^*$ by probing the quantum system $H(s)$ at selected parameter values can be efficient. We formalize this with a binary decision-probe oracle: a probe at parameter value $s$ returns whether $s$ lies to the left or right of the true crossing, and each probe costs $O(1/g(s))$.

**Definition 9.3.1** (Binary decision probe)**.** *For an instance $H$, let $D_H : [0,1] \to \{0,1\}$ be the idealized oracle*

$$D_H(s) = \begin{cases} 0, & s < s^*(H), \\ 1, & s > s^*(H), \end{cases}$$

*with probe cost $O(1/g_H(s))$.*

**Definition 9.3.2** (Adaptive adiabatic protocol)**.** *The protocol operates in two phases.*

Phase 1 (Location). *Initialize $s_{\text{lo}} = 0$, $s_{\text{hi}} = 1$. For $i = 1, \dots, \lceil n/2 \rceil$:*

1. *Set $s_{\text{mid}} = (s_{\text{lo}} + s_{\text{hi}})/2$.*
2. *Query $D_H(s_{\text{mid}})$.*
3. *If $D_H(s_{\text{mid}}) = 0$ (left of crossing), set $s_{\text{lo}} = s_{\text{mid}}$.*
4. *If $D_H(s_{\text{mid}}) = 1$ (right of crossing), set $s_{\text{hi}} = s_{\text{mid}}$.*

*After $\lceil n/2 \rceil$ iterations, $s^*$ is located to precision $O(2^{-n/2})$.*

Phase 2 (Execution). *Reset the state to $|\psi_0\rangle$. Evolve from $s = 0$ to $s = 1$ using the informed local schedule of Theorem 7.4.1, with the crossing position estimated in Phase 1.*

**Lemma 9.3.3** (Decision-probe cost)**.** *Each call to $D_H(s_{\text{mid}})$ costs $O(1/g(s_{\text{mid}}))$.*

*Proof.* Immediate from Definition 9.3.1. □

**Lemma 9.3.4** (Phase 1 cost)**.** *The total time for Phase 1 is $O(T_{\text{inf}})$.*

*Proof.* Let $d_i = |s_{\text{mid},i} - s^*|$ be the distance from the $i$-th midpoint to the true crossing. From the piecewise gap profile established in Chapter 6: outside the crossing window ($|s - s^*| > \delta_s$), the gap satisfies $g(s) \geq c_{\min}|s - s^*|$ where $c_{\min} = \min(c_L, c_R)$ with $c_L = A_1(A_1+1)/A_2$ and $c_R = \Delta/30$ (both positive constants independent of $n$); inside the crossing window ($|s - s^*| \leq \delta_s$), the gap satisfies $g(s) \geq g_{\min}$. Since $g_{\min}$ is the global minimum, both cases combine to

$$g(s_{\text{mid},i}) \geq \max(g_{\min},\ c_{\min} \cdot d_i). \tag{9.3.1}$$

The probe cost at iteration $i$ is therefore

$$O\left(\frac{1}{g(s_{\text{mid},i})}\right) \leq O\left(\min\left(\frac{1}{g_{\min}},\ \frac{1}{c_{\min} \cdot d_i}\right)\right). \tag{9.3.2}$$

The two bounds in (9.3.2) cross at $d_i = g_{\min}/c_{\min}$. Since $g_{\min} = c_L \delta_s \cdot (1 - O(\eta))$ and $c_{\min} \leq c_L$, the crossover distance satisfies $d_{\text{cross}} = g_{\min}/c_{\min} = (c_L/c_{\min})\, \delta_s \geq \delta_s$. The ratio $c_L/c_{\min}$ is a positive constant independent of $n$: both $c_L = A_1(A_1+1)/A_2$ and $c_R = \Delta/30$ are determined by the spectral parameters, so $c_{\min} = \min(c_L, c_R) > 0$ is a fixed constant. At most $O(\log(c_L/c_{\min}) + 1) = O(1)$ binary search midpoints fall in the near regime $d_i \leq d_{\text{cross}}$.

Group the $\lceil n/2 \rceil$ iterations by the distance $d_i$ in dyadic shells $S_j = [2^{-j-1}, 2^{-j}]$. Let $L_i = 2^{-i+1}$ be the binary-search interval width at step $i$. Since the next interval is the half containing $s^*$, the midpoint distances obey

$$d_{i+1} = \left| d_i - \frac{L_i}{4} \right| = \left| d_i - 2^{-i-1} \right|.$$

This recurrence gives $O(1)$ occupancy per shell: for $i > j+1$, $d_i \leq L_i/2 = 2^{-i} < 2^{-j-1}$, so $d_i \notin S_j$; and for $i \leq j$, if $d_i \in (2^{-j-1}, 2^{-j})$, then $d_{i+1} \notin (2^{-j-1}, 2^{-j})$. Thus the shell interior is visited at most once, with only a dyadic-rational edge case where the boundary value $2^{-j-1}$ can appear twice consecutively. Hence each shell contributes $O(1)$ midpoint queries.

*Far shells* ($j < \log_2(1/\delta_s) \approx n/2$): here $d_i > \delta_s$, so the binding bound in (9.3.2) is $O(1/(c_{\min} \cdot d_i)) = O(2^j/c_{\min})$, where $c_{\min}$ enters the implicit constant.

*Near shells* ($j \geq n/2$): here $d_i \leq \delta_s$, so the binding bound is $O(1/g_{\min}) = O(1/\Delta_*) = O(2^{n/2})$.

There are $O(1)$ near shells (at most $O(1)$ midpoints can have $d_i \leq d_{\text{cross}}$ in a binary search). The total cost is:

$$\sum_{j=0}^{n/2-1} O(1) \cdot O(2^j) + O(1) \cdot O(2^{n/2}) = O(2^{n/2}) + O(2^{n/2}) = O(2^{n/2}) = O(T_{\text{inf}}). \tag{9.3.3}$$

The state preparation cost is $O(n)$ per iteration and $O(n)$ iterations, giving $O(n^2) = o(T_{\text{inf}})$. □

**Theorem 9.3.5** (Adaptive adiabatic optimality in the decision-probe model)**.** *The adaptive protocol of Definition 9.3.2 achieves runtime $T_{\mathrm{adapt}} = O(T_{\inf})$ with $\Theta(n)$ measurements.*

*Proof.* Phase 1 locates $s^*$ to precision $O(2^{-n/2}) = O(\delta_s)$ using total time $O(T_{\inf})$ by Lemma 9.3.4. This precision is within the crossing window width $\delta_s = O(\Delta_*)$. Phase 2 has time $O(T_{\inf})$ by Theorem 7.4.1, since the estimate of $s^*$ is accurate to $O(\delta_s)$. The total is $O(T_{\inf}) + O(T_{\inf}) = O(T_{\inf})$. □

**Theorem 9.3.6** (Measurement lower bound)**.** *Any adaptive algorithm in the binary decision-probe model (each measurement returns one bit indicating the ground/excited branch at the probe point) achieving $T = O(T_{\inf})$ requires $\Omega(n)$ measurements.*

*Proof.* The crossing position $s^*$ can lie anywhere in an interval of width $\Theta(1)$. To achieve the informed runtime, the algorithm must locate $s^*$ to precision $\delta_s = O(2^{-n/2})$, since any larger uncertainty incurs the overhead of Theorem 9.2.2. This means distinguishing among $\Omega(2^{n/2})$ possible positions. In the binary decision-probe model, each measurement contributes at most one bit by definition. The information needed is $\log_2(2^{n/2}) = n/2$ bits, requiring $\Omega(n)$ measurements. □

The three adiabatic regimes:

| Strategy | Runtime | Measurements |
|---|---|---|
| Fixed, uninformed | $\Omega(2^{n/2} \cdot T_{\inf})$ | 0 |
| Adaptive | $O(T_{\inf})$ | $\Theta(n)$ |
| Fixed, informed | $O(T_{\inf})$ | 0 |

For the running example ($N = 4$, $d_0 = 1$, $n = 2$): Phase 1 performs $\lceil 1 \rceil = 1$ probe at $s_{\mathrm{mid}} = 0.5$, so the location stage already achieves width $1/2 = O(2^{-n/2})$. The gap there is $g(0.5) = 1/\sqrt{N} = 1/2$, giving probe cost $O(1/g) = O(2) = O(T_{\inf})$.

*Implementation note.* A physical instantiation of $D_H$ can be attempted via phase-estimation-based branch tests on $H(s_{\mathrm{mid}})$. The theorem above is intentionally stated in the ideal decision-probe model; a full finite-sample reliability analysis for this instantiation is separate from the present minimax argument.

The adaptive protocol acquires $A_1$ through measurement; the circuit model bypasses $A_1$ entirely. The Dürr-Høyer quantum minimum-finding algorithm [34] achieves $\Theta(\sqrt{N/d_0})$ by maintaining a threshold and iteratively lowering it using Grover search, never traversing an adiabatic path and never encountering an avoided crossing. The mechanism is amplitude amplification with iterative thresholding, which uses no spectral parameter — no $A_1$, $s^*$, $\Delta$, or gap profile.

**Proposition 9.3.7** ($A_1$-blindness)**.** *Let $X_{\mathrm{DH}}$ denote the output of the amplified Dürr-Høyer algorithm (with $r = \Theta(n)$ repetitions). Then $I(X_{\mathrm{DH}}; A_1 \mid S_0, E_0) \leq 2^{-\Omega(n)}$. Conditioned on success ($X_{\mathrm{DH}} \in S_0$), the mutual information is exactly zero.*

*Proof.* Two problem Hamiltonians $H_z, H'_z$ are ground-equivalent if they share the same ground energy $E_0$ and ground space $S_0$. By symmetry of Grover's algorithm applied to the uniform initial state, the output distribution conditioned on success is $\mathrm{Uniform}(S_0)$, regardless of the excited spectrum. Since $A_1$ depends only on the excited spectrum (via $\{d_k, E_k\}_{k\geq 1}$), we have

$$I(X_{\mathrm{DH}};\, A_1 \mid \mathrm{success}, S_0, E_0) = 0.$$

Let $F$ be the failure indicator of the amplified routine, and fix any prior over ground-equivalent instances conditioned on $(S_0, E_0)$. With $r = \Theta(n)$ repetitions using Boyer-Brassard-Høyer-Tapp amplification [2], the per-trial success probability is at least $2/3$, so

$$p_f := \Pr[F = 1] \leq (1/3)^r = 2^{-\Omega(n)}.$$

Using chain rule and the fact that $F$ is a function of $X_{\mathrm{DH}}$:

$$\begin{aligned} I(X_{\mathrm{DH}};\, A_1 \mid S_0, E_0) &\leq I(X_{\mathrm{DH}}, F;\, A_1 \mid S_0, E_0) \\ &= I(F;\, A_1 \mid S_0, E_0) + I(X_{\mathrm{DH}};\, A_1 \mid F, S_0, E_0) \\ &= I(F;\, A_1 \mid S_0, E_0) + p_f\, I(X_{\mathrm{DH}};\, A_1 \mid F = 1, S_0, E_0) \\ &\leq H(F) + p_f\, H(X_{\mathrm{DH}} \mid F = 1, S_0, E_0). \end{aligned} \tag{9.3.4}$$

The $F = 0$ term vanishes by the conditional independence established above. Now $H(F) \leq h_2(p_f)$, where $h_2(p) = -p \log p - (1-p)\log(1-p)$ is the binary entropy, and $H(X_{\mathrm{DH}} \mid F = 1, S_0, E_0) \leq \log N = n$, so Eq. (9.3.4) gives

$$I(X_{\mathrm{DH}};\, A_1 \mid S_0, E_0) \leq h_2(p_f) + p_f n = 2^{-\Omega(n)}.$$

□

The circuit model does not merely avoid computing $A_1$; it is provably blind to it. The adiabatic model requires and leaks information about $A_1$: a schedule tuned to $A_1$ achieves success probability $\geq 1 - \varepsilon$, while the same schedule applied to a ground-equivalent instance with different $A_1$ yields low success probability. The adaptive adiabatic model sits between: it acquires $A_1$ through $O(n)$ quantum measurements, paying $O(T_{\text{inf}})$ for the acquisition. The three models form a hierarchy of spectral information usage, from full blindness (circuit) through active acquisition (adaptive) to passive dependence (fixed schedule).

The adaptive protocol relies on the rank-one gap profile, which grows linearly from the crossing ($\alpha = 1$). This linear growth is what makes each binary search step informative: the gap at distance $d$ from the crossing is $\Theta(d)$, so the decision-probe cost at distance $d$ is $O(1/d)$, and the geometric series converges. What happens when the gap approaches its minimum more gently?

## 9.4 Gap Geometry and Schedule Optimality

The flatness exponent $\alpha$ parametrizes how the gap approaches its minimum: $g(s) \approx c|s - s^*|^\alpha$ outside the crossing window. For the rank-one profile, $\alpha = 1$, and the runtime is $O(1/\Delta_*)$. Flatter gap profiles ($\alpha > 1$) are worse. Guo and An [25] identified the measure condition — a regularity condition on the gap function controlling whether the power-law schedule of exponent $p = 3/2$ achieves $O(1/g_{\min})$ — and proved its sufficiency. We prove the complementary degradation: for $\alpha > 1$, the measure condition fails and the variationally optimal $p = 3/2$ schedule degrades from $T = O(1/\Delta_*)$ to $T = O(1/\Delta_*^{3-2/\alpha})$. Whether a non-power-law schedule family can achieve $T = O(1/\Delta_*)$ when the measure condition fails remains open. The constant geometric speed (CGS) schedule of Han, Park, and Choi [38] achieves $O(1/g_{\min})$ by adaptively measuring the gap, but it uses runtime quantum feedback and is not a fixed schedule. Among fixed, non-adaptive schedules, no family is known to beat $O(1/\Delta_*^{3-2/\alpha})$ for $\alpha > 1$.

Consider a gap function with flatness exponent $\alpha > 0$: near the minimum, $g(s) = \Delta_* + c|s - s^*|^\alpha$ for a constant $c > 0$. The measure condition requires that $\mu(\{s : g(s) \leq x\}) \leq Cx$ for all $x > 0$, where $C$ is independent of $\Delta_*$.

**Theorem 9.4.1** (Geometric characterization)**.** *The measure condition holds with $C$ independent of $\Delta_*$ if and only if $\alpha \leq 1$.*

*Proof.* For $x \geq \Delta_*$, the sublevel set $\{s : g(s) \leq x\}$ near $s^*$ has measure $\mu = 2((x - \Delta_*)/c)^{1/\alpha}$.

*Case $\alpha \leq 1$.* The ratio $\mu/x = 2((x - \Delta_*)/c)^{1/\alpha}/x$ is an increasing function of $x$ for $\alpha \leq 1$: differentiating, $d(\mu/x)/dx = (2/(c^{1/\alpha}\alpha x^2))\,((x-\Delta_*)/c)^{1/\alpha-1}\,((1/\alpha-1)(x-\Delta_*)+\Delta_*/\alpha)$, where both terms in the parentheses are nonnegative since $1/\alpha - 1 \geq 0$ and $\Delta_* > 0$. But $\mu$ is also capped by 1 (the measure of $[0, 1]$), and the cap is achieved at $x_{\text{cap}} = \Delta_* + c(1/2)^\alpha$, where the sublevel set spans $[0, 1]$. For $x > x_{\text{cap}}$, $\mu/x = 1/x < 1/x_{\text{cap}}$. Taking the supremum: $C = \sup_{x>0} \mu/x \leq 1/x_{\text{cap}} \leq 2^\alpha/c$, independent of $\Delta_*$.

*Case $\alpha > 1$.* At $x = 2\Delta_*$, the ratio is $\mu/x = 2(\Delta_*/c)^{1/\alpha}/(2\Delta_*) = c^{-1/\alpha}\Delta_*^{1/\alpha-1}$. Since $1/\alpha - 1 < 0$, this diverges as $\Delta_* \to 0$. No finite $C$ works for all $\Delta_*$. □

The gap integral $\int_0^1 g(s)^{-\beta}\,ds$ controls the runtime for power-law schedules. A substitution $u = c|s-s^*|^\alpha/\Delta_*$ gives the following scaling.

**Lemma 9.4.2** (Gap integral)**.** *For $\beta > 1/\alpha$,*

$$\int_0^1 g(s)^{-\beta}\,ds = \Theta(\Delta_*^{1/\alpha-\beta}). \tag{9.4.1}$$

*For $\beta = 1/\alpha$, the integral is $\Theta(\log(1/\Delta_*))$. For $\beta < 1/\alpha$, the integral is $\Theta(1)$.*

*Proof.* The substitution $u = (c|s - s^*|^\alpha)/\Delta_*$ transforms the near-minimum contribution to

$$\Delta_*^{1/\alpha-\beta} \int_0^U u^{1/\alpha-1}(1+u)^{-\beta}\,du,$$

where $U = \Theta(1/\Delta_*)$. As $u \to \infty$, the integrand behaves like $u^{1/\alpha-1-\beta}$.

If $\beta > 1/\alpha$, the exponent is strictly less than $-1$, so the $u$-integral converges to a finite constant, yielding $\Theta(\Delta_*^{1/\alpha-\beta})$.

If $\beta = 1/\alpha$, the integrand is asymptotically $u^{-1}$, so the integral contributes $\Theta(\log U) = \Theta(\log(1/\Delta_*))$.

If $\beta < 1/\alpha$, the integral grows as $U^{1/\alpha-\beta}$, which cancels the prefactor $\Delta_*^{1/\alpha-\beta}$, giving $\Theta(1)$.

The contribution from outside a neighborhood of $s^*$ is always $O(1)$: for $|s-s^*| \geq \delta$ with $\delta$ fixed, $g(s) \geq g_0 > 0$ independent of $\Delta_*$, so $\int_{|s-s^*|\geq\delta} g(s)^{-\beta} ds \leq g_0^{-\beta}$. □

**Theorem 9.4.3** (Scaling spectrum)**.** *For a gap function with flatness exponent $\alpha > 2/3$, the adiabatic runtime with the $p = 3/2$ power-law schedule (variationally optimal in the JRS framework [25]) satisfies*

$$T = \Theta(1/\Delta_*^{3-2/\alpha}). \tag{9.4.2}$$

*Proof.* The power-law schedule $u'(s) = c_p\, g(u(s))^p$ has normalization constant $c_p = \int_0^1 g(v)^{-p}\, dv$. The JRS error functional becomes

$$\eta \le \frac{1}{T}\, c_p \int_0^1 g(v)^{p-3}\, dv. \tag{9.4.3}$$

By Lemma 9.4.2, $c_p = \Theta(\Delta_*^{1/\alpha - p})$ (requiring $p > 1/\alpha$) and the second integral is $\Theta(\Delta_*^{1/\alpha + p - 3})$ (requiring $3 - p > 1/\alpha$). Together these require $1/\alpha < p < 3 - 1/\alpha$, an interval of width $3 - 2/\alpha$, which is positive if and only if $\alpha > 2/3$. The symmetric choice $p = 3/2$ lies in this interval for all $\alpha > 2/3$. Their product is

$$c_p \int g^{p-3}\, dv = \Theta(\Delta_*^{(1/\alpha - p) + (1/\alpha + p - 3)}) = \Theta(\Delta_*^{2/\alpha - 3}). \tag{9.4.4}$$

Setting $\eta = O(1)$ gives $T = \Omega(\Delta_*^{-(3-2/\alpha)}) = \Omega(1/\Delta_*^{3-2/\alpha})$. The $p = 3/2$ power-law schedule achieves this scaling, giving a matching upper bound $T = O(1/\Delta_*^{3-2/\alpha})$. ☐

| $\alpha$ | Exponent $\gamma = 3 - 2/\alpha$ | Measure condition | Runtime |
|---|---|---|---|
| 1 | 1 | Holds | $\Theta(1/\Delta_*)$ |
| 2 | 2 | Fails | $\Theta(1/\Delta_*^2)$ |
| 3 | 7/3 | Fails | $\Theta(1/\Delta_*^{7/3})$ |
| $\infty$ | 3 | Fails | $\Theta(1/\Delta_*^3)$ |

The runtime exponents form a continuous spectrum from 1 (V-shaped minimum, best case) to 3 (flat minimum, worst case), refuting any binary dichotomy between "easy" and "hard" gap profiles. For the running example ($M = 2$, $d_0 = 1$, $N = 4$), $\alpha = 1$ and $\gamma = 1$, confirming the optimal $T = \Theta(1/\Delta_*)$ scaling.

**Remark.** *The exponent $\gamma = 3$ at $\alpha = \infty$ reflects the $p = 3/2$ power-law schedule, which is variationally optimal within the JRS error functional but not universally optimal across all adiabatic bounds. The Roland-Cerf schedule ($p = 2$) gives $T = O(1/\Delta_*^2)$ at $\alpha = \infty$ via a tighter adiabatic condition for flat gaps. The table shows the scaling of the JRS-optimal schedule as the gap flattens; different schedule families and adiabatic bounds produce different exponent curves.*

**Proposition 9.4.4** (Structural $\alpha = 1$)**.** *For the rank-one Hamiltonian $H(s) = -(1-s)\,|\psi_0\rangle\langle\psi_0| + sH_z$ with $d_1 \ge 1$ and $\Delta > 0$, the flatness exponent is $\alpha = 1$.*

*Proof.* Near $s^*$, the two lowest eigenvalues form an avoided crossing described by the standard formula $g(s) = \sqrt{g_{\min}^2 + c_L^2 (s - s^*)^2}$. For $|s - s^*| \gg g_{\min}/c_L = \delta_s$, the gap grows linearly: $g(s) \approx c_L |s - s^*|$. The crossing is simple (not higher-order) because the coupling between the two lowest branches is proportional to $|\langle\psi_0\rangle\, \phi_1|^2 = d_1/N > 0$, where $|\phi_1\rangle$ is the symmetric state of the first excited level. A higher-order crossing ($\alpha > 1$) would require this coupling to vanish, which cannot happen when $d_1 > 0$. ☐

No choice of $H_z$ with $d_1 > 0$ and $\Delta > 0$ can produce $\alpha \neq 1$. Different values of $\alpha$ require different interpolation schemes (e.g., quantum phase transitions with $H(s)$ nonlinear in $s$, or systems with symmetry-enforced higher-order crossings). This structural $\alpha = 1$ explains why both the Roland-Cerf analysis and the Guo-An framework achieve the same asymptotic runtime.

Braida et al. [14] and Guo and An [25] are independent works on the same problem class. The former provides the spectral analysis ($A_1$, $s^*$, piecewise gap bounds), while the latter provides the variational optimization (power-law schedule, measure condition).

**Theorem 9.4.5** (Measure condition for the rank-one gap profile)**.** *Under the spectral condition of Chapter 5, the piecewise-linear gap profile satisfies the measure condition with*

$$C \le \frac{3A_2}{A_1(A_1 + 1)} + \frac{30(1 - s_0)}{\Delta}, \tag{9.4.5}$$

*where $s_0$ is the right-arm basepoint defined in Chapter 6.*

*Proof.* Fix $x > 0$. For $x < g_{\min}$, the sublevel set is empty. For $x \geq g_{\min}$, bound the contribution from each piece of the gap profile. The left arm ($g(s) \geq c_L(s^* - s)$) contributes at most $x/c_L$. The crossing window ($|s - s^*| \leq \delta_s$) has width $2\delta_s = 2\hat{g}/c_L$, contributing at most $2x/c_L$ for $x \geq \hat{g}$ (for $g_{\min} \leq x < \hat{g}$: since $g_{\min} \geq (1 - 2\eta)\hat{g}$ and $x \geq g_{\min}$, we have $\hat{g} \leq x/(1 - 2\eta)$; for $\eta \leq 1/6$, this gives $\hat{g} \leq 3x/2$, so the window contribution $2\hat{g}/c_L \leq 3x/c_L$; the condition $\eta \leq 1/6$ holds in the asymptotic regime where $\eta = O(\sqrt{d_0/(NA_2)}) \to 0$). The right arm ($g(s) \geq c_R(s - s_0)/(1 - s_0)$) contributes at most $x \cdot 30(1 - s_0)/\Delta$. Combining and substituting $c_L = A_1(A_1 + 1)/A_2$ gives the bound. □

**Corollary 9.4.6** (Grover measure constant)**.** *For Grover ($M = 2$, $d_0 = 1$, $d_1 = N - 1$, $E_0 = 0$, $E_1 = 1$), the exact measure constant is $C = 1$.*

*Proof.* The exact gap is $g(s)^2 = (2s-1)^2(1-1/N)+1/N$. Solving $g(s) \leq x$ gives $\mu(\{g \leq x\}) = \sqrt{(Nx^2 - 1)/(N - 1)}$ for $x \in [1/\sqrt{N}, 1]$, with $\mu = 1$ for $x > 1$. The ratio $\mu/x$ is increasing on $[1/\sqrt{N}, 1]$ and equals 1 at $x = 1$. □

For the Grover problem, the exact gap integral is $\int_0^1 g(s)^{-2}\, ds = (N/\sqrt{N-1}) \arctan \sqrt{N-1} \to (\pi/2)\sqrt{N}$ as $N \to \infty$. This closed-form evaluation confirms the $O(\sqrt{N})$ runtime from the piecewise analysis and provides the exact constant. For the running example ($N = 4$), $\int_0^1 g(s)^{-2}\, ds = (4/\sqrt{3}) \arctan \sqrt{3} = 4\pi/(3\sqrt{3}) \approx 2.42$, consistent with the runtime $T_{\inf} = O(\sqrt{4}) = O(2)$.

Both the Roland-Cerf $p = 2$ schedule and Guo-An's $p = 3/2$ schedule achieve the same asymptotic runtime $T = O(\sqrt{N/d_0}/\varepsilon)$ (where all spectral parameters $A_1$, $A_2$, $\Delta$ are absorbed into the implicit constant, as declared at the start of this chapter). The RC runtime involves the integral $I = \int_0^1 g(s)^{-2}\, ds$; Guo-An's involves $C^2/g_{\min}$.

**Theorem 9.4.7** (Constant comparison)**.** *Write $a = 3/c_L$ and $r = 30(1 - s_0)/\Delta$. Then $C^2 < I$ if and only if $(c_L - 1)r^2 - 2ar + a(1 - a) > 0$. In the right-arm-dominated regime ($r \gg a$) with $c_L > 1$, this holds, with $C^2/I \to 1/c_L = A_2/(A_1(A_1 + 1))$.*

*Proof.* With $C = a + r$ and $I = a + r^2 c_L$: $I - C^2 = (c_L - 1)r^2 - 2ar + a(1 - a)$. For $c_L > 1$ and $r \gg a$, the leading term $(c_L - 1)r^2$ dominates. □

**Remark.** *The framework comparison extends across gap geometries. For $\alpha < 1$, the Roland-Cerf integral $\int g^{-2}\, ds = \Theta(g_{\min}^{1/\alpha - 2})$ grows slower than $1/g_{\min}$, making the RC analysis tighter. For $\alpha = 1$, both give $\Theta(1/g_{\min})$, and the JRS constant $C^2$ can be smaller than the RC integral $I$ (Theorem 9.4.7). For $\alpha > 1$, the measure constant $C \to \infty$ as $g_{\min} \to 0$, so the JRS framework degrades and only the RC analysis applies. The structural $\alpha = 1$ (Proposition 9.4.4) sits at the exact boundary where both frameworks are valid and neither uniformly dominates.*

For the Grover problem, $c_L \to 2$ as $N \to \infty$, and using exact values $C_{\text{exact}} = 1$, $I_{\text{exact}} \to (\pi/2)\sqrt{N}$, the ratio $C^2/I \to 2/(\pi\sqrt{N}) \to 0$: the JRS certification is asymptotically tighter. The Grover gap has a closed-form expression that makes the exact measure constant computable. For structured Hamiltonians with richer spectra, the exact constants are not available analytically, and the bound-constant ratio from Theorem 9.4.7 provides the comparison. Evaluating the theorem for the open ferromagnetic Ising chain (Equation 5.1.4 with nearest-neighbor coupling $J = 1$ and uniform field $h = 1$, $n = 10$ spins) gives $C^2/I = 0.71$: the JRS advantage persists, though with a weaker margin than Grover. The two frameworks are complementary, not competing. The spectral analysis [14] identifies $A_1$, $s^*$, and the piecewise gap structure. The variational optimization [25] determines the optimal power-law exponent. Together they give a complete picture: the rank-one $\alpha = 1$ gap sits at the exact boundary where both frameworks apply and the measure condition holds with a bounded constant.

The complementarity extends to their sensitivity under partial spectral knowledge. The RC framework ($p = 2$) constructs its schedule from the crossing position $s^*$, so its runtime degrades on the crossing-localization scale: $T_{\text{RC}}(\varepsilon_{A_1}) = T_{\text{RC},\infty} \cdot \Theta(\max(1, \varepsilon_{A_1}/\delta_{A_1}))$, where $\delta_{A_1} = 2\sqrt{d_0 A_2/N}$ is the precision threshold from Theorem 9.2.2. The JRS framework ($p = 3/2$) instead requires certified bounds $(C_+, g_-)$ on the measure constant and minimum gap, producing a multiplicative overhead $((1 + \delta_C/C)^2)/(1 - \delta_g/g_{\min})$ where $\delta_C$ and $\delta_g$ are the estimation errors. The two frameworks have qualitatively different sensitivity profiles: RC needs $s^*$ to exponentially small precision $\delta_s = \Theta(2^{-n/2})$, while JRS needs $C$ and $g_{\min}$ only to constant relative precision. When spectral parameters are partially known — the situation forced by NP-hardness — the JRS framework may be more robust to imprecise inputs, even though both frameworks achieve the same asymptotic scaling.

The gap geometry and optimality analysis above assumes the rank-one interpolation $H(s) = -(1-s)\,|\psi_0\rangle\langle\psi_0| + sH_z$. The rank-one structure is a design choice, not a physical constraint. Can a different design — different initial state, ancilla qubits, multi-segment path — avoid the $A_1$ dependence entirely?

## 9.5 Anatomy of the Barrier

No instance-independent modification within the rank-one framework can make $s^*$ spectrum-independent. The argument proceeds through four theorems that progressively close escape routes, culminating in a no-go theorem.

Recall from Chapter 5 that for any initial state $|\psi\rangle \in \mathbb{C}^N$, the weights $w_k(\psi) = \sum_{z\in\Omega_k} |\langle z\rangle\, \psi|^2$ determine the effective spectral parameter $A_1^{\text{eff}}(\psi) = \sum_{k\geq 1} w_k(\psi)/(E_k - E_0)$ and the effective crossing position $s^*(\psi) = A_1^{\text{eff}}(\psi)/(A_1^{\text{eff}}(\psi)+1)$. For the uniform superposition $|\psi_0\rangle$, $w_k = d_k/N$ and $A_1^{\text{eff}} = A_1$.

**Theorem 9.5.1** (Product ancilla invariance)**.** *For any product initial state $|\Psi\rangle = |\psi_0\rangle \otimes |\phi\rangle$ and uncoupled final Hamiltonian $H_f = H_z \otimes I_{2^m}$, the extended Hamiltonian $H_{\text{ext}}(s) = -(1-s)\,|\Psi\rangle\langle\Psi| + s(H_z \otimes I_{2^m})$ has the same crossing position $s^* = A_1/(A_1+1)$ as the bare system.*

*Proof.* Decompose the extended Hilbert space $\mathbb{C}^N \otimes \mathbb{C}^{2^m}$ into the subspace $\mathcal{V}_\phi = \mathbb{C}^N \otimes |\phi\rangle$ and its orthogonal complement. States $|z\rangle \otimes |a\rangle$ with $\langle\phi\rangle\, a = 0$ satisfy $\langle\Psi\rangle\, z, a = 0$, making them exact eigenstates of $H_{\text{ext}}(s)$ with eigenvalue $sE(z)$. These $N(2^m-1)$ states do not participate in the avoided crossing. The restriction of $H_{\text{ext}}(s)$ to $\mathcal{V}_\phi$ is unitarily equivalent to the bare Hamiltonian $H(s)$ via the isomorphism $|\psi\rangle \otimes |\phi\rangle \mapsto |\psi\rangle$. □

**Remark.** *The crossing position is invariant, but the gap of $H_{\text{ext}}(s)$ is strictly smaller than the bare gap: for $d_0 = 1$, the extra eigenvalues at $sE_0$ (from states $|z\rangle\otimes|a\rangle$ with $z \in \Omega_0$, $a \perp |\phi\rangle$) sit between the ground eigenvalue $\lambda_0(s) < sE_0$ and the crossing branch. Uncoupled ancillas make the gap worse, not better.*

**Theorem 9.5.2** (Universality of uniform superposition)**.** *Among all states $|\psi\rangle \in \mathbb{C}^N$, the uniform superposition $|\psi_0\rangle$ is the unique state (up to per-basis-element phases) for which the weights $w_k(\psi)$ depend only on $\{E_k, d_k\}$ and not on the specific assignment of energies to computational basis states.*

*Proof.* An energy assignment is a function $\sigma : \{0,\ldots,N-1\} \to \{E_0,\ldots,E_{M-1}\}$ with $|\sigma^{-1}(E_k)| = d_k$. The weights under assignment $\sigma$ are $w_k(\psi,\sigma) = \sum_{z:\sigma(z)=E_k} |\langle z\rangle\, \psi|^2$. We require $w_k(\psi,\sigma) = w_k(\psi,\sigma')$ for all assignments $\sigma, \sigma'$ with the same degeneracies.

Any two such assignments are related by a permutation $\pi$ of $\{0,\ldots,N-1\}$. The condition becomes $\sum_{z\in\Omega_k} |\langle z\rangle\, \psi|^2 = \sum_{z\in\Omega_k} |\langle \pi^{-1}(z)\rangle\, \psi|^2$ for all $k$ and all permutations $\pi$.

*Necessity.* Consider two-level spectra with $d_0 = 1$. For any two basis states $z_a, z_b$, the transposition swapping them maps the assignment $\sigma$ (with $\sigma(z_a) = E_0$) to $\sigma'$ (with $\sigma'(z_b) = E_0$). The condition forces $|\langle z_a\rangle\, \psi|^2 = |\langle z_b\rangle\, \psi|^2$. Since $z_a, z_b$ are arbitrary, $|\langle z\rangle\, \psi|^2 = 1/N$ for all $z$.

*Sufficiency.* If $|\langle z\rangle\, \psi|^2 = 1/N$ for all $z$, then $w_k = d_k/N$ regardless of the assignment. □

**Corollary 9.5.3.** *Any instance-independent adiabatic algorithm (same Hamiltonian for all energy assignments with the same degeneracy structure) must use the uniform superposition as initial state, fixing the crossing at $s^* = A_1/(A_1+1)$.*

**Theorem 9.5.4** (Coupled ancilla limitation)**.** *Consider an extended Hamiltonian $H_{\text{ext}}(s) = -(1-s)\,|\Psi\rangle\langle\Psi| + s(H_z \otimes I + V)$ where $|\Psi\rangle = |\psi_0\rangle \otimes |\phi\rangle$ and $V$ is instance-independent. No fixed $V$ makes $A_1^{\text{eff}}$ constant across all problem instances.*

*Proof.* Consider the two-level family parametrized by $\Delta > 0$: $E_0 = 0$, $E_1 = \Delta$, $d_0 = 1$, $d_1 = N-1$. For $\Delta > 2\|V\|$, by Weyl's inequality each eigenvalue of $H_f(\Delta) = H_z(\Delta) \otimes I + V$ lies within $\|V\|$ of an eigenvalue of $H_z(\Delta) \otimes I$, so the spectrum splits into two well-separated clusters: one near energy 0 (within $\|V\|$ of 0) and one near energy $\Delta$ (within $\|V\|$ of $\Delta$). Each eigenvalue $E_j$ in the excited cluster satisfies $|E_j - \Delta| \leq \|V\|$, so the excited contribution to $A_1^{\text{eff}}$ is $\sum_{j\in\text{excited}} |\langle\Psi\rangle\, \phi_j|^2/(E_j - E_0) = (1 - d_0/N)/(\Delta + O(\|V\|)) = \Theta(1/\Delta)$ for $\Delta \gg \|V\|$. Since $\|V\|$ is a fixed constant independent of $\Delta$, this contribution varies with $\Delta$, so $A_1^{\text{eff}}(\Delta)$ is non-constant. □

**Theorem 9.5.5** (Multi-segment rigidity)**.** *Consider a two-segment path where segment 2 has Hamiltonian $H_2(t) = -(1-t)\,|\psi_{\text{mid}}\rangle\langle\psi_{\text{mid}}| + tH_z$. If the algorithm is instance-independent, then the intermediate state $|\psi_{\text{mid}}\rangle$ must be the uniform superposition, giving the same crossing $B_1 = A_1$.*

*Proof.* Segment 2 is a rank-one adiabatic Hamiltonian with initial state $|\psi_{\text{mid}}\rangle$. Its crossing position is $t^* = B_1/(B_1+1)$ where $B_1 = \sum_{k\geq 1} w_k(\psi_{\text{mid}})/(E_k - E_0)$. If segment 1 does not involve $H_z$, then $|\psi_{\text{mid}}\rangle$ is determined entirely by segment 1's Hamiltonian, which is instance-independent. Since $|\psi_{\text{mid}}\rangle$ is then the same for all energy assignments with the same degeneracy structure, Theorem 9.5.2 forces $w_k = d_k/N$, so $B_1 = A_1$. If segment 1 involves $H_z$, then $|\psi_{\text{mid}}\rangle$ already depends on the spectrum, and the algorithm is not instance-independent. □

**Theorem 9.5.6** (No-go)**.** *For any adiabatic algorithm using a rank-one initial Hamiltonian, a final Hamiltonian whose ground state encodes the solution, and instance-independent design, the crossing position cannot be made independent of the problem spectrum.*

*Proof.* Combine Theorems 9.5.1–9.5.5: Theorem 9.5.2 forces the uniform superposition; Theorem 9.5.1 shows uncoupled ancillas preserve $s^*$; Theorem 9.5.4 shows coupled ancillas shift $s^*$ but cannot make it constant; Theorem 9.5.5 shows multi-segment paths within the rank-one framework cannot escape. □

For the running example ($N = 4$, $d_0 = 1$), product ancilla invariance (Theorem 9.5.1) implies that appending any number of ancilla qubits in a product state leaves the crossing at $s^* = 3/7$.

The no-go theorem applies specifically to the rank-one framework with instance-independent design. Higher-rank initial Hamiltonians are a natural candidate for circumventing the rank-one obstruction. They do not succeed: the following propositions show that rank-$k$ projectors cannot make crossing positions spectrum-independent, first on two-level families and then on general multilevel families via a trace argument. For rank-$k$ projectors $P = UU^\dagger$, the secular equation generalizes to the $k\times k$ determinant condition $\det(I_k - (1-s)G(\lambda, s)) = 0$ where $G(\lambda, s) = U^\dagger(sH_z - \lambda I)^{-1}U$. On the two-level family ($E_0 = 0$, $E_1 = \Delta$), this reduces to $\det(I_k - (x/\Delta)B) = 0$ where $B = U_{\text{exc}}^\dagger U_{\text{exc}}$ and $x = (1-s)/s$. Each positive eigenvalue $\mu$ of $B$ gives a crossing branch $s(\Delta) = 1/(1 + \Delta/\mu)$, which is non-constant as a function of $\Delta$.

**Proposition 9.5.7** (Rank-$k$ two-level obstruction)**.** *Fixed rank-$k$ projectors cannot make crossing positions spectrum-independent on fixed-degeneracy two-level families unless the projector has zero support on excited states.*

For the general multilevel case, the trace argument provides a clean obstruction.

**Proposition 9.5.8** (Trace no-go)**.** *For a rank-$k$ projector $P = UU^\dagger$ and the multilevel family with gaps $\Delta_1, \ldots, \Delta_{M-1}$, define the reduced matrix $A(\Delta) = \sum_{\ell=1}^{M-1} B_\ell/\Delta_\ell$ where $B_\ell = U_\ell^\dagger U_\ell \succeq 0$ collects the excited-level contributions. If $B_j \neq 0$ and $\Delta_j$ varies, then $\operatorname{tr}(A(\Delta)) = \sum_\ell \operatorname{tr}(B_\ell)/\Delta_\ell$ is non-constant in $\Delta_j$. By Weyl's eigenvalue monotonicity theorem, each eigenvalue of $A(\Delta)$ is a continuous function of $\Delta_j$, and the sum of the positive eigenvalues equals $\operatorname{tr}(A)$. Since the trace changes, at least one positive eigenvalue — and hence at least one crossing position — must change with $\Delta_j$.*

**Remark.** *When the excited blocks commute ($[B_\ell, B_m] = 0$ for all $\ell, m$), the reduced crossing equation admits simultaneous diagonalization, giving explicit per-branch formulas: each active branch $r$ with $G_r(\Delta) = \sum_\ell \mu_{\ell r}/\Delta_\ell > 0$ has crossing position $s_r = G_r/(1+G_r)$, and varying any gap $\Delta_j$ gives $\partial s_r/\partial\Delta_j = -\mu_{jr}/(\Delta_j^2(1+G_r)^2) \leq 0$, with strict inequality whenever the branch has support on the varied level ($\mu_{jr} > 0$). The commuting case thus provides explicit, quantitative non-constancy for each individual branch, complementing the trace argument's aggregate statement. Even the most tractable generalization of the secular equation — simultaneous diagonalization with explicit formulas — cannot achieve spectrum-independent crossings.*

The barrier is structural within the rank-one framework and extends to higher-rank families. Whether time-dependent couplings or non-rank-one intermediate Hamiltonians provide a genuine escape remains open. But the no-go is specific to the monotone-schedule adiabatic framework. Dropping the monotone constraint reveals that constant controls already suffice on the restricted two-level family.

**Proposition 9.5.9** (Constant-control optimality on two-level family)**.** *For $H_z = I - P_0$ where $P_0$ projects onto the $d_0$-dimensional ground space, the continuous-time rank-one Hamiltonian $H = -|\psi_0\rangle\langle\psi_0| + H_z$ with constant controls achieves $p_0(t^*) = 1$ at $t^* = (\pi/2)\sqrt{N/d_0}$, with controls independent of $A_1$ (on the two-level family $H_z = I - P_0$).*

*Proof.* Let $\mu = d_0/N$, $|G\rangle = d_0^{-1/2}\sum_{x\in S_0}|x\rangle$, and $|B\rangle = (N-d_0)^{-1/2}\sum_{x\notin S_0}|x\rangle$. The initial state is $|\psi_0\rangle = \sqrt{\mu}\,|G\rangle + \sqrt{1-\mu}\,|B\rangle$. Dropping the global identity term, the effective Hamiltonian in the $(|G\rangle, |B\rangle)$ basis is

$$\widetilde{H} = -\begin{pmatrix} \mu & \sqrt{\mu(1-\mu)} \\ \sqrt{\mu(1-\mu)} & -\mu \end{pmatrix}, \tag{9.5.1}$$

which satisfies $\widetilde{H}^2 = \mu I_2$. The matrix exponential is $e^{-it\widetilde{H}} = \cos(\sqrt{\mu}\,t)\,I_2 - i\sin(\sqrt{\mu}\,t)\,\widetilde{H}/\sqrt{\mu}$. Applying to $|\psi_0\rangle$ and computing the ground-state probability:

$$p_0(t) = |\langle G\rangle\, e^{-it\widetilde{H}}|\psi_0|^2 = \mu + (1-\mu)\sin^2(\sqrt{\mu}\,t). \tag{9.5.2}$$

At $t^* = (\pi/2)/\sqrt{\mu} = (\pi/2)\sqrt{N/d_0}$, $\sin^2(\sqrt{\mu}\,t^*) = 1$, so $p_0(t^*) = 1$. □

On the two-level family, the Hamiltonian self-calibrates via Rabi-like oscillation at frequency $\sqrt{\mu} = \sqrt{d_0/N}$: the time-independent Hamiltonian $H_r = -|\psi_0\rangle\langle\psi_0| + r \cdot H_z$ with $r = 1$ achieves optimality without knowing $A_1$ [39]. For general spectra, the resonance shifts to $r^* = A_1$ [39], moving the calibration problem from computing $A_1$ classically to detecting a spectral resonance quantumly.

A natural approach is Loschmidt echo measurement: evolve under $H_r$ and measure the return probability $|\langle\psi_0\rangle\, e^{-iH_r t}\psi_0|^2$, which oscillates with large amplitude near resonance and stays close to 1 off resonance. On the two-level family, this works cleanly: a binary search over $r$ with $O(n)$ probe measurements, each of cost $O(1/g_{\min})$, locates $r^*$ with polynomial overhead; the details appear in [39]. For general multilevel spectra, higher excited states contribute additional oscillation frequencies that mask the resonance signal. Whether the multilevel Loschmidt echo can be deconvolved efficiently, or whether a different calibration observable circumvents this interference, is open.

The constant-control counterexample applies only to the two-level family $H_z = I - P_0$. Under normalized controls, the barrier reappears.

**Proposition 9.5.10** (Normalized-control lower bound)**.** *Under normalized controls $|g(t)| \leq 1$ and the scaled family $H_z^{(\delta)} = \delta(I - P_0)$ with minimum excitation $\delta \in (0, 1]$, any instance-independent algorithm achieving success probability $\geq 2/3$ requires $T = \Omega(\sqrt{N/d_0}/\delta)$.*

*Proof.* The oracle-dependent term $g(t)H_z^{(\delta)} = \delta g(t)(I - P_0)$ has instantaneous oracle strength $\delta|g(t)|$. The total oracle action is $\mathcal{A} = \int_0^T \delta|g(t)|\,dt \leq \delta T$. The continuous-time query lower bound for unstructured search with $d_0$ marked items among $N$ gives $\mathcal{A} = \Omega(\sqrt{N/d_0})$ [40], so $T = \Omega(\sqrt{N/d_0}/\delta)$. □

For $\delta = N^{-1/2}$, this gives $T = \Omega(N/\sqrt{d_0})$, the same exponential penalty as the fixed-schedule adiabatic model. The barrier reappears on worst-case instances even for general continuous-time rank-one algorithms, provided the controls are normalized. The scope of the barrier is therefore precise: it is a consequence of monotone schedules with bounded controls, not of continuous-time quantum computation in general.

## 9.6 Computational Nature of $A_1$

The barrier cannot be designed away. What kind of computational hardness does it represent? The quantity $A_1$ is not merely NP-hard to compute — its hardness is counting hardness, inherited from the partition function. The tractability boundary does not align with optimization hardness, is not determined by the number of solutions, and depends on structural properties of the energy landscape.

The quantity $A_1$ encodes spectral information beyond the minimum gap. Consider three energy levels with $E_0 = 0$ ($d_0 = 1$), $E_1 = 1/n$ ($d_1 = 1$), $E_2 = 1$ ($d_2 = N - 2$). Then $\Delta = 1/n \to 0$ but $A_1 = (n + N - 2)/N \to 1$, so $1/\Delta \to \infty$ while $A_1 = \Theta(1)$. The tail of $N - 2$ states at energy 1 contributes $(N - 2)/N \approx 1$ to $A_1$, dominating the single state at the gap edge that contributes $n/N \approx 0$. The crossing position $s^* = A_1/(A_1 + 1) \approx 1/2$ is determined by the bulk of the spectrum, not by the gap, making $A_1$ fundamentally a whole-spectrum quantity that $\Delta$ alone cannot predict.

The distinction between NP-hardness at precision $1/\mathrm{poly}(n)$ (Theorem 8.1.2) and #P-hardness exactly (Theorem 8.2.4) matters because $A_1$ is fundamentally a counting quantity.

**Proposition 9.6.1** ($A_1$ hardness is counting hardness)**.** *For Boolean CSPs where counting satisfying assignments is #P-hard (including k-SAT for $k \geq 2$), computing $A_1$ of the clause-violation Hamiltonian is #P-hard even restricted to satisfiable instances.*

*Proof.* Encode the CSP as $H_z = \sum_{j=1}^m C_j$ where each $C_j(x) = 1$ if assignment $x$ violates clause $j$. The interpolation argument (Theorem 8.2.4) recovers all degeneracies $d_k$ from polynomially many evaluations of $A_1$ with shifted parameters, via Lagrange interpolation on the rational function $f(x) = \sum_k d_k/(\Delta_k + x/2)$. For satisfiable CSPs, $d_0$ counts satisfying assignments, and counting is #P-hard by hypothesis. □

The partition function connection makes this precise. Shifting energies so that $E_0 = 0$ and defining the Laplace partition function $Z(\beta) = \sum_x e^{-\beta E(x)}$, the spectral parameter admits the integral representation

$$A_1 = \frac{1}{N}\int_0^\infty (Z(\beta) - d_0)\,d\beta. \tag{9.6.1}$$

For integer spectra with $E(x) \in \{0, 1, \ldots, m\}$, the ordinary generating function $Z(t) = \sum_x t^{E(x)}$ gives $A_1 = (1/N)\int_0^1 (Z(t) - d_0)/t\,dt$. Both representations appear to require knowing $d_0$, which is itself a counting-hard quantity for many CSPs. However, for additive approximation it suffices to replace $d_0$ by the single evaluation $Z(\tau)$ at a small $\tau > 0$. Define the $\tau$-truncated proxy

$$A_1^{(\tau)} = \frac{1}{N}\int_\tau^1 \frac{Z(t) - Z(\tau)}{t}\,dt. \tag{9.6.2}$$

The additive error satisfies $0 \le A_1 - A_1^{(\tau)} \le \tau(1 + \ln(1/\tau))$, so choosing $\tau = O(\eta/\ln(1/\eta))$ gives an $\eta$-approximation to $A_1$ without direct access to $d_0$. When $E_0$ is known, even the coarse version is useful: sampling from the Boltzmann distribution at inverse temperature $\beta$ gives an unbiased estimator of $Z(\beta)/Z(0) = Z(\beta)/N$, and integrating via (9.6.1) yields an additive approximation of $A_1$ without computing $d_0$ directly. These representations turn "compute $A_1$" into partition function evaluation, connecting tractability of $A_1$ directly to tractability of counting problems.

**Proposition 9.6.2** (Bounded treewidth tractability). *For local energy functions $E(x) = \sum_j E_j(x_{S_j})$ with bounded locality $|S_j| \le k$ and a tree decomposition of the primal graph of width $w$, $A_1$ is computable exactly in $\mathrm{poly}(n, m) \cdot 2^{O(w)}$ time.*

*Proof.* Write the partition function polynomial $Z(t) = \sum_x t^{E(x)} = \sum_{q=0}^m d_q t^q$ in factor-graph form: $Z(t) = \sum_x \prod_j t^{E_j(x_{S_j})}$. Variable elimination on the tree decomposition computes $Z(t)$ exactly. At each elimination step, factor tables have at most $2^{w+1}$ entries, each a polynomial of degree at most $m$; multiplying factors convolves the polynomials (cost $O(m^2)$ per entry), and summing out a variable adds two polynomials (cost $O(m)$). After $n$ elimination steps, the result is $Z(t) = \sum_q d_q t^q$. Then $A_1 = (1/N)\sum_{q>E_0} d_q/(q - E_0)$. □

The treewidth condition is sufficient but not necessary. A simpler criterion applies whenever the spectrum itself is simple: if $H_z$ has at most $\mathrm{poly}(n)$ distinct energy levels with known energies and degeneracies, then $A_1 = (1/N)\sum_{k\ge1} d_k/(E_k - E_0)$ is directly computable in $\mathrm{poly}(n)$ time from the defining sum. This criterion is complementary to bounded treewidth — it applies to spectra that are structurally simple regardless of the interaction graph. For instance, Hamming-distance cost functions $E(x) = |x \oplus z_0|$ for a fixed target $z_0$ have $M = n + 1$ levels with degeneracies $d_k = \binom{n}{k}$ and energies $E_k = k$, so $A_1 = (1/N)\sum_{k=1}^n \binom{n}{k}/k$ depends only on $n$ and is trivially computable.

The partition function bridge is one-directional: tractable $Z$ implies tractable $A_1$ (via the integral representations above), but exact $A_1$ does not determine low-temperature $Z(\beta)$.

**Proposition 9.6.3** (Reverse bridge obstruction). *There exist two diagonal Hamiltonians $H_z$, $H_z'$ on $N = 2^n$ states with the same ground degeneracy ratio $d_0/N$, same minimum excitation $\Delta_{\min}$, and $A_1(H_z) = A_1(H_z')$ exactly, yet $|Z_{H_z}(\beta) - Z_{H_z'}(\beta)|/N \ge 1/100$ at $\beta = O(1/\Delta_{\min})$.*

*Proof.* Fix an integer $B \ge 3$. Define two spectra, both with $d_0/N = 1/2$ and $\Delta_{\min} = 1/B$: the first has $N/8$ states at energy $1/B$ and $3N/8$ states at energy $B$; the second has $N/16$ states at energy $1/B$ and $7N/16$ states at energy $c_B = 7B/(B^2 + 6)$. Direct computation gives $A_1 = (B^2 + 3)/(8B)$ for both. At $\beta = B$: $Z_1(B)/N = 1/2 + e^{-1}/8 + 3e^{-B^2}/8$ while $Z_2(B)/N = 1/2 + e^{-1}/16 + (7/16)e^{-7B^2/(B^2+6)}$. Since $7B^2/(B^2 + 6) \ge 4.2$ for $B \ge 3$, the difference is at least $e^{-1}/16 - (7/16)e^{-4.2} > 1/100$. □

Three natural conjectures about easy instances of $A_1$ computation are all false.

**Proposition 9.6.4** (Unique solution does not imply easy $A_1$). *There exist instances with $d_0 = 1$ for which computing $A_1$ is #P-hard.*

*Proof.* The proof of Proposition 9.6.1 applies to satisfiable instances with $d_0 = 1$: the interpolation reduction recovers $d_1, \ldots, d_{M-1}$ from $A_1$ evaluations, and counting the number of assignments at each violation level is #P-hard. Concretely, for a satisfiable 3-SAT instance with $m$ clauses and a unique satisfying assignment, the clause-violation Hamiltonian $H_z = \sum_j C_j$ has $d_0 = 1$ and $A_1 = \sum_{k=1}^m d_k/(kN)$, where $d_k$ counts assignments violating exactly $k$ clauses. Recovering these counts from $A_1$ (via shifted parameters) is #P-hard. □

**Proposition 9.6.5** (Bounded degeneracy is vacuous). *If all $d_k \le \mathrm{poly}(n)$ and $M \le \mathrm{poly}(n)$, then $d_0 \ge N - \mathrm{poly}(n)^2$, and the optimization problem is trivially solvable by random sampling.*

*Proof.* The total state count satisfies $\sum_{k=0}^{M-1} d_k = N = 2^n$. If $d_k \le \mathrm{poly}(n)$ for all $k$ and $M \le \mathrm{poly}(n)$, then $\sum_{k\ge1} d_k \le (M - 1) \cdot \mathrm{poly}(n) \le \mathrm{poly}(n)^2$, so $d_0 \ge N - \mathrm{poly}(n)^2$. For $n$ large enough, $d_0/N \ge 1 - o(1)$, and a random sample finds a ground state with probability $1 - o(1)$. □

**Proposition 9.6.6** (Hard optimization does not imply hard $A_1$)**.** *The tractability of $A_1$ is independent of optimization hardness. 2-SAT is in P but #2-SAT is #P-complete [28], giving easy optimization with hard $A_1$. In the reverse direction, Grover search with a promised ground degeneracy $d_0$ gives hard optimization but trivial $A_1 = (N - d_0)/(N\Delta)$, computable in $O(1)$ from the promise.*

The tractability boundary for $A_1$ is subtle. It does not align with optimization hardness, is not determined by the number of solutions, and depends on structural properties of the energy landscape (treewidth, partition function tractability) rather than on the difficulty of finding the ground state.

## 9.7 The Complexity Landscape

The quantum query complexity of $A_1$ estimation at the algorithmically relevant precision $\varepsilon = 2^{-n/2}$ is $O(2^{n/2} \cdot \mathrm{poly}(n))$ (Theorem 8.3.3), the classical lower bound is $\Omega(2^n)$ (Theorem 8.3.4), and no polynomial-interpolation scheme can establish #P-hardness at this precision (Theorem 8.3.2). The quantum bound is tight.

**Theorem 9.7.1** (Tight quantum query complexity at schedule precision)**.** *At the schedule-relevant precision $\varepsilon = \Theta(2^{-n/2})$, the quantum query complexity of $A_1$ estimation is $\Theta(2^{n/2}) = \Theta(1/\varepsilon)$. The lower bound is achieved on two-level instances with $\Delta_1 = 1$.*

*Proof.* For $\varepsilon = \Theta(2^{-n/2})$ and $\Delta_1 = 1$, Theorem 8.3.3 gives an upper bound $O(\sqrt{N} + 1/\varepsilon) = O(2^{n/2})$. For the lower bound, consider $M = 2$ instances with $\Delta_1 = 1$: estimating $A_1 = (N - d_0)/N$ to precision $\varepsilon$ reduces to approximate counting. The Grover iterate $G = (2\left|+\right\rangle\left\langle+\right| - I)(I - 2\Pi_S)$ has eigenphases $\pm 2\theta$ with $\sin^2\theta = d_0/N$. After $T$ sequential applications of $G$, the probe state acquires phase $T\phi$ where $\phi = 2\arcsin\left(\sqrt{d_0/N}\right)$, and the quantum Fisher information for estimating $\phi$ from $T$ sequential applications is $F_Q = 4T^2$ (the standard Heisenberg limit for phase accumulation in sequential quantum metrology [41, 37]). The quantum Cramér-Rao bound gives $\mathrm{Var}(\hat{\phi}) \geq 1/F_Q = 1/(4T^2)$. The adversary chooses $d_0 = N/2$ so that $\sin^2\theta = 1/2$, where $|d(\sin^2\theta)/d\theta| = |\sin 2\theta| = 1$. Estimating $A_1 = 1 - \sin^2\theta$ to precision $\varepsilon$ at this operating point requires estimating $\theta$ to precision $\varepsilon$, hence $1/(4T^2) \leq \varepsilon^2$, giving $T \geq 1/(2\varepsilon)$ applications of $G$, each costing $O(1)$ oracle queries. With $\varepsilon = \Theta(2^{-n/2})$, this is $\Omega(2^{n/2})$, so the complexity is $\Theta(2^{n/2}) = \Theta(1/\varepsilon)$. ☐

The lower bound is worst-case over the unknown parameter $d_0$: the adversary fixes $d_0 = N/2$ to maximize the estimation difficulty. The Heisenberg limit $F_Q = 4T^2$ for sequential unitary applications is a fundamental result of quantum metrology that applies to all quantum estimation strategies, not just phase estimation — it follows from the unitarity of quantum evolution and the Cramér-Rao inequality, as shown by Braunstein and Caves [41] and extended to the sequential setting by Giovannetti, Lloyd, and Maccone [37]. Alternatively, the $\Omega(1/\varepsilon)$ lower bound follows directly from quantum approximate counting: estimating $d_0/N$ to additive precision $\varepsilon$ requires $\Omega(1/\varepsilon)$ quantum queries [35, 42], and the reduction to $A_1$ is immediate on $M = 2$ instances.

This result connects directly to the adaptive protocol of section 9.3: the adaptive protocol achieves $T_{\mathrm{adapt}} = O(T_{\mathrm{inf}}) = O(2^{n/2})$, which is the same order as the tight quantum query complexity $\Theta(2^{n/2})$ for $A_1$ estimation at the algorithmically relevant precision $\delta_{A_1} = \Theta(2^{-n/2})$. This is not a coincidence — both tasks require distinguishing $\Omega(2^{n/2})$ possibilities with $O(1)$ information per quantum measurement.

In the high-precision regime relevant to schedule placement, the quadratic quantum advantage persists.

**Proposition 9.7.2** (Precision phase diagram)**.** *For two-level instances with $\Delta_1 = 1$ and precision $\varepsilon \leq c/\sqrt{N}$ (constant $c$), the query complexity of $A_1$ estimation is $\Theta(1/\varepsilon)$ quantum and $\Theta(1/\varepsilon^2)$ classical. The quantum-to-classical ratio is $\Theta(1/\varepsilon)$ in this regime.*

*Proof.* In this regime, $1/\varepsilon \geq \sqrt{N}/c$, so the upper bound of Theorem 8.3.3 becomes $O(\sqrt{N} + 1/\varepsilon) = O(1/\varepsilon)$. The matching quantum lower bound is inherited from two-level approximate counting (Theorem 9.7.1). The classical lower bound $\Omega(1/\varepsilon^2)$ follows from Theorem 8.3.4, and Monte Carlo sampling gives the matching upper bound $O(1/\varepsilon^2)$. ☐

**Theorem 9.7.3** (ETH computational complexity)**.** *Under the Exponential Time Hypothesis (ETH), any classical algorithm computing $A_1$ at precision $2^{-n/2}$ requires $2^{\Omega(n)}$ time.*

*Proof sketch.* The NP-hardness reduction (Theorem 8.1.2) maps 3-SAT on $n_{\mathrm{var}}$ variables to $A_1$ estimation of a 3-local Hamiltonian on $n = O(n_{\mathrm{var}})$ qubits at precision $1/\mathrm{poly}(n)$. By the Impagliazzo-Paturi-Zane sparsification lemma [43], 3-SAT on $n_{\mathrm{var}}$ variables can be reduced to instances with $O(n_{\mathrm{var}})$ clauses, giving $n = O(n_{\mathrm{var}})$ qubits. Any algorithm computing $A_1$ at precision $2^{-n/2}$ can, in particular, compute $A_1$ at the coarser precision $1/\mathrm{poly}(n)$ (since $2^{-n/2} < 1/\mathrm{poly}(n)$ for large $n$), and thus solves 3-SAT by the reduction. Under ETH, 3-SAT on $n_{\mathrm{var}} = \Omega(n)$ variables requires $2^{\Omega(n_{\mathrm{var}})} = 2^{\Omega(n)}$ time. ☐

Under ETH, the quadratic quantum advantage extends from the query model to the computational model.

**Corollary 9.7.4** (Quantum pre-computation cost)**.** *Estimating $A_1$ to the schedule-relevant precision $\delta_{A_1} = \Theta(2^{-n/2})$ via quantum amplitude estimation costs $\Theta(2^{n/2} \cdot \mathrm{poly}(n))$ time, matching the adaptive protocol's runtime. The classical pre-computation cost at the same precision is $\Omega(2^n)$.*

In terms of parameterized complexity, the corollary places $A_1$ estimation at precision $2^{-n/2}$ in FBQTIME($2^{n/2}\cdot$ poly($n$)): the problem is not polynomial-time in the standard sense but admits a quantum algorithm whose runtime matches the Grover scale. The information cost of fixed-schedule adiabatic optimization matches the quantum speedup scale: estimating the missing $n/2$ bits of $A_1$ costs $\Theta(2^{n/2})$ quantumly, the same scale as Grover search and the informed adiabatic runtime. The circuit model achieves that scale without this pre-step because amplitude amplification directly solves the search task.

The generic extrapolation barrier (Theorem 8.3.2) shows that the interpolation breakdown at precision $2^{-n/2}$ is not an artifact of a specific construction. Any polynomial extrapolation scheme with $d = \mathrm{poly}(n)$ nodes faces Lebesgue amplification $\Lambda_d(x^*) \geq 2^{d-1}$ when the evaluation point is at distance at least $b - a$ from the sample interval $[a, b]$; this geometric condition must be checked in each interpolation setup and is not implied solely by $x^* = \Theta(2^{-n/2})$ with nodes in $[0, 1/\mathrm{poly}(n)]$. Under that condition, polynomial-interpolation reductions for $A_1$ require precision $2^{-\Omega(n)}$.

**Proposition 9.7.5** (Two-level worst-case reduction)**.** *The two-level family ($M = 2$) is a worst-case subclass for $A_1$ estimation at schedule-relevant precision: any worst-case lower bound for approximate counting on this subclass applies to general $A_1$ estimation.*

*Proof.* Worst-case complexity over all instances is at least the complexity on any subclass. Restricting to $M = 2$ gives

$$A_1 = \frac{N - d_0}{N\Delta_1},$$

so for fixed $\Delta_1 = 1$, estimating $A_1$ to additive precision $\varepsilon$ is exactly approximate counting for $d_0/N$ at precision $\varepsilon$. Therefore, any lower bound for approximate counting on this subclass is automatically a lower bound for general $A_1$ estimation. □

The worst-case hardness of $A_1$ estimation does not hide in complex spectra. Simple two-level instances, where $A_1$ reduces to counting, already saturate the query lower bound. Algorithms exploiting the sum-of-reciprocals structure of $A_1$ for multilevel spectra cannot beat algorithms for plain mean estimation.

At the schedule precision, bounded-treewidth instances remain tractable for $A_1$ computation (Proposition 9.6.2). For ferromagnetic Ising models, the partition function $Z(\beta)$ can be multiplicatively approximated in polynomial time [44], which gives an additive approximation of $A_1$ at coarse precision via the integral representations of section 9.5. However, achieving precision $\delta_{A_1} = \Theta(2^{-n/2})$ requires the multiplicative accuracy $\mu = O(2^{-n/2}/B)$ where $B = O(\log(1/\delta_{A_1})/\Delta_{\min})$, and the FPRAS runtime scales as poly($1/\mu$). Since $\mu = O(2^{-n/2}/B)$ with $B = O(n/\Delta_{\min})$, this gives $\mathrm{poly}(1/\mu) = 2^{\Omega(n)}$. The ferromagnetic Ising approximation does not remain tractable at the algorithmically relevant precision.

The interpolation theorem (Theorem 9.2.2) provides the quantitative link between information and runtime. To formalize this, consider a communication setting: Alice holds the complete classical description of $H_z$ (all eigenvalues and degeneracies), Bob holds a quantum computer with oracle access to $H_z$, and Alice can send $C$ classical bits to Bob. Bob's goal is to find a ground state using at most $T$ queries. In the circuit-oracle model, $C = 0$ suffices for $T = O(\sqrt{N/d_0})$: Bob runs the Dürr-Høyer algorithm without any communication. In the fixed-schedule adiabatic model, Bob must construct a schedule with velocity matched to the crossing, requiring $s^*$ to precision $\Delta_* = O(2^{-n/2})$, which costs $C = \Theta(n)$ bits. Each additional bit of $A_1$ precision halves the adiabatic runtime, until $n/2$ bits suffice for optimality. Formally, if Alice communicates $C$ bits encoding $A_1$ to precision $\varepsilon = \Theta(2^{-C})$, the adiabatic runtime satisfies $T(C) = T_{\inf} \cdot \Theta(\max(1, 2^{n/2-C}))$.

**Theorem 9.7.6** (Bit-runtime information law)**.** *The classical communication cost for the adiabatic model to achieve target runtime $T$ is $C^*(T) = \max(0, n/2 - \log_2(T/T_{\inf}))$ bits, while $C^*_{\mathrm{circuit}}(T) = 0$ for all $T \geq T_{\inf}$.*

*Proof.* Inverting $T(C) = T_{\inf} \cdot 2^{n/2-C}$ gives $C = n/2 - \log_2(T/T_{\inf})$. Clamping $C \geq 0$ and noting that the circuit model achieves $T = T_{\inf}$ at $C = 0$ by the Dürr-Høyer algorithm gives both formulas. □

The complete model comparison, synthesizing results from this chapter and Chapter 8, is:

| Model | Info needed | Runtime | Communication |
|---|---|---|---|
| Circuit (Dürr-Høyer) | None | $\Theta(\sqrt{N/d_0})$ | 0 bits |
| Fixed AQO, informed | $A_1$ to $2^{-n/2}$ | $O(\sqrt{N/d_0})$ | $\Theta(n)$ bits |
| Fixed AQO, $C$ bits | $A_1$ to $2^{-C}$ | $T_{\text{inf}} \cdot 2^{n/2-C}$ | $C$ bits |
| Fixed AQO, uninformed | None | $\Omega(N/\sqrt{d_0})$ | 0 bits |
| Adaptive AQO | $O(n)$ measurements | $O(\sqrt{N/d_0})$ | 0 bits |
| Constant-control, two-level | None | $\Theta(\sqrt{N/d_0})$ | 0 bits |
| Quantum $A_1$ estimation | $\varepsilon = 2^{-n/2}$ | $\Theta(2^{n/2})$ queries | — |
| Classical $A_1$ estimation | $\varepsilon = 2^{-n/2}$ | $\Theta(2^n)$ queries | — |

The circuit model and the adaptive adiabatic model both achieve optimal performance with zero classical communication. The fixed adiabatic model traces a diagonal: each missing bit doubles the runtime. The $\Theta(n)$-bit gap between the circuit model and the fixed adiabatic model is exactly the information content of $A_1$ at the algorithmically relevant precision. The communication cost is a property of the computational model, not of the computational task.

For the running example ($N = 4$, $d_0 = 1$, $n = 2$): the circuit model uses $O(2)$ queries at $C = 0$; the informed adiabatic model uses $O(2)$ queries at $C = 1$ bit; the uninformed adiabatic model uses $\Omega(4)$ queries at $C = 0$. The one missing bit accounts for the factor-of-two gap.

The information gap is now resolved in all three of its meanings. The spectral gap determines the runtime: within the adiabatic framework, the minimum gap $g_{\min}$ sets the time scale $T = O(1/g_{\min})$, and the gap profile $g(s)$ determines how the schedule must be shaped. The gap in knowledge determines what runtime is achievable: with no knowledge of where $g_{\min}$ occurs, the runtime blows up by a factor of $(s_R - s_L)/\Delta_*$; with $\varepsilon$-precision knowledge, the overhead is $\Theta(\max(1, \varepsilon/\delta_{A_1}))$; with $O(n)$ quantum measurements, the overhead vanishes. And whether the gap in knowledge matters at all depends on the computational model: in the circuit model, the quantity $A_1$ is irrelevant and invisible; in the fixed-schedule adiabatic model, it is essential and NP-hard; in the adaptive adiabatic model, it is acquirable at polynomial cost.

The ignorance taxonomy has five levels, where the overhead is the multiplicative ratio $T/T_{\text{inf}}$. Level 0 (no information): $\Omega(2^{n/2})$ overhead. Level 1 (precision $\varepsilon$): $\Theta(\max(1, \varepsilon/\delta_{A_1}))$ overhead. Level 2 (bounded interval $[u_L, u_R]$): constant overhead proportional to $u_R - u_L$. Level 3 (quantum measurement): $O(1)$ overhead with $O(n)$ measurements. Level 4 (circuit model): overhead 1, no spectral information needed.

The adiabatic approach to unstructured search works, achieves the Grover speedup, and is optimal among all schedules. But its information requirements are a structural consequence of the rank-one interpolation path. These requirements are not a fundamental limitation of quantum computation — they are a property of the adiabatic model. The next chapter translates these results into machine-checked formal proofs.

Chapter 10

# Formalization

Chapter 11

# Conclusion

# Bibliography


[1] Lov K. Grover. A fast quantum mechanical algorithm for database search. In *Proceedings of the 28th Annual ACM Symposium on Theory of Computing*, pages 212–219, 1996. doi:10.1145/237814.237866.

[2] Michel Boyer, Gilles Brassard, Peter Høyer, and Alain Tapp. Tight bounds on quantum searching. *Fortschritte der Physik*, 46(4-5):493–505, 1998. doi:10.1002/(SICI)1521-3978(199806)46:4/5<493::AID-PROP493>3.0.CO;2-P.

[3] Dorit Aharonov, Wim van Dam, Julia Kempe, Zeph Landau, Seth Lloyd, and Oded Regev. Adiabatic quantum computation is equivalent to standard quantum computation. *SIAM Journal on Computing*, 37 (1):166–194, 2007. doi:10.1137/S0097539705447323.

[4] Jeremie Roland and Nicolas J. Cerf. Quantum search by local adiabatic evolution. *Physical Review A*, 65 (4):042308, 2002. doi:10.1103/PhysRevA.65.042308.

[5] Edward Farhi, Jeffrey Goldstone, Sam Gutmann, and Daniel Nagaj. How to make the quantum adiabatic algorithm fail. *International Journal of Quantum Information*, 6(03):503–516, 2008. doi:10.1142/S021974990800358X.

[6] Charles H. Bennett, Ethan Bernstein, Gilles Brassard, and Umesh Vazirani. Strengths and weaknesses of quantum computing. *SIAM Journal on Computing*, 26(5):1510–1523, 1997. doi:10.1137/S0097539796300933.

[7] Marko Žnidarič and Martin Horvat. Exponential complexity of an adiabatic algorithm for an NP-complete problem. *Physical Review A*, 73:022329, 2006. doi:10.1103/PhysRevA.73.022329.

[8] Itay Hen. Continuous-time quantum algorithms for unstructured problems. *Journal of Physics A: Mathematical and Theoretical*, 47(4):045305, 2014. doi:10.1088/1751-8113/47/4/045305.

[9] F. Barahona. On the computational complexity of Ising spin glass models. *Journal of Physics A: Mathematical and General*, 15(10):3241, 1982. doi:10.1088/0305-4470/15/10/028.

[10] Andrew Lucas. Ising formulations of many NP problems. *Frontiers in Physics*, 2:5, 2014. doi:10.3389/fphy.2014.00005.

[11] Tameem Albash and Daniel A. Lidar. Adiabatic quantum computation. *Reviews of Modern Physics*, 90: 015002, 2018. doi:10.1103/RevModPhys.90.015002.

[12] Arthur Braida. *Analog Quantum Computing for NP-Hard Combinatorial Graph Problems*. PhD thesis, Université d'Orléans, 2024.

[13] Boris Altshuler, Hari Krovi, and Jérémie Roland. Anderson localization makes adiabatic quantum optimization fail. *Proceedings of the National Academy of Sciences*, 107(28):12446–12450, 2010. doi:10.1073/pnas.1002116107.

[14] Arthur Braida, Shantanav Chakraborty, Leonardo Novo, and Jérémie Roland. Unstructured adiabatic quantum optimization: Optimality with limitations. *arXiv preprint arXiv:2411.05736*, 2024.

[15] Gene H. Golub. Some modified matrix eigenvalue problems. *SIAM Review*, 15(2):318–334, 1973. doi:10.1137/1015032.

[16] Shantanav Chakraborty, Leonardo Novo, and Jérémie Roland. Optimality of spatial search via continuous-time quantum walks. *Physical Review A*, 102:032214, 2020. doi:10.1103/PhysRevA.102.032214.

[17] Jack Sherman and Winifred J. Morrison. Adjustment of an inverse matrix corresponding to a change in one element of a given matrix. *The Annals of Mathematical Statistics*, 21(1):124–127, 1950. doi:10.1214/aoms/1177729893.

[18] W. van Dam, M. Mosca, and U. Vazirani. How powerful is adiabatic quantum computation? In *Proceedings 42nd IEEE Symposium on Foundations of Computer Science*, pages 279–287, 2001. doi:10.1109/SFCS.2001.959902.

[19] Tosio Kato. On the adiabatic theorem of quantum mechanics. *Journal of the Physical Society of Japan*, 5 (6):435, 1950.

[20] Andrew M. Childs and Jeffrey Goldstone. Spatial search by quantum walk. *Physical Review A*, 70:022314, 2004. doi:10.1103/PhysRevA.70.022314.

[21] Sabine Jansen, Mary-Beth Ruskai, and Ruedi Seiler. Bounds for the adiabatic approximation with applications to quantum computation. *Journal of Mathematical Physics*, 48(10):102111, 2007. doi:10.1063/1.2798382.

[22] Sergio Boixo, Emanuel Knill, and Rolando Somma. Eigenpath traversal by phase randomization. *Quantum Information and Computation*, 9(9):833–855, 2009.

[23] Joseph Cunningham and Jérémie Roland. Eigenpath traversal by Poisson-distributed phase randomisation. In *19th Conference on the Theory of Quantum Computation, Communication and Cryptography (TQC 2024)*, pages 7:1–7:20, 2024. doi:10.4230/LIPIcs.TQC.2024.7.

[24] Alexander Elgart and George A. Hagedorn. A note on the switching adiabatic theorem. *Journal of Mathematical Physics*, 53(10), 2012. doi:10.1063/1.4748968.

[25] Xi Guo and Dong An. Improved gap dependence in adiabatic state preparation by adaptive schedule. *arXiv preprint arXiv:2512.10329*, 2025.

[26] Julia Kempe, Alexei Kitaev, and Oded Regev. The complexity of the local Hamiltonian problem. *SIAM Journal on Computing*, 35(5):1070–1097, 2006. doi:10.1137/S0097539704445226.

[27] M.R. Garey, D.S. Johnson, and L. Stockmeyer. Some simplified NP-complete graph problems. *Theoretical Computer Science*, 1(3):237–267, 1976. doi:10.1016/0304-3975(76)90059-1.

[28] Leslie G. Valiant. The complexity of enumeration and reliability problems. *SIAM Journal on Computing*, 8(3):410–421, 1979. doi:10.1137/0208032.

[29] George M. Phillips. *Interpolation and Approximation by Polynomials*, volume 14. Springer Science & Business Media, 2003. doi:10.1007/b97417.

[30] Ramis Movassagh. The hardness of random quantum circuits. *Nature Physics*, 19(11):1719–1724, 2023. doi:10.1038/s41567-023-02131-2.

[31] Ramamohan Paturi. On the degree of polynomials that approximate symmetric Boolean functions. In *Proceedings of the 24th Annual ACM Symposium on Theory of Computing*, pages 468–474, 1992. doi:10.1145/129712.129758.

[32] Scott Aaronson and Alex Arkhipov. The computational complexity of linear optics. In *Proceedings of the 43rd Annual ACM Symposium on Theory of Computing*, pages 333–342, 2011. doi:10.1145/1993636.1993682.

[33] Adam Bouland, Bill Fefferman, Chinmay Nirkhe, and Umesh Vazirani. On the complexity and verification of quantum random circuit sampling. *Nature Physics*, 15(2):159–163, 2019. doi:10.1038/s41567-018-0318-2.

[34] Christoph Dürr and Peter Høyer. A quantum algorithm for finding the minimum. *arXiv preprint quant-ph/9607014*, 1996.

[35] Gilles Brassard, Peter Høyer, Michele Mosca, and Alain Tapp. Quantum amplitude amplification and estimation. *Contemporary Mathematics*, 305:53–74, 2002. doi:10.1090/conm/305/05215.

[36] Lucien Le Cam. Convergence of estimates under dimensionality restrictions. *The Annals of Statistics*, 1 (1):38–53, 1973. doi:10.1214/aos/1176342150.

[37] Vittorio Giovannetti, Seth Lloyd, and Lorenzo Maccone. Quantum metrology. *Physical Review Letters*, 96: 010401, 2006. doi:10.1103/PhysRevLett.96.010401.

[38] Mancheon Han, Hyowon Park, and Sangkook Choi. The constant speed schedule for adiabatic state preparation: Towards quadratic speedup without prior spectral knowledge, 2025.

[39] Eduardo Araújo, Shantanav Chakraborty, and Leonardo Novo. Advantages and limitations of analog quantum search methods. *In preparation*, 2025.

[40] Edward Farhi and Sam Gutmann. Analog analogue of a digital quantum computation. *Physical Review A*, 57(4):2403–2406, 1998. doi:10.1103/PhysRevA.57.2403.

[41] Samuel L. Braunstein and Carlton M. Caves. Statistical distance and the geometry of quantum states. *Physical Review Letters*, 72(22):3439–3443, 1994. doi:10.1103/PhysRevLett.72.3439.

[42] Ashwin Nayak and Felix Wu. The quantum query complexity of approximating the median and related statistics. In *Proceedings of the 31st Annual ACM Symposium on Theory of Computing (STOC)*, pages 384–393, 1999. doi:10.1145/301250.301349.

[43] Russell Impagliazzo, Ramamohan Paturi, and Francis Zane. Which problems have strongly exponential complexity? *Journal of Computer and System Sciences*, 63(4):512–530, 2001. doi:10.1006/jcss.2001.1774.

[44] Mark Jerrum and Alistair Sinclair. Polynomial-time approximation algorithms for the ising model. *SIAM Journal on Computing*, 22(5):1087–1116, 1993.